

AD720857

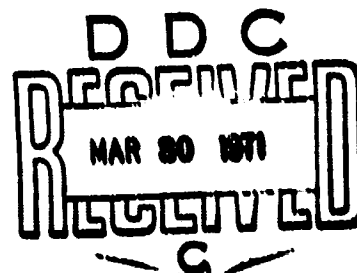
AFML - TR - 70 - 259

**STRESS - CORROSION AND CORROSION - FATIGUE  
SUSCEPTIBILITY OF HIGH-STRENGTH  
ALUMINUM ALLOYS**

**G.E. NORDMARK, B.W. LIFKA, M.S. HUNTER,  
AND J.G. KAUFMAN**

**ALUMINUM COMPANY OF AMERICA  
ALCOA RESEARCH LABORATORIES  
NEW KENSINGTON, PA.**

**TECHNICAL REPORT AFML - TR - 70 - 259  
NOVEMBER 1970**



**THIS DOCUMENT HAS BEEN APPROVED FOR PUBLIC  
RELEASE AND SALE ; ITS DISTRIBUTION IS UNLIMITED**

**Reproduced by  
NATIONAL TECHNICAL  
INFORMATION SERVICE  
Springfield, Va. 22151**

**AIR FORCE MATERIALS LABORATORY  
AIR FORCE SYSTEMS COMMAND  
WRIGHT - PATTERSON AIR FORCE BASE, OHIO**

**BEST**

**AVAILABLE**

**COPY**

EXEMPTED TO	
BY	WRITE SECTION
DO	OFF SECTION
EXEMPTED TO	
AUTHORITY	
BY	
DISTRIBUTION/AVAILABILITY CODES	
DET.	AVAIL. CODE OF SPECIAL
A	

## NOTICES

When Government drawings, specifications, or other data are used for any purpose other than in connection with a definitely related Government procurement operation, the United States Government thereby incurs no responsibility nor any obligation whatsoever; and the fact that the Government may have formulated, furnished, or in any way supplied the said drawings, specification, or other data, is not to be regarded by implication or otherwise as in any manner licensing the holder or any other person or corporation, or conveying any rights or permission to manufacture, use, or sell any patented invention that may in any way be related thereto.

Copies of this report should not be returned unless return is required by security considerations, contractual obligations, or notice on a specific document.

**STRESS-CORROSION AND CORROSION-FATIGUE  
SUSCEPTIBILITY OF HIGH-STRENGTH  
ALUMINUM ALLOYS**

**G. E. Nordmark  
B. W. Lifka  
M. S. Hunter  
J. G. Kaufman**

This document has been approved for public release and sale; its distribution is unlimited.


## FOREWORD

This investigation was conducted by the Alcoa Research Laboratories, Aluminum Company of America, New Kensington, Pennsylvania, under USAF Contract No. AF33(615)-67-C-1922, Project No. 7381, "Stress-Corrosion and Corrosion-Fatigue Susceptibility of High-Strength Aluminum Alloys". The work was under the direction of the Air Force Materials Laboratory, Wright-Patterson Air Force Base, Ohio 45433, with Mr. H. W. Zoeller (LAA) as project engineer.

The investigation was made under the supervision of Mr. R. L. Moore and, later, Dr. J. W. Clark. Project leaders were: Mr. G. E. Nordmark for fatigue testing; Mr. B. W. Lifka for corrosion and stress corrosion; Mr. J. G. Kaufman for mechanical properties and fracture behavior; Mr. M. S. Hunter for metallography; and Mr. R. S. Barker for residual stress measurements.

This final report covers work done from June 1967 through October 1970. The report was released by the authors for publication in October 1970.

This technical report has been reviewed and is approved.

  
D. A. SHINN, Chief  
Aeronautical Systems Support Branch  
Materials Support Division  
AF Materials Laboratory

## ABSTRACT

The "stress-corrosion-fatigue" performance of several high strength-aluminum alloys was investigated by tests of hydraulic cylinders and other types of specimens. Specimens were prepared from forgings and forging stock of alloys 2014-T6, 7075-T6, 7075-T73, 7079-T6, and X7080-T7 and from premium castings of alloy CH70-T7. The alternating internal pressure loading of the cylinders at frequencies between 0.15 and 20 cpm in corrosive environment included hold times at load of as much as 5.4 minutes. Corrosive environment was provided by a warm salt fog at 12 hour intervals.

Alloy 7075-T73 rated best in the corrosion-fatigue tests; no stress-corrosion cracking occurred in this alloy, and the lives of forged cylinders subjected to repeated loadings to 80% of design stress in a corrosive environment were at least 10 times as long for this alloy as for forged cylinders of alloys 2014-T6, 7075-T6, or 7079-T6. Fractographic examination showed that stress-corrosion cracking as well as fatigue cracking occurred in alloys 2014-T6, 7075-T6, and 7079-T6 in the stress-corrosion-fatigue tests. The investigation demonstrated that stress corrosion and fatigue can interact under certain conditions to produce failures in shorter times and fewer cycles than for either phenomenon occurring by itself.

### Key Words

corrosion-fatigue  
stress-corrosion  
internal  
pressure  
hydraulic  
cylinders  
C-rings  
forgings  
rolled rod  
casting  
mechanical properties  
fracture  
toughness  
tear

fatigue  
pressure  
axial-stress  
metallography  
fracture-mechanics  
cracking  
fractography  
frequency  
aluminum alloys  
7075-T6  
7075-T73  
7079-T6  
X7080-T7  
2014-T6  
CH70-T7

## TABLE OF CONTENTS

<u>SECTION</u>		<u>PAGE</u>
I	Introduction	1
II	Summary	2
III	Materials	4
IV	Specimens	7
V	Procedures	9
VI	Test Results	14
VII	Conclusions	29
VIII	Recommendations	32
	References	34

## LIST OF ILLUSTRATIONS

	<u>Page</u>
Fig. 1 Steps in Processing of Test Cylinders from Die Forgings	35
Fig. 2 Kahn Type Tear Test Specimen	36
Fig. 3 Notch-Bend Fracture Toughness Specimen	37
Fig. 4 Compact Tension Fracture Toughness Specimen	38
Fig. 5 Fracture Paths of Tear Specimens	39
Fig. 6 Hydraulic Cylinder Fatigue Test Cell - Specimen Detail	40
Fig. 7 "C" Ring Specimen for Hydraulic Cylinder Fatigue and Corrosion Test	41
Fig. 8 Residual Stress Patterns in Test Section of Cylinder Specimens Quenched at Different Water Temperatures in Heat Treatment	42
Fig. 9 Axial Stress Fatigue Specimen for Tests in Laboratory Atmosphere or Submerged in Highly Corrosive Liquid	43
Fig. 10 Arrangement of Cylinder for Fatigue Test in Controlled Environment	44
Fig. 11 Assembly of Cylinders on Test Rack	45
Fig. 12 Facilities for Fatigue Testing of Hydraulic Cylinders	46
Fig. 13 Calibration of 7075 Cylinder Loaded Hydrostatically	47
Fig. 14 Apparatus for Fatigue Testing C-Rings in Controlled Environment	48
Fig. 15 Machine for Fatigue and Corrosion-Fatigue Tests of C-Rings in Controlled Environment	49
Fig. 16 Comparison of Measured and Calculated Stresses in C-Rings	50



LIST OF ILLUSTRATIONS (continued)

	<u>Page</u>
Fig. 17 Axial Stress Fatigue Tests of Alloy 7075-T6	51
Fig. 18 Axial Stress Fatigue Tests of Alloy 7079-T6	52
Fig. 19 Axial Stress Fatigue Tests of Alloy X7080-T7	53
Fig. 20 Axial-Stress Fatigue Tests of Alloy 2014-T6	54
Fig. 21 Axial Stress Fatigue Tests of Alloy 7075-T73	55
Fig. 22 Axial Stress Fatigue Tests of Alloy CH70-T7	56
Fig. 23 Fatigue Lives of Cylinders - No Corrosive Environment	57
Fig. 24 Failure of 7075-T6 Die Forged Specimen #18 in Static Stress-Corrosion Tests in Simulated Seacoast Environment	58
Fig. 25a Effect of Environment on Fatigue Life of Hydraulic Cylinders	59
Fig. 25b Effect of Environment on Fatigue Life of Hydraulic Cylinders	60
Fig. 26 Fatigue Lives of C-Rings - No Corrosive Environment	61
Fig. 27 Comparison of the Stress-Corrosion Performance of Static-Loaded C-Rings from the Die Forgings and Castings in Three Corrosive Environments	62
Fig. 28 Comparison of the Stress-Corrosion Performance of Static-Loaded C-Rings from the Rolled Rod Stock in Three Corrosive Environments	63
Fig. 29 Static Stress-Corrosion Cracking of C-Ring from 2014-T6 Rolled Rod Stock in Alternate Immersion Test	64
Fig. 30 Static Stress-Corrosion Cracking of C-ring from 7075-T6 Rolled Rod Stock in Alternate Immersion Test	65
Fig. 31 Static Stress-Corrosion Cracking of C-ring from 7075-T6 Forging in Simulated Seacoast Environment	66
Fig. 32 Typical Stress-Corrosion Failures of Statically Loaded C-rings	67

LIST OF ILLUSTRATIONS (continued)

	<u>Page</u>
Fig. 33 Stress-Corrosion Fatigue Tests of 7075-T6 and 7075-T73 Cylinders	68
Fig. 34a Stress-Corrosion-Fatigue Tests of 7075-T6 Cylinders and C-rings	69
Fig. 34b Stress-Corrosion-Fatigue Tests of 7079-T6 Cylinders and C-rings	70
Fig. 35 Fracture of 7079-T6 Cylinder No. 7 Resulting from Fatigue Crack Propagating from Outside Surface	71
Fig. 36 Fracture of 7075-T73 Cylinder No. 7 Resulting from Fatigue Crack Propagating from Inside Surface	72
Fig. 37 Failures of CH70-T7 Cylinders Resulting from Fatigue Cracks Propagating from Inside Surface	73
Fig. 38 Longitudinal Splitting of Cylinder in Corrosion-Fatigue Test	74
Fig. 39 Single Initiation Site in Fig. 38 at Higher Magnification	75
Fig. 40 Multiple Cracking Sites and Difference in Appearance of Slow and Fast-Fracture Regions Characteristic of 2014-T6 and 7075-T6 Cylinders in Corrosion-Fatigue Test	75
Fig. 41 Multiple Auxiliary Cracks Adjacent to Main Fracture in 7075-T6 Corrosion-Fatigue Specimen	76
Fig. 42 Multiple Auxiliary Cracks Adjacent to Main Fracture in 2014-T6 Corrosion-Fatigue Specimen	76
Fig. 43 Intergranular and Interfragmentary Path of One of the Auxiliary Cracks in 2014-T6 Cylinder in Corrosion-Fatigue Test	77
Fig. 44 Intergranular and Interfragmentary Path of Auxiliary Crack in 7075-T6 Cylinder from Corrosion-Fatigue Test	77
Fig. 45 Intergranular and Interfragmentary Path of Auxiliary Crack in 7075-T6 Cylinder from Stress-Corrosion Test	78

LIST OF ILLUSTRATIONS (continued)

		<u>Page</u>
Fig. 46	Cross Sections of Auxiliary Cracks in Cylinders from Rod Exposed to Corrosion-Fatigue Test	79
Fig. 47	Scanning Electron Micrograph (SEM) of Fracture Surface in Slow-Fracture Region of 7079-T6 Cylinder in Corrosion-Fatigue Test	80
Fig. 48	SEM of Fracture Surface in Slow-Fracture Region of 2014-T6 Cylinder in Corrosion-Fatigue Test	80
Fig. 49	SEM of Fracture Surface in Slow-Fracture Region of 7075-T6 Cylinder in Corrosion-Fatigue Test	81
Fig. 50	SEM of Fracture Surface in Slow-Fracture Region of 7075-T6 Cylinder in Stress-Corrosion Test	81
Fig. 51	SEM of Slow-Fracture Surface of Cylinder from X7080-T7 Forging in Corrosion-Fatigue Test	82
Fig. 52	Transmission Electron Micrograph Typical of Fracture Appearance in Slow-Fracture Region of 7079-T6, 7075-T6 and 2014-T6 Cylinder in Corrosion-Fatigue Test	83
Fig. 53	TEM Showing Dimpled Rupture Characteristic of Tensile Failure in Fast-Fracture Region of Cylinders in Corrosion-Fatigue Test	84
Fig. 54	TEM Showing Striations Typical of Fatigue Failure in Slow Fracture Region of Cylinders in Corrosion-Fatigue Test	85
Fig. 55	TEM Showing Faceted Appearance of Slow-Fracture Region of 7075-T6 Cylinder in Stress-Corrosion Test	86
Fig. 56	Granular Appearance of Fracture and Intergranular Path of Auxiliary Crack in 2014-T6 Cylinder	87
Fig. 57	Granular Appearance at Origin and Adjoining Ray Pattern	88
Fig. 58	Granular Appearance at Origin	88

LIST OF ILLUSTRATIONS (continued)

		<u>Page</u>
Fig. 59	SEM of Fracture of C-Ring from 2014-T6 Forging Exposed in Corrosion Fatigue Test	89
Fig. 60	SEM Typical of C-Rings from 7079-T6, 70 1-T6 and X7080-T7 Forgings Exposed to Corrosion-Fatigue Test	90
Fig. 61	Cross Sections of Auxiliary Cracks in C-Rings Indicating Mixed Fracture Mode	91
Fig. 62	SEM Showing Appearance Typical of Fractures Having Inside Origin in Cylinder Subjected to Fatigue in Laboratory Air	92
Fig. 63	SEM Showing Appearance of Fracture Having Outside Origin in Cylinder Subjected to Fatigue in Laboratory Air	93
Fig. 64	Fracture Appearance as Affected by Cycle Rate	94
Fig. 65	SEM of Fracture Surface of Cylinder from 2014-T6 Rod Having Long Life in Corrosion-Fatigue Test	95

# LIST OF TABLES

		<u>Page</u>
Table I.	Tensile Properties of Materials	96
Table II.	Results of Tear Tests	97
Table III.	Results of Plane-Strain Fracture-Toughness Tests of Notch-Bend Specimens	98
Table IV.	Results of Plane-Strain Fracture Toughness Tests of Compact Tension Specimens	99
Table V.	Summary of Plane-Strain Fracture Toughness Data	100
Table VI.	Cylinder Dimensions and Calculated Hoop Tensions for 8000 psi Test Pressure	101
Table VI..	Results of Axial Stress Fatigue Tests	102
Table VIII.	Results of Fatigue Tests of Hydraulic Cylinders - Alloy 7075-T6	103
Table IX.	Results of Fatigue Tests of Hydraulic Cylinders - Alloy 7079-T6	104
Table X.	Results of Fatigue Tests of Hydraulic Cylinders - Alloy X7080-T7	105
Table XI.	Results of Fatigue Tests of Hydraulic Cylinders - Alloy 2014-T6	106
Table XII.	Results of Fatigue Tests of Hydraulic Cylinders - Alloy 7075-T73	107
Table XIII.	Results of Fatigue Tests of Hydraulic Cylinders - Alloy CH70-T7	108
Table XIV.	Summary of Fatigue Test Results of Hydraulic Cylinders Under Hoop Tensions Equal to 80% of Design Stresses	109
Table XV.	Summary of Fatigue Test Results of Hydraulic Cylinders Under Hoop Tensions Equal to 50% of Design Stresses	110

LIST OF TABLES (continued)

		<u>PAGE</u>
Table XVI.	Results of Fatigue Tests of C-Rings - Alloy 7075-T6	111
Table XVII.	Results of Fatigue Tests of C-Rings - Alloy 7079-T6	112
Table XVIII.	Results of Fatigue Tests of C-Rings - Alloy X7080-T7	113
Table XIX.	Results of Fatigue Tests of C-Rings - Alloy 2014-T6	114
Table XX.	Results of Fatigue Tests of C-Rings - Alloy 7075-T73	115
Table XXI.	Results of Fatigue Tests of C-Rings - Alloy CH70-T7	116
Table XXII.	Results of Stress-Corrosion Tests on Static-Loaded C-Rings Exposed for 84 Days to Alternate-Immersion Test in 3.5% NaCl Solution	117
Table XXIII.	Results of Stress-Corrosion Tests on Static-Loaded C-Rings Exposed in Laboratory to Simulated Seacoast Environment	118
Table XXIV.	Results of Stress-Corrosion Tests on Static-Loaded C-Rings Exposed to Seacoast Atmosphere at Point Judith, R. I.	119
Table XXV.	Summary of Flexural Fatigue Test Results of C-Rings Stressed to 80% of Design Stresses	120
Table XXVI.	Summary of Flexural Fatigue Test Results of C-Rings Stressed to 50% of Design Stresses	121
Table XXVII.	Comparison of Specimen Lives in Corrosion-Fatigue and Various Types of Static Stress-Corrosion Test	122
Table XXVIII.	Results of Fatigue Tests of Hydraulic Cylinders in Noncorrosive Environment	123
Table XXIX.	Fracture-Mechanics Analysis of Fatigue Failures in Hydraulic Cylinders	124

STRESS-CORROSION AND CORROSION-FATIGUE  
SUSCEPTIBILITY OF HIGH STRENGTH  
ALUMINUM ALLOYS

SECTION I

INTRODUCTION

Forged aluminum cylinders used for landing gear, stabilizers and other aircraft systems are exposed to various combinations of cyclic loading in corrosive environments. Although these components have performed well in most applications, some parts have suffered fatigue or stress-corrosion failures. Such failures have focused attention on the need for a better understanding of the interaction of corrosion and fatigue. Corrosion-fatigue tests conducted at normal machine speeds of 120 to 10,000 cpm do not allow sufficient time for the corrosion or stress-corrosion action which may occur in less severe service environments. The possible interaction of corrosion and fatigue complicates the problem.

The Air Force Materials Laboratory, in an effort to establish a better basis for selecting aluminum alloys for hydraulic cylinders and other aircraft structural components, sponsored this research program to study the combined effects of stress-corrosion and corrosion-fatigue under appropriate loading rates and exposure conditions. Two types of test were made: (1) fatigue tests of cylinders under internal pressure in which alloy, temper, method of fabrication, stress, external environment and frequency were variables, and (2) tests of coupons taken from cylinder blanks. The latter include corrosion-fatigue tests and stress-corrosion tests of C-rings, corrosion-fatigue tests of axial-stress specimens and tensile, tear and fracture-toughness tests.

## SECTION II

### SUMMARY

The corrosion-fatigue and stress-corrosion performance of several high strength aluminum alloys was investigated by tests of hydraulic cylinders, C-rings and axial-stress fatigue specimens. Specimens were prepared from forgings and forging stock of alloys 2014-T6, 7075-T6, 7075-T73, 7079-T76, and X7080-T7 and also from premium cast alloy CH70-T7. The primary purpose was to evaluate these alloys and fabrication processes by tests of cylinders subjected to cyclic internal pressure in a corrosive environment. A secondary objective was to determine the extent to which conventional stress-corrosion and corrosion-fatigue tests of the same materials would have predicted the "stress-corrosion-fatigue" susceptibility of the cylinders.

Frequencies of loading for the corrosion-fatigue tests of the cylinders and C-rings were in the range of 0.15 to 10 cpm. The load cycle included a hold-time at maximum load to allow time for stress corrosion to occur. These tests can be regarded as stress-corrosion tests in which the stress was periodically removed. The corrosive environment was provided by subjecting the specimens to a warm salt fog at 12-hr intervals.

In general, the investigation demonstrated that stress-corrosion cracking may occur under cyclic loading, especially at low frequencies, and that stress-corrosion and fatigue can interact under certain conditions to produce failures in shorter times and fewer cycles than for either phenomenon occurring by itself.

Overall, alloy 7075-T73 gave the best performance. Stress-corrosion cracking did not occur in any 7075-T73 specimens in the various types of tests, and cylinders of this alloy subjected to repeated loading to 80% of design stress in a corrosive environment lasted 10 times as long as any forged cylinders of 2014-T6, 7075-T6, or 7079-T6. The three latter alloys developed stress-corrosion cracks in these tests. The premium cast CH70-T7 specimens also did not exhibit any stress-corrosion cracking. In only one test did stress-corrosion cracking occur in X7080-T7 specimens.



Electron microscopic examination indicated failures to be either pure stress corrosion, pure fatigue, one followed by the other, or mixtures of the two, depending on the alloy and temper, stress level, rate of cycling, and conditions of exposure. Mixed mode failures generally started from stress-corrosion origins; apparently these cracks propagated by stress corrosion where the grains were favorably oriented and by fatigue where they were not.

In tests in laboratory air the lowest fatigue strengths were those of the cast CH70-T7 cylinders; however, at the higher stress levels in the corrosion-fatigue tests, the lives of the cast cylinders were longer than those of the wrought specimens which failed by stress corrosion. For alloy 7075-T73 and X7080-T7 cylinders tested to 80% of design stress, the fatigue lives were reduced by half as a result of introducing a hold time in the fatigue cycle.

The majority of the fatigue and stress-corrosion failures of the forged cylinders occurred in the region of a parting plane. However, the rolled rod stock, which does not contain a parting plane, was only slightly more resistant to corrosion-fatigue cracking than were the die forgings.

The static stress-corrosion tests of C-rings ranked the alloys in the same high-low resistance categories as did the stress-corrosion-fatigue tests of cylinders; but, of course, they could not predict the fatigue performance of the alloys. Neither corrosion-fatigue tests of axial-stress specimens nor corrosion-fatigue tests of C-rings in the same environments as the cylinders gave results which would have predicted the performance of the cylinders. Recommendations are made for improving the C-ring corrosion-fatigue tests.

The crack sizes (fatigue or stress-corrosion cracks) which were associated with unstable fractures of the cylinders correlated well with the critical sizes predicted from fracture-toughness tests.

## SECTION III

### MATERIALS

#### 1. Production

a. Rolled rod forging stock, 4-1/2-in. diameter, in alloys 7075, 7079, X7080 and 2014. This stock was produced at Alcoa's Massena Works from 12 x 12-in. or 14 x 14-in. cast ingot. Processing was standard but extra ultrasonic inspection and metallurgical surveillance was practiced. All of the bloom stock met contact ultrasonic inspection standards, in addition 35% of the 4-1/2-in. diameter stock was inspected to Class A, ASNT standards. No discontinuities were detected.

b. Die forgings made at Alcoa's Cleveland Works from a portion of the 4-1/2-in. diameter stock described above. The shape selected (Fig. 1a) is a commercial die forging, normally made from 4-1/2-in. diameter stock. Its dimensions are such that the desired cylinder blanks (Fig. 1b) could be obtained with a minimum removal of parting-plane structure. The die forgings were ultrasonically inspected at Cleveland and found to meet standards for aircraft forgings.

c. Premium strength cast cylinder blanks (Fig. 1b) of alloy CH70, an alloy similar to K01 and X201.0. These were made and heat treated at Alcoa's Cleveland Research Foundry.

The die forgings and rolled forging stock were machined to cylinder blanks, 2.3 in. I.D. by 4.08 in. O.D. by 18-in. (Fig. 1b) at Alcoa's New Kensington Works. These were heat treated and aged at the Alcoa Research Laboratories to the specified tempers in accordance with recommended practices.

#### 2. Tensile, Tear and Fracture Properties

Longitudinal and transverse tensile, tear and fracture toughness specimens were taken from cylinder blanks; the transverse specimens were taken both across and 90° from the parting line. The tensile and fracture toughness specimens were prepared and tested in accordance with ASTM Standard Methods E8<sup>1</sup> and E399<sup>2</sup>, respectively. The tear specimens were tested as described in reference 3. The tear and fracture toughness specimens are shown in Figs. 2 - 4.

---

\*Numbers refer to references at end of report.

Table I lists the results of the tensile-property survey made on the test materials. All alloys and products met the minimum property levels.

The most significant criteria of toughness from the tear (Table II) and fracture-toughness (Tables III and IV for notch-bend and compact tension specimens, respectively) tests are the ratios of tear strength to tensile yield strength, the unit propagation energies, and the critical plane-strain stress-intensity factors,  $K_{Ic}$ . Clear comparisons of the various alloys, tempers and products on the basis of some of these parameters are made difficult by two factors: First, many of the tear specimens taken from the longitudinal direction did not crack straight across the specimen (see Fig. 5), so that useful values of the unit propagation energies were not obtained in these cases. Second, because of the limitations imposed on the thickness and fatigue cracking of the fracture-toughness specimens, many of the values of  $K_Q$  obtained were not technically valid values of  $K_{Ic}$ . Candidate values of  $K_{Ic}$  are designated  $K_C$ , in accordance with ASTM standard methods, and their validity checked before they are designated to be equal to  $K_{Ic}$ .

However, broad comparisons among the various alloys, tempers and products can still be made by utilizing all the data together, and recognizing that some of the fracture toughness data, though not technically valid, provide a reasonable estimate of the true  $K_{Ic}$ . In the latter regard, those data from specimens which: (a) were fatigue cracked at stress intensities slightly higher than the present limit, i.e., at  $K_Q$  between 60 and 75% of  $K_{Ic}$ ; or (b) contained a crack slightly longer than the present limit were considered to be meaningful values of  $K_{Ic}$ , and are so designated in the tables. These values were considered together with the entirely valid data in appraising the toughness of the materials. For those tests from which the data were clearly invalid, it was considered that it was probable (though not certain) that the true value of  $K_{Ic}$  was higher than the calculated  $K_Q$ . The summary listing of  $K_{Ic}$  values in Table V was developed upon these bases, and was used along with the tear test data in developing general ratings of the toughness of various alloys and products.

Of the materials tested the 7075-T73 and X7080-T7 samples, particularly the lower strength rolled rod samples, had the highest toughness of the group. There was not much difference, however, between the toughness of the die forgings of these materials (which had relatively high tensile yield strengths) and the toughness of the 7075-T6 and 7079-T6 samples,

particularly in the transverse direction. Alloy 2014-T6 rated lowest in all test directions for both rolled rod and die forgings. The cast CH70-T7 samples showed less directionality than the other materials. In the longitudinal direction, alloy CH70-T7 rated about on a par with alloy 7075-T6, but in the transverse direction it had higher toughness than any of the other samples.

With regard to test direction, all the wrought alloys had higher toughness in the longitudinal direction than in the transverse direction. For the die forgings, the toughness in the transverse direction across the parting plane was generally lower than that away from the parting plane (X7080-T7 was an apparent exception); the rolled rod thus has an advantage in not having this lower-toughness zone.

The specific use of some of the fracture-toughness data in analyzing the conditions under which fracture took place at the conclusion of the fatigue tests is presented in Section VI-9.

## SECTION IV

### SPECIMENS

#### 1. Preparation

The investigation was concerned primarily with tests of two types of specimens taken from the 18-in. long cylinder blanks: (1) cylinders of the dimensions shown in Fig. 6, and (2) C-rings of comparable test section dimensions as shown in Fig. 7. The dimensions of the die forged and cast cylinders, shown in Fig. 6 and Table VI, were proportioned so that an internal pressure of 8000 psi would produce maximum stresses equal to 80% of the allowable design stresses, which are defined as being  $2/3$  of the minimum transverse tensile strengths. The cylinders from rolled stock were made to the same dimensions as those from the forgings of the same alloy.

All machined cylinders were subjected to ultrasonic inspection and met the requirements for Class A - ASNT Standards for wrought aluminum products. Inspections by fluorescent penetrants did not show any significant surface defects.

A C-ring specimen (Fig. 7) for corrosion-fatigue tests was cut from the end of each blank from which a cylinder was machined. The same specimen number was used for the two types of specimens from a blank. Similar specimens for stress-corrosion tests were cut from other cylinder blanks. In the case of the die forgings, the C-rings were oriented so that the parting plane coincided with the section of maximum bending.

#### 2. Residual Quenching Stresses

Residual stresses were investigated in cylinders of 7075-T73, 7075-T6 and X7080-T7, whose quench water temperatures were approximately 70F, 150F and 212F, respectively. Three bonded resistance strain gages, each having elements in the circumferential and axial directions, were located 120 deg. apart around the circumference of each specimen. A 3-in. length of cylinder, containing the gages at midlength, was isolated from the specimen. This section was bored out in stages and the relaxed strains at the outer surface measured after each removal. The corresponding residual stresses were determined by the Sach's boring-out method<sup>4</sup>.

Figure 8 shows the distribution of circumferential and axial residual stress determined for the three specimens. As expected, the lower the temperature of the quench water, the higher the residual stresses. The stress gradients, all varying from tension in the interior to compression on the exterior, indicate that the bore surface was quenched less rapidly than the exterior. Residual stresses of these magnitudes (circumferential stresses of 1-4 ksi tension on the inside and 1-4 ksi compression on the outside) should have only a minor effect on fatigue performance.

## SECTION V

### PROCEDURES

#### 1. Axial-Stress Fatigue and Corrosion-Fatigue Tests

A common short-time method of evaluating relations between fatigue and corrosion is to determine conventional S-N curves, without corrosion, and then to repeat the fatigue tests in a corrosive environment. Specimens for these tests, shown in Fig. 9, were of such a size as to be limited to the longitudinal direction of the cylinder blanks. The fatigue tests were made in ambient air. In the corrosion-fatigue tests the specimens were continuously immersed in an acidic (pH 0.8) salt-dichromate solution containing 30 g/l potassium dichromate, 36 g/l chromic acid, and 3 g/l sodium chloride. This electrolyte was selected because it causes rapid intergranular attack of alloys or tempers susceptible to this form of corrosion without causing appreciable general surface corrosion. The 5 kip Krouse fatigue testing machines utilized for these tests operate at a speed of 1100 cpm.

#### 2. Cylinder Fatigue Tests

New equipment and procedures were designed for the cylinder corrosion-fatigue tests. The cylinders were closed at the ends with threaded aluminum caps fitted with O-ring seals. As is indicated in Fig. 10 they were enclosed in chambers so that the exterior surfaces were in a controlled atmospheric environment, with or without the addition of corrosive media. The test chambers were mounted on racks as shown in Figs. 11 and 12. Provision was made in the racks for 39 specimens.

Internal hydraulic pressure was provided by an MTS closed-loop, electro-hydraulic loading system coupled to a 10,000 psi capacity pressure intensifier. The pressure fluid was oil with a corrosion inhibitor added (MIL Spec. 052-600-0605). Pressures in the system were monitored by a fluid pressure transducer in the line supplying the specimens. The pressurization system shut down by the loss of oil when a specimen failed.

In order to check the reliability of the cylinder-fatigue-test procedure, a static pressure-strain survey was made

on one specimen. The results, Fig. 13, showed good agreement between measured and calculated hoop tensions at the center of the cylinder over the full 8000 psi range of test pressures. Both circumferential and longitudinal stresses at the end of the cylindrical test section were greater than calculated, indicating a small stress concentration.

The fluctuating pressures for the fatigue tests are controlled by a calibrated pressure cell located at the intensifier. For the sinusoidal loadings the pressures were applied at the maximum rate at which good correlation could be maintained between the measured stresses in a cylinder located near the end of the line, the pressure cell reading at the end of the line and the pressure cell at the intensifier.

The volume of each cylinder was about 78 cu in. Sixty cubic inches of this were taken up by a piece of aluminum rod, 2-1/4 in. diameter by 15-1/2 in. long, placed in the cylinder cavity. This was done to reduce the required volume of hydraulic fluid.

Air, at a humidity controlled generally to 50  $\pm$  5%, was circulated through the test chambers; control was accomplished using an Aminco Unit. It was desired to control metal temperatures to 85F to ensure condensation of the salt fog. However, cylinder temperatures were influenced by room temperature and speed of pressurizing, so that the metal temperature varied from 85 to 110F. Temperature variation in this range was believed not to have a major effect on the test results.

#### a. Simulated Seacoast Environment

The simulated seacoast environment was provided by fogging the test chambers at 12-hour intervals with a warm salt fog. For one minute the test chambers were sprayed with a 115F solution of 5% sodium chloride (NaCl) in deionized water buffered to a pH range of 4-5. Air valves on the inlets closed the chambers off during the salt fog and during a subsequent seven-minute period of draining and purging. For the remainder of the 12-hour period, conditioned air, at a humidity of 50  $\pm$  5%, was circulated through the chamber.

#### b. Loading of Cylinders Tested in Simulated Seacoast Environment

To allow time for corrosive action to occur, the pressures in the simulated seacoast environment were cycled at a frequency



such that, for most all  $\sigma$ , it would require six months or more to accumulate the number of loadings which produced fatigue failure in the tests in laboratory air. The pressure was held at maximum for 80% of the period and then cycled, using a sine type curve, to minimum and back to maximum. For example, the hold time was 5.4 minutes per cycle for the tests to 80% of design stress. These tests could also be considered to be interrupted stress-corrosion tests.

### 3. Cylinder Stress-Corrosion Tests

A limited investigation was made of the stress-corrosion cracking characteristics of cylinders under constant internal pressure. Duplicate specimens of 7075-T6 and 7075-T73 were placed in test chambers at the same time as the corrosion-fatigue tests, but the hydraulic pressure was held constant at 8000 psi by means of check valves.

### 4. C-Ring Fatigue Tests

Figures 14 and 15 show the apparatus developed to conduct these tests. Provision was made for testing 36 specimens at one time. The rings were loaded to produce maximum tensile stresses on the inside surface equal to the interior hoop tensions applied to the cylinders. Bending stress-deflection relations were determined for typical C-rings and these were used as a basis for the machine loadings.

The moving parts of the mechanism are actuated by small automobile brake cylinders. Oil pressure moves each piston and the attached yokes as far as the preset stops will permit. In this way C-rings, attached to the moving yoke, are strained to the desired level. A small preload is maintained on the C-ring by a spring and when a ring cracks the resulting drop in preload trips a timer, indicating the time to failure.

Figure 16 shows relations between C-ring deflection and bending stresses on the section of maximum moment. The interesting point to be noted is that the circumferential tension at midwidth is 15 to 20% higher than at the edges of the specimen. Although not indicated in the figure, the stress distribution is reversed on the outside surface of the C-ring, with the edge stresses being higher. This situation, not covered by the usual stress and deflection formulas, results from restraint of transverse bow. Since the average measured bending stresses in Fig. 16 are in fair agreement with calculated values for a given ring deflection, this relationship was adopted for loading the C-rings for all flexural fatigue and stress-corrosion tests. This means

that the midwidth stresses were higher, and the edge stresses slightly lower, than the computed stresses.

The tests in conditioned air, without salt-fog injections, were made as rapidly as equipment permitted. Under corrosive conditions, however, the cycle times were increased by the use of hold times as in the cylinder tests.

The C-ring tests differed from the cylinder tests in three important respects: (1) The test surface of the C-ring was 1/4 in. from the original forged surface while that of the cylinder was about 1/2 in. from this surface; consequently, the C-ring had a more pronounced parting plane structure; (2) The C-rings were stressed by constant deformation and the cylinders were stressed by constant load (pressure); thus, in the C-ring test the load tends to relax as cracks propagate through the thickness, resulting in longer lives; and (3) In the cylinder tests, the simulated seacoast environment was fairly uniform in the various test chambers; however, in the C-ring tests the concentration of salt deposits varied along the length of the chamber, and was fairly light on specimens remote from the nozzles. This latter behavior probably accounted for some of the scatter in C-ring test results, since triplicate C-ring specimens from a given alloy and product were positioned at different locations relative to the nozzle.

## 5. C-Ring Stress-Corrosion Tests

Because the C-ring is a standard stress-corrosion test specimen appropriate for cylinder parts, tests of this type were made on all alloys and products. The purpose of these tests was to establish the stress-corrosion resistance of the test materials and to investigate possible correlations between stress-corrosion and corrosion-fatigue behavior. The C-rings were of the same size as used in the fatigue tests. They were stressed statically by means of threaded studs located on the C-ring diameter. Expansion of the diameter induced tensile stresses on the inner surface, as in the corrosion-fatigue tests. C-rings were stressed to 80, 55, and 30% of the design stresses for the different alloys.

The following exposures were used in the C-ring stress-corrosion tests:

1. Simulated seacoast environment as described in Section V.2.a. The lower two chambers on the rack of the C-ring fatigue apparatus shown in Fig. 15 were used for this purpose.

2. Seacoast atmosphere at Alcoa's exposure station at Point Judith, Rhode Island. The Point Judith facilities, facing south into the Atlantic Ocean, are located 300 feet from the water's edge on a rocky beach, a few feet above sea level. Specimens face the ocean but are tilted 45° upward. The specimens are inspected periodically for failures.

3. Alternate immersion in a 3.5% NaCl solution, which is the most widely used test for many aluminum alloys and therefore established a common reference datum. These tests employed a 3.5% by weight NaCl solution made from reagent grade salt and distilled water. The salt concentration was maintained by frequent additions of water to compensate for loss of water by evaporation. The pH was maintained within a range of 6.7 to 7.4.

The alternate-immersion cycle consisted of total immersion of the specimens for 10 minutes each hour. For the remaining 50 minutes per hour the specimens air dried at 75 to 80F and 45 to 50% relative humidity. The specimens were tested for the standard exposure period of 84 days. They were inspected daily for failure.

## SECTION VI

### TEST RESULTS

#### 1. Fatigue and Corrosion-Fatigue Tests of Axial-Stress Specimens

The results of the fatigue tests of 1/8-in. thick, longitudinal, axial-stress specimens are presented in Table VII and Figs. 17 to 22. For reference, a scatter band reported for axial-stress fatigue tests<sup>5</sup> of round specimens for the strongest alloy, 7075-T6, is shown on each plot. Also, the average S-N curve from Fig. 17 for 7075-T6 specimens tested in the acidic salt-dichromate solution is shown on the plots for the other alloys. For each of the wrought alloys the results for the specimens tested in air tend to cluster about the lower bound of the scatter band. This is reasonable since it is common for rectangular specimens to give lower results than round specimens in the range of  $10^5$  to  $10^6$  cycles. The results for the rolled rod and forged specimens of the five alloys are equivalent. For lives beyond  $10^5$  cycles the fatigue strengths of the cast CH70-T7 specimens are half or less than the strengths of the wrought products.

Testing these specimens in the acidic salt-dichromate solution dropped the fatigue strength of the wrought products by 50% or more. In this medium there is little difference between the results for the sand castings and the wrought materials. However, there does appear to be some advantage for alloys 7079-T6 and X7080-T7.

#### 2. Fatigue Tests of Cylinders in Air

The results of the fatigue tests of cylinders tested in laboratory atmosphere with controlled humidity are listed in Tables VIII to XIII and plotted in Fig. 23. Clearly, the cast cylinders had the lowest fatigue strengths. There is substantial overlap of the lives obtained for the wrought cylinders stressed to 80% of design stress, but alloys 2014-T6 and 7075-T73 showed some advantage.

The maximum test pressure in the wrought cylinders which did not fail in six million cycles to 3,000 psi (30% of design stress) was increased to 5,000 psi; and for those cylinders which did not fail in eight million cycles to that pressure, the pressure was increased to 6,500 psi. To determine if the prior stressing affected the life, one of the 7075-T6 and one of the 7075-T73 cylinders, having such a history, were tested to failure

at 8,000 psi. The lives of these specimens were greater than those of virgin specimens of these alloys tested at 8,000 psi. Obviously, the prior life was not detrimental. For the lower test pressures alloy 7079-T6 had the shortest lives and 7075-T73 the longest.

If the above comparisons were made on the basis of maximum net stress, as on a normal stress-cycle plot, the evaluation would be altered somewhat. Because the sand cast specimens were the lowest stressed, the advantage of the wrought products would be greater. The advantage of alloy 7075-T73 would be reduced since it was the lowest stressed of the wrought alloys.

### 3. Static Stress-Corrosion Tests of Cylinders

The two 7075-T6 cylinders subjected to hydrostatic pressures of 8,000 psi (80% of design) failed by stress corrosion after 7 and 8 days' exposure to the simulated seacoast environment. One of these failures is pictured in Fig. 24a. Neither of the 7075-T73 cylinders failed in 15 months. Thus, these tests confirm that alloy 7075-T73 is highly resistant to stress corrosion.

### 4. Stress-Corrosion-Fatigue Tests of Cylinders in Simulated Seacoast Environment

As is listed in Tables VIII to XIII, both stress-corrosion and fatigue failures occurred in the cylinders subjected to repeated loading in the simulated seacoast environment. The lives for the various alloys are compared in Tables XIV and XV and in Fig. 25. For alloys 7079-T6, 2014-T6 and 7075-T6, failures occurred by stress-corrosion cracking at a pressure of 8,000 psi after fewer than 1/10 as many loadings as required to cause fatigue failures in the tests in air. Thus, their lives were much shorter than those of alloys 7075-T73, X7080-T7 and CH70-T7 which failed by fatigue. The longest lives were for alloy 7075-T73.

The fatigue lives of the 7075-T73 and X7080-T7 cylinders pressurized to 80% of design stress in the simulated seacoast environment are about half the lives of specimens tested in air. Because the failures of these specimens initiated on the inside surface, the difference is obviously not a result of the salt spray. Apparently, it is a result of the 5.4 min. hold time in the load cycle. The fact that the one 7075-T73 cylinder pressurized along with those being sprayed, but not itself sprayed, had a life only slightly longer than those being sprayed adds credence to this conclusion. The hold times did not reduce the lives of the cast cylinders. Many of the specimens subjected to the hold time at

80% of design stress had multiple fatigue origins, whereas only a single origin was visible in the fracture surfaces of the wrought specimens subjected to the uninterrupted sinusoidal loadings.

Two of the 7075-T6 forged cylinders pressurized to 50% of design stress failed at a life less than 1% of that at which the sinusoidal tests were stopped without any failure of the 7075 specimens. The lives of most of the X7080-T7 cylinders were also surprisingly short. Because the failures of these short-lived specimens initiated on an inside surface, the short lives must be a result of the load cycle rather than corrosion. However, stress-corrosion cracking did occur in all three cylinders from 2014-T6 forgings and in two of the 7079-T6 cylinders from rolled rod. At the longer lives, most of the fatigue failures initiated externally at corrosion pits. Four of six 7075-T73 cylinders survived 1,000,000 or more pressurizations to this stress level; only one other specimen, a 2014-T6 cylinder of rolled rod stock, survived this many loadings.

Overall, the best cylinder performance in the corrosion-fatigue, as well as air-fatigue tests, was obtained with alloy 7075-T73. Second rating should probably go to alloy X7080-T7 because it was more resistant to stress-corrosion than alloys 2014-T6, 7075-T6 and 7079-T6. The cast alloy would rate ahead of alloys 7079-T6 and 7075-T6 in the corrosion-fatigue tests.

The parting plane of the forgings was a common location of failure of the cylinders. Eighteen of 29 failures of the forged specimens tested in laboratory air initiated in a parting plane. For the forgings tested in the simulated seacoast environment, the corrosion fatigue or stress-corrosion origins were usually in a parting plane. Some of the specimens had many stress-corrosion cracks in the region of the parting plane. However, the rolled rod stock, which does not contain a parting plane, was only slightly more resistant to stress-corrosion cracking than were the die forgings.

## 5. Fatigue Tests of C-Rings in Air

The results of the C-ring tests in laboratory air (50 +5% humidity) are listed in Tables XVI to XXI and plotted in Fig. 26. As for the cylinders, the CH70-T7 rings were the only ones to fail at a stress of 30% of design stress; however, at 80% of design stress the cast C-rings had lives as long as most of the wrought specimens. Generally, the results of the C-rings do not correspond very well with those of the cylinders. Typically the lives of the C-rings were on the order of ten times those of the cylinders though this ratio varied substantially for different alloys. The X7080-T7 C-rings stressed to 80% of design stress had extraordinarily long lives. However, shorter

lives were obtained at a stress of 65% of design stress for two specimens which had previously been stressed to 30 and 50% of design stress. An X7080-T7 specimen subjected to the same lower stresses had a short life when stressed to 80% of design stress. The life of a 7075-T73 specimen having a similar load history was within the wide scatter of specimens stressed only to 80% of design stress.

At stresses of 65% of design stress the large scatter in the lives for 7079-T6 and X7080-T7 rings encompasses the relatively short lives of alloy 2014-T6 and the longer lives of alloy 7075-T73.

#### 6. C-Ring Stress-Corrosion Tests

The results of the stress-corrosion tests of static-loaded C-rings are given in Tables XXII to XXIV. A comparison of the stress levels resulting in failures is made in Fig. 27 for the die forgings and the casting and in Fig. 28 for the rolled rod stock.

Because the C-ring specimens were stressed in bending to a constant deflection, it was possible that the occurrence of many tiny cracks would cause sufficient stress relaxation to prevent obvious, visible cracking. Consequently, specimens that did not show visible cracks were examined metallographically to determine whether or not they contained minute cracks. Examples where metallographic examination revealed minute stress-corrosion cracks are shown in Figs. 29 - 31.

These tests are significant from two aspects:

(1) they establish the resistance to stress-corrosion cracking of the actual lots of material involved in the contract; and

(2) they put the special environment developed for the corrosion-fatigue tests in perspective with an actual seacoast exposure and with a well known accelerated test medium.

##### a. Stress-Corrosion Resistance of Contract Materials

The results obtained in all three environments are in good agreement with prior experience on the products and alloys involved.

Perhaps the obvious observation is that, for susceptible alloys and tempers, the short-transverse grain structure in the parting plane of die forgings is more critical than is the less directional, transverse grain structure in the rolled rod. This is indicated to some extent by failure times in alternate immersion (Table XXII) but is more apparent from the levels of stress causing failures in the other two environments (compare Figs. 27 and 28).

As expected, alloys 7075-T73 and CH70-T7 were the most resistant to stress-corrosion cracking; even at the highest stress no failures occurred in any environment. The next most resistant alloy was X7080-T7 for which the only failures were die forged specimens at the 80% stress level (34.6 ksi) in the simulated seacoast environment (Fig. 27). It should be pointed out that the alternate immersion test is not the most discriminating stress-corrosion cracking test for alloy X7080 and that three to five years of atmospheric exposure are required to define susceptibility to stress-corrosion cracking with reasonable confidence.

The other three alloys, 2014-T6, 7075-T6 and 7079-T6, were susceptible at all stress levels in the alternate immersion test and at the high stresses in the other two environments. In the simulated and actual seacoast environments 2014-T6 was slightly more resistant than the other two alloys.

#### b. Simulated Seacoast Environment

The intent of the special acidic-salt spray environment was to simulate, under reproducible laboratory conditions, exposure to seacoast atmosphere, which is one of the most potent stress-corrosion cracking media of commonly encountered, natural environments. If successful, such a test medium has the advantage of: (a) permitting frequent inspection of the specimens; and (b) eliminating seasonal climatic variations.

The stress-corrosion cracking data on the static-loaded C-rings (Tables XXII to XXIV and Figs. 27 and 28) show good agreement between the stress levels at which failure occurred in the simulated and natural seacoast environments; both of these environments were somewhat less severe than alternate immersion. It was hoped that the simulated environment would be somewhat accelerated over the natural atmosphere. Unfortunately, the inspection periods at the Point Judith station were not frequent enough to provide a precise comparison. The ranges in failure times available, however, show appreciably quicker failures in the simulated environment only for the 7075-T6 and 7079-T6



die forged specimens at the 80 and 55% stress levels and the X7080-T7 and 2014-T6 die forgings at the 80% stress. For all other cases, either no failure has occurred or failure times are similar.

It was hoped that the stress-corrosion cracking failure times in the simulated environment would be such that there would be opportunity for both stress-corrosion and corrosion-fatigue mechanisms of failure to be operative at the particular loading cycles employed in the corrosion fatigue tests. However, because stress-corrosion cracking failure times vary with both applied stress and alloy, this objective cannot be attained without adjustment of the loading cycle for individual alloy and stress conditions.

As shown by Fig. 32, the depth and extent of general pitting attack in the simulated environment was similar to that in seacoast atmosphere. In both these media numerous shallow pits developed that resulted in a general roughened or "weathered" surface condition. In contrast, the alternate immersion test caused deeper and discrete sites of attack.

#### 7. Stress-Corrosion-Fatigue Tests of C-Rings in Simulated Seacoast Environment

The results of the fatigue tests of C-rings in the simulated seacoast environment are included in Tables XVI to XXI and summarized in Tables XXV and XXVI. Alloy 7079-T6 C-rings had the shortest lives at a stress of 80% of design stress. The lives of the other alloys overlapped, with the 7075-T73 specimens tending to have the longest lives. The lives of the CH70-T7 C-rings were longer than most of the C-rings from the forgings and rolled rods. Generally, the C-rings from the forgings had shorter lives than those of the rod. The fact that most of the failures occurred in the midwidth of the C-rings is consistent with the stress being higher there than at the edges.

The reduction in life was less for the C-rings stressed to 50% of design stress than for any of the other tests in the salt spray. This is probably due to the fact that the hold time (4.8 sec) was least for these tests. The lives of two of the forged 7075-T6 specimens were within the scatter of results for the specimens tested in laboratory air. The lives of the cast specimens were shorter than those of all but two wrought specimens. Alloys 7079-T6 and 7075-T6 would rate lowest of the wrought alloys in these tests.

## 8. Comparison of Stress-Corrosion Tests

Table XXVII compares the time to produce stress-corrosion failure in several types of tests. For the rolled rod specimens, and to a lesser degree for the forged specimens, the times required to produce failure in the corrosion-fatigue tests of C-rings were generally less than those of the statically loaded C-rings tested in the same environment.

Figure 33 is an interaction diagram, which compares the stress-corrosion, corrosion-fatigue, and fatigue results for the 7075-T6 and 7075-T73 cylinders pressurized to 80% of design stress. The points on the horizontal line are the results of fatigue tests in laboratory air, which were run at 20 cpm; the diagonal line is for the stress-corrosion-fatigue tests in the simulated seacoast environment, and the vertical line shows the results of static stress-corrosion tests in the simulated seacoast environment. The advantage of alloy 7075-T73 in the simulated seacoast environment is obvious. As was discussed previously, the 7075-T73 cylinders tested at 0.15 cpm failed from the interior surface so the reduction in life for these specimens was apparently a result of the hold time in the cycle.

Figure 34a shows a similar plot for the 7075-T6 C-rings and cylinders. The fatigue lives obtained for the cylinders and C-rings tested in laboratory air overlap but in the stress-corrosion tests the C-rings lasted several times as long as the cylinders. Surprisingly, the 7075-T6 C-rings tested at 1.5 cpm in corrosive environment did not suffer any reduction in fatigue life. More typical behavior is shown in Fig. 34b for 7079-T6 C-rings and cylinders.

As noted on Fig. 34a and 34b, a 7075-T6 C-ring and a 7079-T6 C-ring that were inspected after failure showed evidence of both stress-corrosion and fatigue, whereas the cylinders that were likewise inspected gave evidence only of stress corrosion. This difference is consistent with the different rates of loading used, as reflected by the location on the chart of the lines corresponding to the cylinder and C-ring tests. For a given time of exposure, the cylinders were not subjected to as many fatigue cycles.

There are other differences between the cylinder and C-ring test conditions which may account for the lack of correlation in the test results. For one thing, as mentioned previously, the cylinders were tested under constant load while

the C-ring test was a constant deformation-type test, so that the load (stress) relaxed as a crack propagated through the thickness. In addition, the state of stress was not the same in the two tests: in the cylinder the ratio of hoop to longitudinal stress was 2:1; while in the C-ring the hoop stress was about 6 times the transverse stress. Also, the entire periphery of the cylinder was stressed uniformly while only a small area of the C-ring was stressed to the maximum level. This is believed to be significant because salt buildup occurred predominantly on upward surfaces and the region of maximum stress in the C-rings was in the vertical plane. Finally, the salt buildup was not uniform in the C-ring test chambers. A modification of the C-ring equipment to provide more uniform wetting of the specimens would be desirable.

#### 9. Fracture-Mechanics Analysis of Cylinders

Of the 102 cylinders subjected to cyclic loading in various environments, complete fractures of the entire 8-in. length of test section were obtained in 71. In these a fatigue or stress-corrosion crack, or a combination of the two grew in size to the point where unstable crack growth resulted in fracture. Table XXVIII shows the shape and measured principal dimensions of the cracks in specimens tested in air. This type of data, together with the average hoop tensions producing failure and the average transverse values of  $K_{IC}$  from Table V, were used to analyze those fractures which took place by unstable crack growth.

The fracture-mechanics analysis was made using the procedures described in Ref. 6. The stress intensity at fracture,  $K_{If}$ , was calculated from the relationship

$$K_{If} = (1.1) \sqrt{\pi} \sigma \sqrt{a/Q} \quad (1)$$

where  $\sigma$  = average (through-the-thickness) gross-section circumferential stress in the cylinder wall at maximum pressure, ksi

$a$  = maximum depth of part-through crack at instability, in.

$$Q = \phi^2 - 0.212 \left( \frac{\sigma}{\sigma_{YS}} \right)^2$$

$\phi$  = complete elliptical integral of the second kind in which  $a/2c$  is the argument

$\sigma_{YS}$  = tensile yield strength, ksi

$2a$  = maximum length of part-through crack, in.

By assuming that  $K_{If}$  should be equal to the known value of  $K_{Ic}$ , the fracture conditions can be predicted for a particular crack size or operating stress, as either:

$$a/Q = \frac{1}{1.21\pi} \left( \frac{K_{Ic}}{\sigma} \right)^2, \text{ or} \quad (2)$$

$$\sigma = \frac{K_{Ic}}{(1.21\pi a/Q)^{1/2}} \quad (3)$$

The calculations were based on the assumption that the analysis of part-through cracks under plane-strain conditions was appropriate. It is recognized that the analysis is not strictly applicable in many cases because the depth of the crack exceeded one-half the wall thickness; where this occurred, the ligament between the crack tip and the opposite wall was probably too thin to maintain plane-strain conditions, hence, some type of mixed mode or plane-stress failure would be expected. Another simplification was the use of the average stress on the wall; it is recognized that the circumferential stresses were not uniform through the wall thickness and, in fact, stresses at the inner surface may have been as much as 30 per cent greater than those at the exterior surface. Finally, no correction factors were applied to compensate for other geometrical effects (i.e., bending curvature, or multiple cracks). These simplifications are controversial to some extent, so the raw data for the wrought alloys are included in Table XXIX.

The results of the analyses are shown in Table XXIX. In general, the values of stress intensity at fracture,  $K_{If}$ , agreed reasonably well with the  $K_{Ic}$  values, independent of the nature of the cracks. Average  $K_{If}$  values ranged from 14 per cent below to 14 per cent above the  $K_{Ic}$  values, with individual values from 28 per cent below to 31 per cent above  $K_{Ic}$ . While the  $K_{If}$  values were about evenly split above and below the  $K_{Ic}$  values, there was a trend for the  $K_{If}$  value to be below  $K_{Ic}$  when the cyclic stress was relatively low, and above  $K_{Ic}$  when the cyclic stress was relatively high.

Overall, these computations indicate that the fracture-mechanics analysis does a fair job of analyzing the conditions under which fractures developed in these cylinders, particularly when one considers that prior to the advent of fracture mechanics there was no analytical way to make such calculations. The differences observed may be related as much to problems in measuring  $K_{Ic}$  accurately, as to shortcomings of the analysis.

An additional point to be made is the fact that no unstable fractures developed for CH70-T7, the alloy with the highest indicated transverse fracture toughness ( $K_{Ic} = 33 \text{ ksi}\sqrt{\text{in.}}$ ); instead failures were by leakage from through cracks. The computed stress intensities,  $K_I$ , for some of these cracks were about  $30 \text{ ksi}\sqrt{\text{in.}}$ . Thus the fact that no unstable fractures developed is further support for the usefulness of  $K_{Ic}$  to judge whether fracture would be expected by leakage or unstable fracture.

## 10. Metallographic Examinations

Metallographic examinations of selected samples were made: (1) to determine the type of failure; (2) to characterize the various fracture modes; and (3) to determine the degree of interaction between fatigue and corrosion as represented by the features of fracture surfaces. This work involved visual examination, light microscope examinations of sections polished and etched by conventional procedures, transmission electron microscope (TEM) examinations using the standard oxide replica technique, and direct examination of fracture surfaces with the scanning electron microscope (SEM). Examinations were concerned primarily with cylinder and C-ring specimens exposed to the simulated seacoast environment. Some examinations were made of cylinder specimens fatigued in air, and special comparisons were made to determine the effects on fracture appearance of specimen life in the corrosion-fatigue test.

### a. Cylinders Exposed to Simulated Seacoast Environment at 80% of Design Stress

The group of specimens selected for examination consisted primarily of corrosion-fatigue specimens from forgings and rod of 7079-T6, 7075-T6 and 2014-T6 alloys, forged X7080-T7 and cast CH70-T7. Fractures, extending the full length of the test section, occurred after only a small portion of the cross sectional area had been penetrated (Fig. 24). With 7079-T6 cylinders, failures initiated on the outer surface and resulted from the development of a single crack (Fig. 38). There was a gradual transition from the cracked region (slow fracture) to the region of rapid tension failure (fast fracture) (Fig. 39). In 2014-T6 and 7075-T6 cylinders, in which fracture also initiated on the outer surface, the fracture surface included many cracks, and the areas of slow and fast fracture could be readily distinguished (Fig. 40). With these two alloys, there were also many small auxiliary cracks adjacent and parallel to the main fracture (Figs. 41 and 42). Fractures in the X7080-T7 and CH70-T7 samples initiated on the inner surface of the cylinders and appeared similar to those shown in Figs. 37 and 38.

Light microscope examinations were made as an aid in establishing the fracture type in cylinders from 7079-T6, 7075-T6 and 2014-T6 forgings. Little information could be gained from cross sections of the fracture surface and, since the 7079-T6 specimens had no auxiliary cracks, the failure of 7079-T6 could

not be diagnosed by this means. With the 2014-T6 and 7075-T6 cylinders, however, sections of auxiliary cracks indicated the fracture mode. In both 2014-T6 and 7075-T6 specimens auxiliary cracks followed an intergranular and interfragmentary path and had no transgranular segments which would suggest fatigue cracking (Figs. 43 and 44). In addition, the auxiliary cracks followed the directionality of the microstructure which was at a considerable angle to the direction of maximum stress. These features are strong indication that the failures were primarily the result of stress corrosion.

Examinations were also made of sections of the auxiliary cracks in the 7075-T6 cylinders stressed under constant pressure and exposed to the simulated seacoast environment (stress-corrosion test). These cracks also developed along intergranular and interfragmentary paths and followed the directionality of the microstructure (Fig. 45). The similarity between these cracks and those in the corrosion-fatigue cylinders indicated that failures in the corrosion-fatigue test were primarily the result of stress corrosion rather than fatigue.

Light microscope examinations were also made of cross sections of auxiliary cracks in cylinder specimens from 7075-T6 and 2014-T6 rod (there were no auxiliary cracks in 7079-T6 specimens). All cracks followed intergranular or interfragmentary paths (Fig. 46). While the crack path was the same in specimens from forgings and rod, crack propagation was more difficult in the rod material because the pronounced microstructural directionality of the forging was absent. This accounts for the longer lives encountered with specimens from rod when the failure mode was stress-corrosion cracking.

In addition to the visual and light microscope examinations, fracture surfaces in the slow-fracture region were examined with the scanning electron microscope (SEM). In cylinder specimens from forgings and rod of 7079-T6, 7075-T6 and 2014-T6 from the corrosion-fatigue tests and of forged 7075-T6 from the stress-corrosion test, all fractures had a faceted appearance characteristic of stress corrosion, with cracks and corrosion penetrating along grain and fragment boundaries (Figs. 47 - 50). A thorough search was made of the slow fracture regions of these corrosion-fatigue specimens, looking particularly for striations and other features indicative of fatigue fracture. None were found. Thus, the cracking was by the stress-corrosion mode until the sample could no longer sustain the load and sudden failure occurred.

Fracture in the X7080-T6 cylinder, which initiated on the inner surface, was characterized by a distinct ray pattern at the initiation point and striations in other areas of the slow-fracture region (Fig. 51) both of which are characteristic of fatigue failure. Fracture in CH70-T7 also initiated on the inside of the cylinder and was, therefore, of the fatigue type, although typical fatigue markings were not prominent.

In a further characterization of fracture appearance, specimens from forgings of 7079-T6, 7075-T6 and 2014-T6 subjected to the fatigue and corrosion-fatigue test and of 7075-T6 exposed to the stress-corrosion test (constant load) were examined with the TEM, using oxide replica techniques. For the corrosion-fatigue specimens, the slow-fracture region had a faceted appearance of the type shown in Fig. 52. This was in sharp contrast to the dimpled surface seen in the fast-fracture region (Fig. 53), which is characteristic of tensile fracture. It also differed greatly from the striation patterns characteristic of the fatigue fractures (Fig. 54). The slow-fracture region of the 7075-T6 specimen in the stress-corrosion test also showed the faceted appearance (Fig. 55). This confirms the conclusion that the failures of these cylinders in the corrosion-fatigue test were solely of the stress-corrosion variety.

**b. Cylinders Exposed to Simulated Seacoast Environment at 50% of Design Stress**

Metallographic examinations were made of the fracture of cylinders of all products in which failures initiated on the outside (7079 rod and forgings of 2014-T6 and 7075-T6), and of 7079-T6, 7075-T6 and X7080-T7 cylinders having inside fracture origins. The fracture of the shortest lived 2014-T6 specimen had a granular appearance throughout the slow-fracture region, and auxiliary cracks followed an intergranular path (Fig. 56). Failure was therefore of the stress-corrosion type. The fractures of a 7075-T6 and two 7079-T6 cylinders had a granular appearance at the crack initiation point (Figs. 57 and 58) but ray patterns (Fig. 57) and striations elsewhere. It was concluded that these failures were of the fatigue type, initiating at stress-corrosion cracks. The failures of some of the longer lived specimens initiated at corrosion pits.

The cylinders having inside origins were of 7079-T6, 7075-T6 and X7080-T7. All had ray patterns from the origin as well as fatigue striations away from the origin and were typical fatigue fractures. Their appearance was of the type shown in Fig. 51.

**c. C-Rings Exposed to Simulated Seacoast Environment at 80% of Design Stress**

Metallographic examinations were also made of C-ring specimens from forgings of 7079-T6, 7075-T6, X7080-T7 and 2014-T6 alloys. As has been described previously, these specimens were taken so that the most highly stressed region in the C-ring was at the parting plane of the forging. Thus, the stress was in the short transverse direction with respect to the microstructure, the most critical situation as regards stress-corrosion cracking.

Scanning electron microscope examinations of fracture surfaces showed a purely stress-corrosion fracture in the one sample of 2014-T6 examined. The fracture initiation region had a very granular appearance and the ray pattern that has been generally characteristic of fatigue was absent (Fig. 59a). Elsewhere, the faceted appearance and intergranular penetration typical of stress corrosion was evident (Fig. 59b).

In contrast, fracture surfaces showed a very definite mixture of fracture modes in 7079-T6, 7075-T6 and X7080-T7 alloys. At the fracture initiation points, ray patterns characteristic of fatigue fracture were apparent but they were frequently rather indistinct and had a granular appearance (Fig. 60a). In areas primarily in the early fracture region, but not exclusively in such regions, areas having the distinct features of stress-corrosion cracking were apparent (Fig. 60b). In other regions, generally more prevalent toward the end of the slow-fracture region, the striation patterns typical of fatigue were found, (Fig. 60c). Thus, at high magnifications, there were no visible indications of interaction between the two fracture modes. The change in the appearance of the ray pattern at the fracture initiation point, however, is definite evidence of interaction.

Additional evidence of the mixed-fracture mode was seen in light microscope cross sections of auxiliary cracks in C-rings of 7075-T6 and X7080-T7. These examinations were complicated by the fact that the alloys were unrecrystallized and either fatigue or stress-corrosion cracks would develop in the same general direction. At relatively low magnification (Fig. 61) the mixed modes are suggested, and at higher magnification, separate areas in which cracking followed intergranular and transgranular paths were observed.

d. C-Rings Exposed to Simulated Seacoast Environment at 50% of Design Stress

Metallographic examinations in this group were concerned only with the stress-corrosion-susceptible alloys 7079-T6, 7075-T6 and 2014-T6. In the 7079-T6 specimens examined, considerable corrosion of the fracture surface made diagnosis uncertain. It appeared, however, that failure was of the mixed-mode type, as had been the case at the higher stress level. With the 7075-T6 and 2014-T6 specimens, failures were definitely of the mixed-mode type, showing an indistinct ray pattern near the origin and separate areas of intergranular faceted fracture and fatigue striations. Appearance was similar to that shown in Fig. 60.



#### e. Cylinders Fatigue Tested in Air

In the fatigue tests of cylinders in laboratory air at 50% relative humidity, it had been expected that failures would initiate on the inner surface because the stress was appreciably higher there than on the outer surface. In a number of specimens, however, failure initiated on the outside surface. SEM examinations were made to compare the surfaces of fractures initiating on the outer and inner surfaces. Fractures originating on the inner surface were characterized by ray patterns at the origin and pronounced striation patterns (Fig. 62). Some of those originating on the outer surface showed the same characteristics, indicating that they were of the fatigue variety and had presumably initiated at a stress raiser. Other fractures originating on the outer surface had a granular pattern at the origin and no semblance of a ray pattern (Fig. 63a). Away from the origin, however, these fractures showed the pronounced striations characteristic of fatigue (Fig. 63b). Thus, cracks of this type were substantially fatigue cracks having a stress-corrosion crack as their origin.

#### f. Effect of Cycle Rate and Waveform in Fatigue

Earlier in this report it was pointed out the hold period at maximum stress and the rate of cycling had an apparent effect on fatigue life. SEM examinations were made to determine whether this difference was reflected in fractographic features. For this comparison, two 7075-T73 cylinder specimens, both of which had failed from an inside origin, were selected. One had been stressed sinusoidally at a rate of 20 cycles per minute; the other had been stressed at 0.15 cycles per minute with a hold time at maximum stress of 5.4 minutes on each cycle. The appearance of the fractures at the origin and at approximately equal distances away from the origin is shown by Fig. 64. There is indication that the ray and striation patterns are more distinct with the combination of slower cycling rate and hold time, although more samples would have to be examined to determine whether this was the general case. Measurements indicate a somewhat faster propagation rate for the slow rate-hold time combination. This difference in striation spacing is roughly proportional to the fatigue lives of the specimens (22,000 vs 39,000).

#### g. Effect of Specimen Life in Corrosion-Fatigue Test on Fracture Appearance

In the corrosion-fatigue tests of cylinders stressed to 80% of design stress, most specimens of the stress-corrosion-

susceptible alloys 7079-T6, 7075-T6 and 2014-T6 failed after relatively short lives. All those examined failed by a purely stress-corrosion mode. To answer the question of whether fracture appearance differed with test life, special examinations were made of two cylinders from 2014-T6 rod having lives of 1573 and 18,920 cycles. The slow-fracture region of the short-lived specimen had a granular faceted appearance throughout, similar to that shown in Fig. 48. The long-term failure had primarily the same appearance, although because of the longer exposure, the grains near the origin were heavily pitted after the stress-corrosion crack had passed (Fig. 65a). Near the outer edge of the slow-fracture region, however, and just before ultimate failure, a few areas of fatigue striations were observed (Fig. 65b). While the two types of failure were found on this fracture, no interaction of one failure mode with the other was observed and the failure was judged to be of the stress-corrosion type.

#### h. Possible Stress-Corrosion-Fatigue Failure Mechanisms

The mixed mode failures suggest one mechanism by which stress-corrosion and fatigue can interact in a corrosion-fatigue test. A number of fractures initiated as stress-corrosion cracks and then changed to the mixed-mode type. These were characterized by regions having the features of either stress corrosion or fatigue without any other distinctive features that could be attributed to the combination of the two. Other investigations<sup>6</sup> have shown that the propagation of stress-corrosion cracks is highly dependent on the directionality of grain structure with respect to the stressing direction. Combining these observations suggests that the mixed mode cracks were stress-corrosion cracks as long as a favorable grain orientation was available. When a region having unfavorable boundary orientation was encountered, the stress-corrosion crack would be stalled while it sought favorably oriented structure to either side of the difficult area. This would increase the local stress on this area and, with the cyclic stressing, fatigue action would breach the obstacle. Once the unfavorably oriented area had been passed, stress-corrosion cracking could resume.

## SECTION VII

### CONCLUSIONS

The corrosion-fatigue and stress-corrosion performance of several high strength aluminum alloys was investigated by tests of hydraulic cylinders, C-rings and axial-stress fatigue specimens. Specimens were prepared from forgings and forging stock of alloys 2014-T6, 7075-T6, 7075-T73, 7079-T6, and X7080-T7 and also from premium cast alloy CH70-T7. The cyclic loads of the cylinders and C-rings in the corrosion-fatigue tests were in the 0.15 to 10 cpm frequency range and included a hold time at load to allow time for stress corrosion to occur. The investigation led to the following principal conclusions for the tests in the corrosive environment.

1. In general, it was demonstrated that stress-corrosion cracking may occur under cyclic loading, especially at low frequencies, and that stress corrosion and fatigue can interact under certain conditions to produce failures in shorter times and fewer cycles than for either phenomenon occurring by itself.

2. Electron microscope examination indicated failures to be either pure stress corrosion, pure fatigue, one followed by the other, or mixtures of the two, depending on the alloy and temper, stress level, rate of cycling and conditions of exposure. Mixed mode failures generally started from stress-corrosion origins. Apparently, these cracks propagated by stress corrosion where the grains were favorably oriented and by fatigue in other areas.

3. Overall, alloy 7075-T73 gave the best performance; no stress-corrosion failures occurred in this alloy. The lives of forged cylinders loaded by cyclic internal pressure to 80% of design stress in a simulated seacoast environment were at least 10 times as long for 7075-T73 as for alloys 2014-T6, 7075-T6, and 7079-T6.

4. Stress-corrosion cracking did not occur in any of the premium cast CH70-T7 specimens. Alloy X7080-T7 also demonstrated good resistance to stress-corrosion cracking, with no failures of this kind occurring under most test conditions.

5. All but one of the cylinders of alloys 2014-T6, 7075-T6 and 7079-T6 that were cycled to 80% of design stress developed stress-corrosion failures. Stress corrosion also

occurred in some of the lower stressed cylinders and many of the C-rings of these alloys.

6. The static stress-corrosion tests of C-rings ranked the alloys in the following decreasing order of resistance to stress-corrosion cracking:

- (1) 7075-T73, CH70-T7 (no failures)
- (2) X7080-T7 (some failures at 80% of design stress)
- (3) 2014-T6, 7075-T6, 7079-T6 (susceptible at 30, 55, and 80% of design stress)

This is also the general ranking obtained in the stress-corrosion-fatigue tests of cylinders except that alloy X7080-T7 ranked ahead of CH70-T6 in the cylinder tests.

7. Although the corrosion-fatigue tests of coupons did not rank the alloys in the same order as that obtained in the stress-corrosion-fatigue tests of cylinders, the results of this investigation suggest that for given service loading conditions a useful laboratory test using coupons could be developed.

The following observations, although not having a direct bearing on stress-corrosion-fatigue behavior, are also of interest:

1. Reducing frequency of loading and introducing a hold time at load reduced by 50% or more the fatigue lives of the wrought cylinders which failed by fatigue action. However, the difference in load cycle did not appear to affect the lives of the cast cylinders.

2. The fatigue failures of some of the 7079-T6 cylinders tested using sinusoidal loading in laboratory air appeared to develop from stress-corrosion cracks.

3. When tested in air, alloy CH70-T7 generally had significantly lower fatigue strengths than the wrought products, even though it performed better in stress-corrosion-fatigue than several of the wrought alloys.

4. For the die forgings the fracture-toughness values obtained in the transverse and longitudinal directions for alloys 7075-T6 and 7079-T6 were almost as high as those of 7075-T73

and X7080-T7. Alloy 2014-T6 rated the lowest from a fracture-toughness standpoint. For transverse specimens the fracture toughness of the alloy CH70-T7 was higher than that of any of the wrought alloys.

5. The crack sizes (fatigue or stress-corrosion crack) which were associated with unstable fracture of the cylinders correlated well with values predicted from the fracture-toughness tests.

6. In the static stress-corrosion tests the simulated seacoast environment proved to be quite similar to actual seacoast atmosphere both as regards the stress levels causing failures and the extent of general corrosion.

## SECTION VIII

### RECOMMENDATIONS

The results of this investigation serve to emphasize the complex nature of the stress-corrosion, corrosion and fatigue interaction. It is proposed that additional work be done to provide more information on the stress-corrosion-fatigue behavior of high-strength aluminum alloys, as follows:

1. Additional tests of cylinders should be made to fill in some of the gaps in the results for the alloys evaluated in this investigation. These should include tests under a steady stress in a stress-corrosion environment of alloys 2014-T6, 7079-T6 and X7080-T7, for comparison with the results of stress-corrosion-fatigue tests reported herein. Additional cylinder tests should be made at higher loading rates in the corrosive environment to obtain more information on the interaction of corrosion and fatigue. The effect of loading rate on fatigue strength in laboratory air is also in question as a result of this investigation, and some additional tests should be made to provide further data on this point. Finally, a few tests should be made at different hold-times under stress in the fatigue cycle to determine whether the time to stress-corrosion failure under intermittent loading depends more on the time under stress or the total time in the corrosive environment.

2. Because the corrosion-fatigue tests of cylinders appeared to be effective in rating alloys in regards to performance of hydraulic cylinders in a relatively mild saline environment, additional tests of this nature should be made to evaluate new forging alloys such as 7175-T736, 7049-T73 and MA15-T7X.

3. The test of C-rings should be modified to provide more uniform specimen exposure and to obtain more rapid stress corrosion, with reduced local corrosion. With these alterations C-ring tests should provide an economical method of seeking answers to some of the following basic questions regarding the stress-corrosion-fatigue interaction:

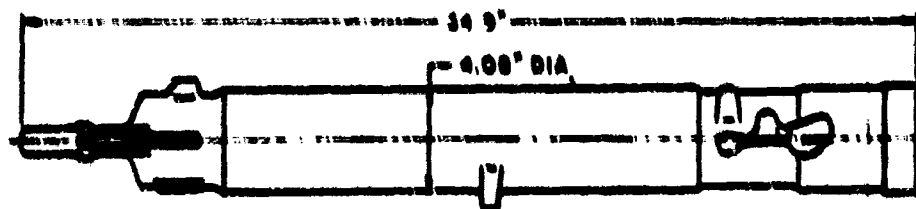
- A. What effect does the interaction of stress-corrosion mode of failure and fatigue mode of failure have on:

- (1) Relationship between stress and cycles to failure in fatigue tests?
- (2) Relationship between stress and time to failure in stress-corrosion tests?
- B. In what range of cyclic loading conditions will stress-corrosion cracking occur?
- C. Will some conditions of cyclic loading lower the threshold stress for stress-corrosion cracking obtained in static tests?
- D. What effect does aging treatment have on above factors?

### REFERENCES

1. "Standard Methods of Tension Testing of Metal Materials," E8-70, 1970 Book of ASTM Standards, Part 31.
2. "Tentative Method of Test for Plane-Strain Fracture Toughness of Metallic Materials," Designation E399-70T, ASTM Standards, Part 31, July 1970, pp 911-927.
3. J. G. Kaufman and Marshall Holt, "Fracture Characteristics of Aluminum Alloys," ARI Technical Paper No. 18, Aluminum Co. of America, 1965.
4. G. Sachs and G. Espey, "The Measurement of Residual Stresses in Metals," Iron Age (1948) 148, No. 12, pp 63-71; (1948) 148 No. 13, pp 36-42.
5. F. Howell and J. Miller, "Axial Stress Fatigue Strength of Structural Aluminum Alloys," Proc. ASTM, 1956.
6. C. F. Tiffany and J. N. Masters, "Applied Fracture Mechanics," Fracture-Toughness Testing and Its Applications, ASTM STP 381, April 1965, pp 249-277.
7. Alcoa Aluminum Handbook, Aluminum Co. of America, 1967.
8. M. S. Hunter and W. G. Fricke, Jr., "Study of Crack-Initiation Phenomena Associated With Stress Corrosion of Aluminum Alloys," Contr. No. NAS8-20396, George C. Marshall Space Flight Center, Final Summary Report, October 6, 1969.
9. W. F. Brown, Jr., Editor, Review of Developments in Plane Strain Fracture Toughness Testing, ASTM STP 436, 1970.

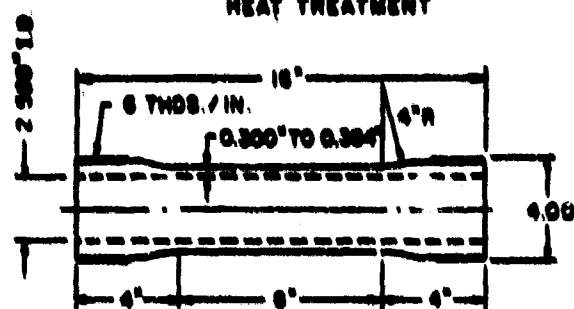




(a) ORIGINAL FORGING

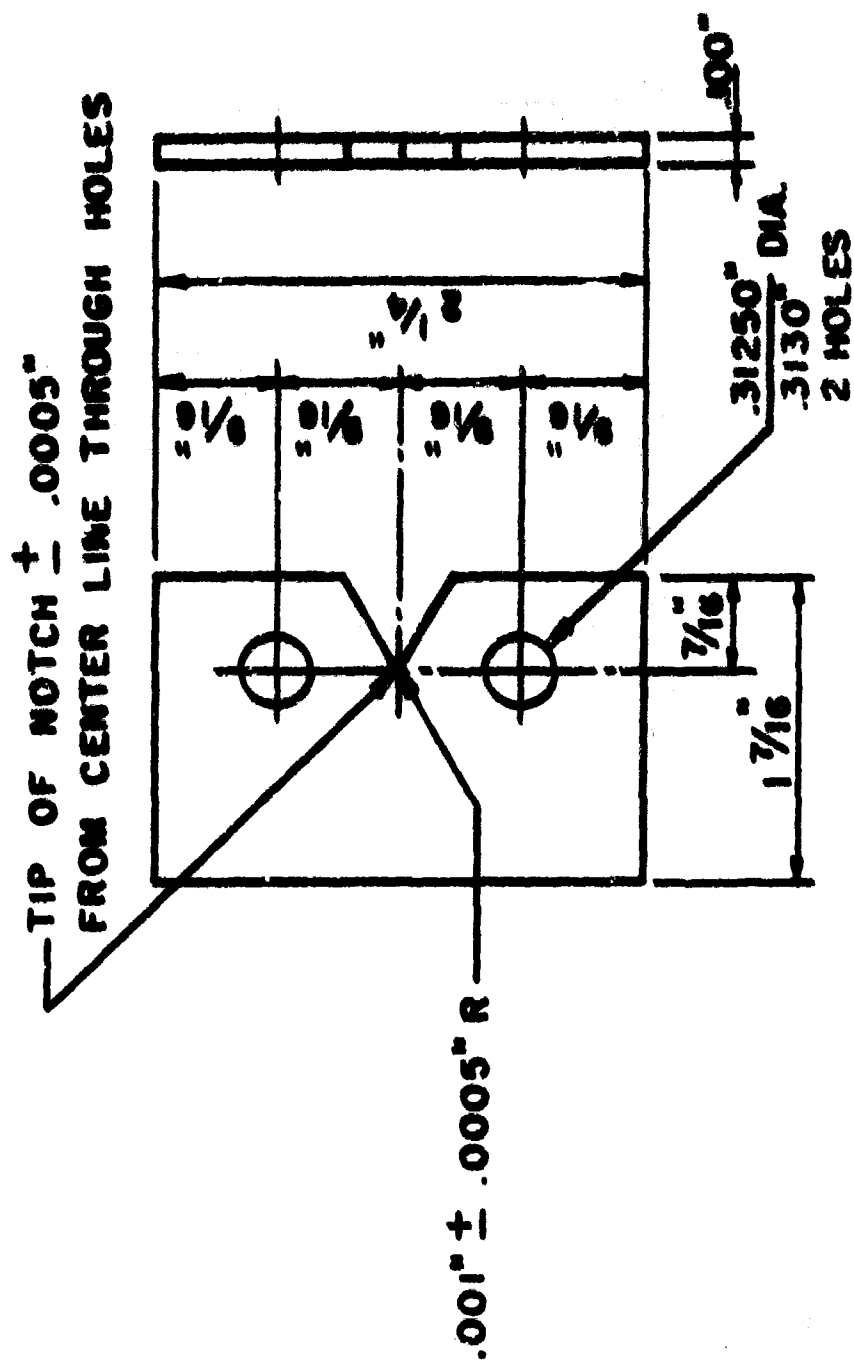


(b) CYLINDER BLANK FOR  
HEAT TREATMENT

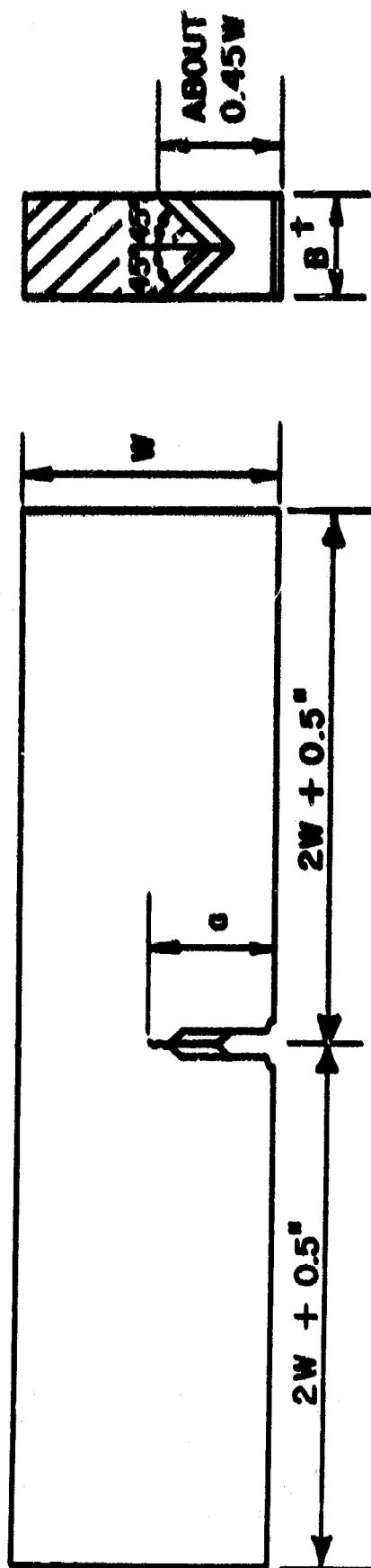


(c) TEST CYLINDER

FIG. 1 - STEPS IN PROCESSING OF TEST  
CYLINDERS FROM DIE FORGINGS.



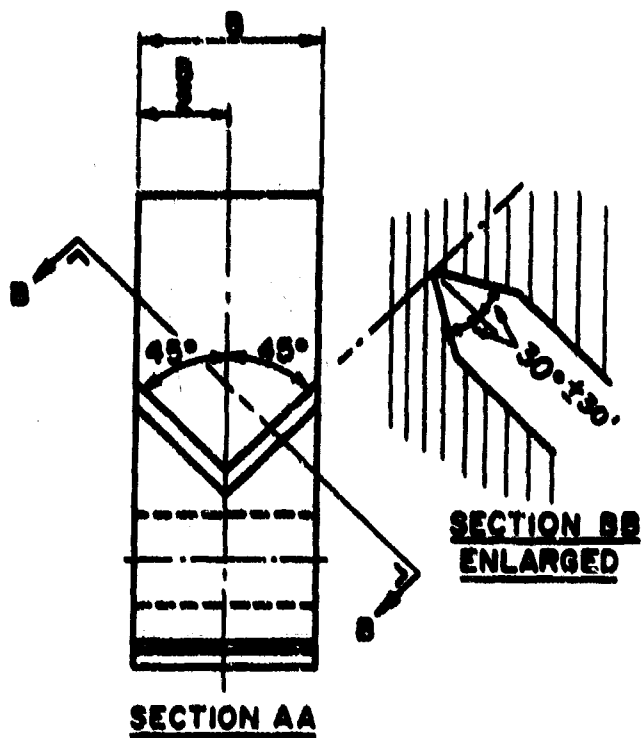
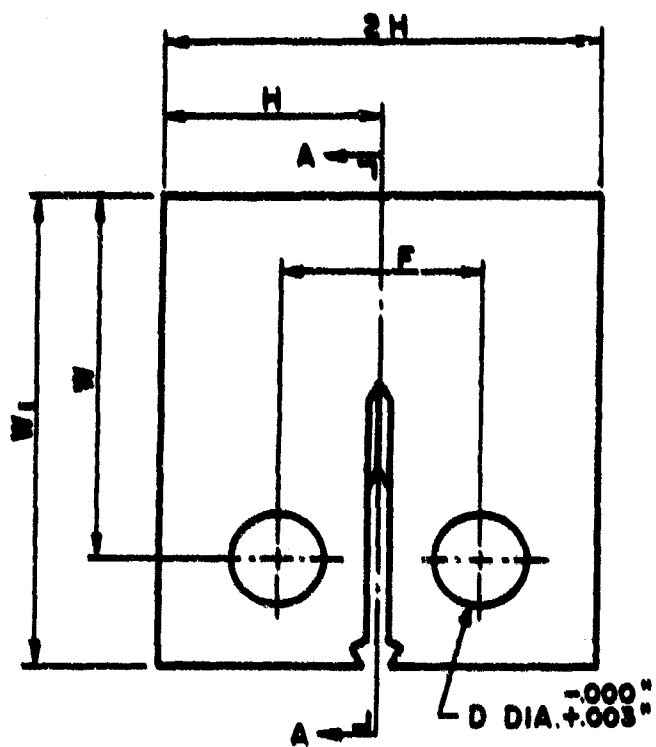
KAHN TYPE TEAR TEST SPECIMEN



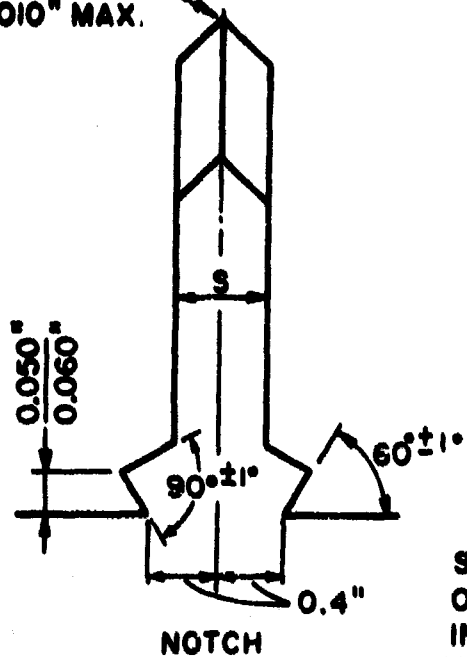
	THICKNESS, B, IN.	WIDTH, W, IN.	LENGTH, IN.	CRACK LENGTH, $a_0$ *, IN.
W-L	1/4	1/2	3	1/4
L-W	3/4	1-1/2	7	3/4

\* INCLUDING AT LEAST 0.050 IN. OF FATIGUE CRACK

NOTCH - BEND FRACTURE TOUGHNESS SPECIMEN  
FIGURE 3



NOTCH ROOT  
RADIUS .010" MAX.



NOTCH ENLARGED VIEW

#### PROPORTIONS

$B = \text{THICKNESS} = 0.75''$

$a = B = c = .75''$

$W = 2B, N_1 = 2.5B$

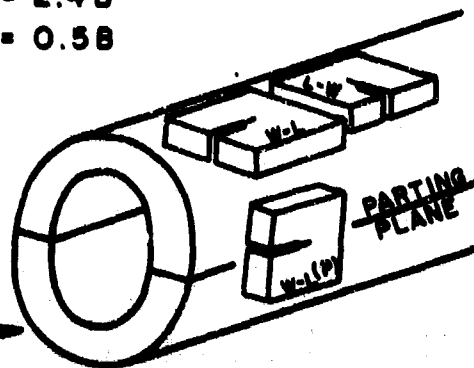
$S = 0.1B$

$F = 1.10B$

$H = 2.4B$

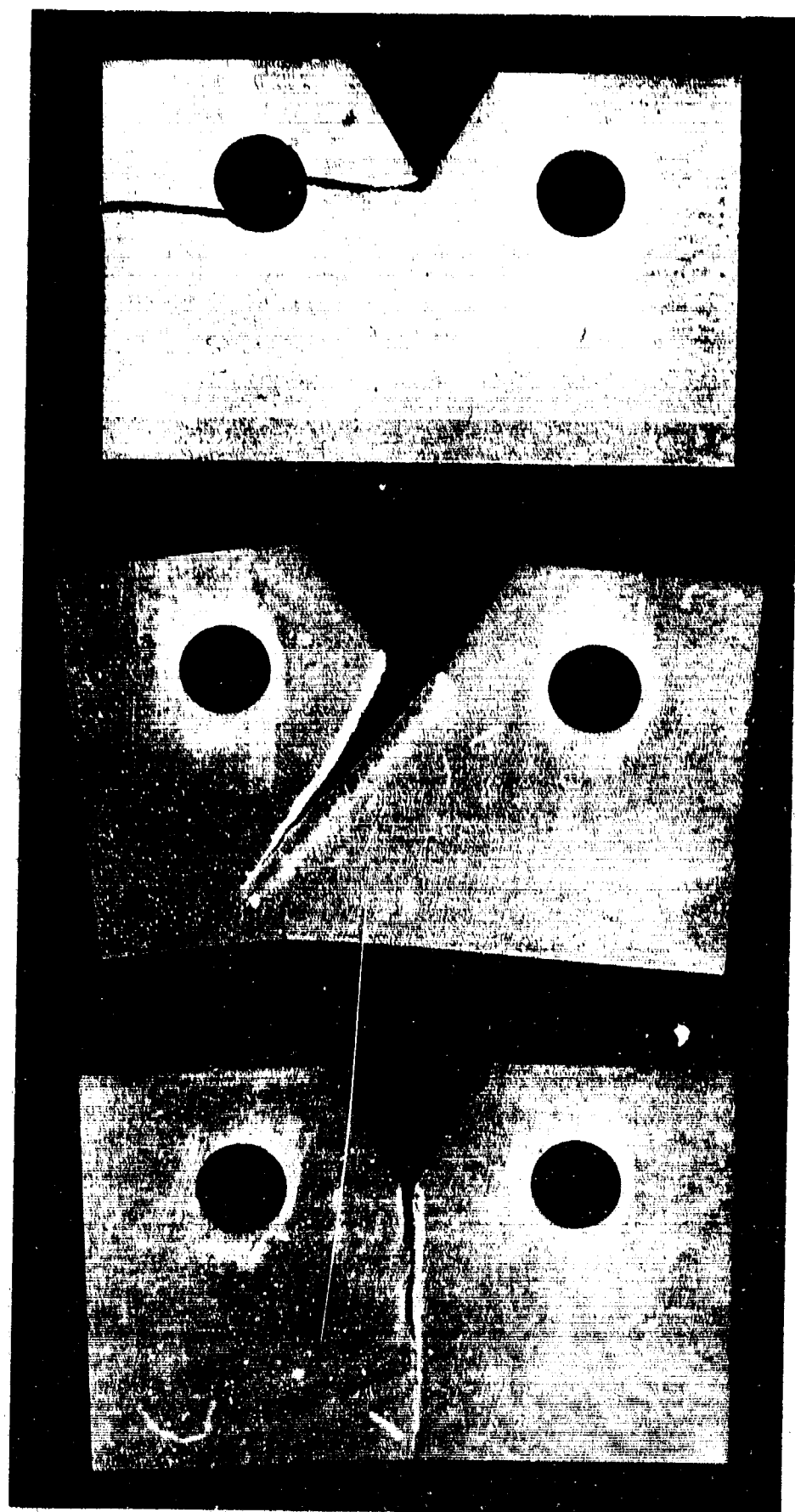
$D = 0.5B$

SPECIMEN  
ORIENTATION  
IN CYLINDER  
BLANK.



COMPACT TENSION FRACTURE TOUGHNESS SPECIMEN

FIGURE 4

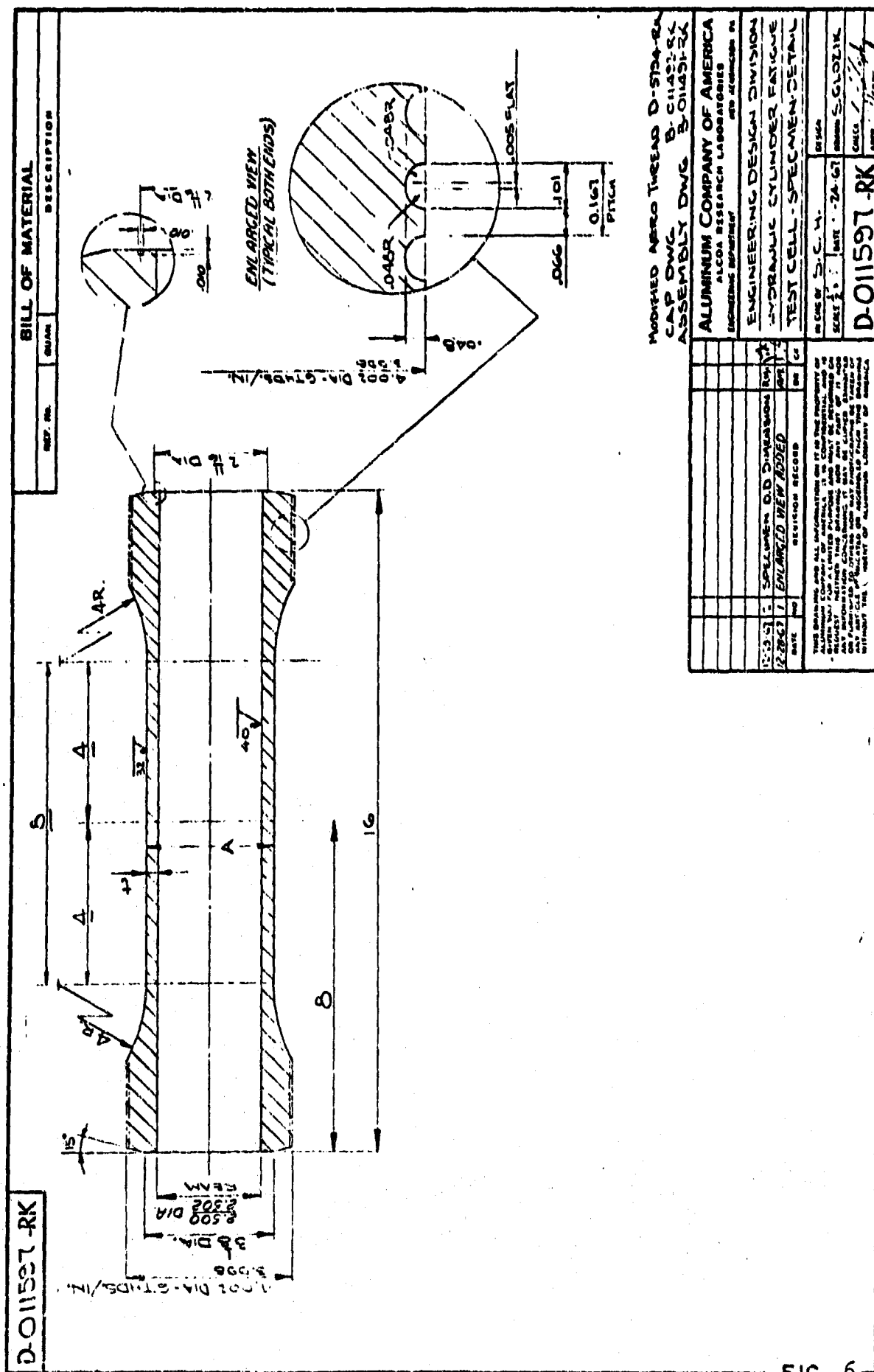


Normal

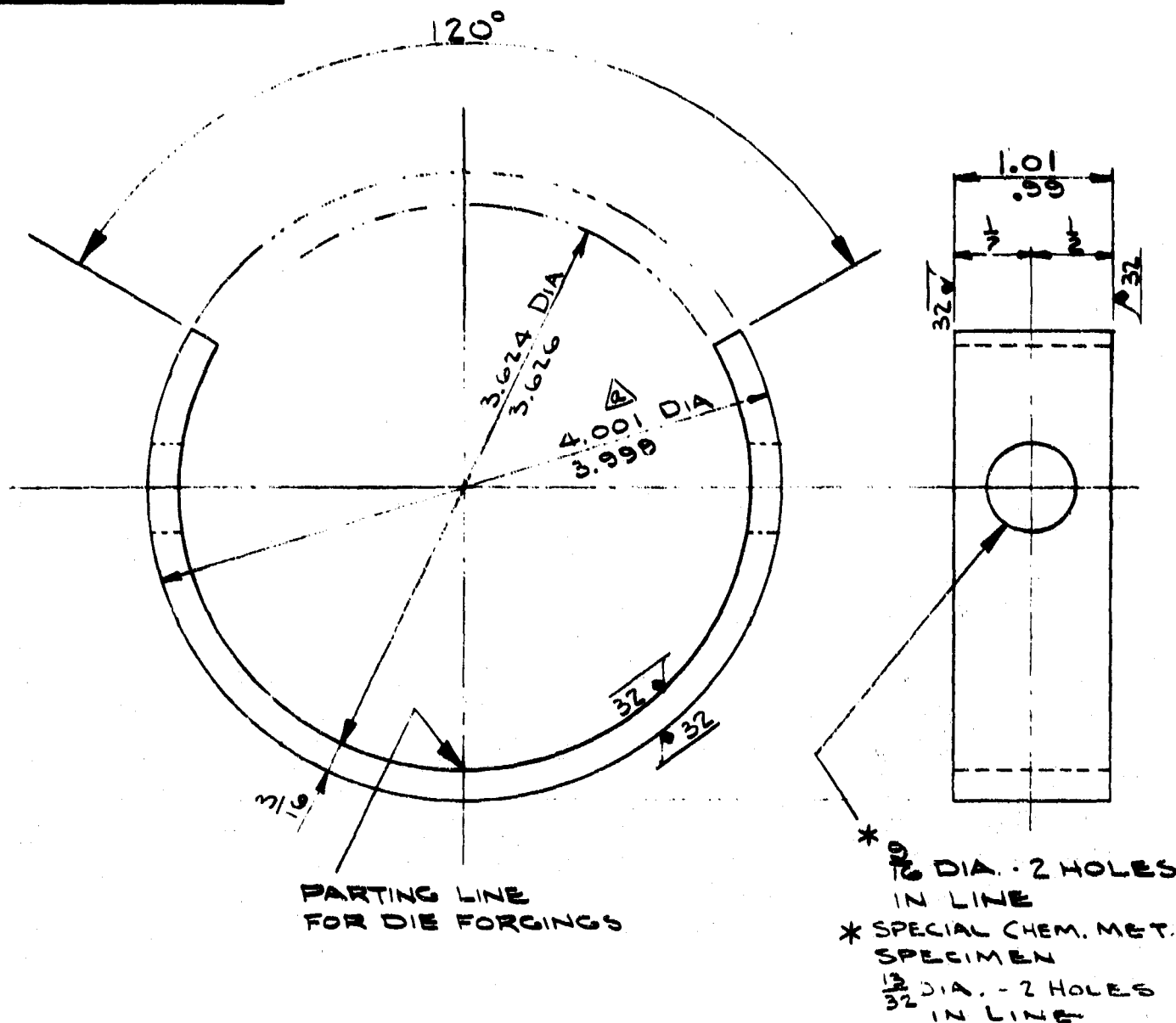
Diagonal

Pin-hole

FIG. 5. FRACTURE PATHS OF TEAR SPECIMENS, SERIES 18 AND 19.



**L-011614-RK**



**SPECIMEN**   **REQD.**

**ASSEMBLY DWG B-011495-RK**

12-29-67	2	* NOTE ADDED	RM	
12-29-67	1	△ WAS 4.001 DIA	RM	
DATE	NO.	REVISION RECORD	DR	CK

**ALUMINUM COMPANY OF AMERICA**  
ALCOA RESEARCH LABORATORIES  
ENGINEERING DEPARTMENT NEW KENSINGTON, PA.

**ENGINEERING DESIGN DIVISION**  
**"C" RING SPECIMEN FOR HYDRAULIC**  
**CYLINDER FATIGUE & CORROSION TEST**

THIS DRAWING AND ALL INFORMATION ON IT IS THE PROPERTY OF ALUMINUM COMPANY OF AMERICA. IT IS CONFIDENTIAL AND IS GIVEN YOU FOR A LIMITED PURPOSE AND MUST BE RETURNED ON REQUEST. NEITHER THIS DRAWING NOR ANY PART OF IT NOR ANY INFORMATION CONCERNING IT MAY BE COPIED, EXHIBITED OR FURNISHED TO OTHERS NOR MAY PHOTOGRAPHS BE TAKEN OF ANY ARTICLE FABRICATED OR ASSEMBLED FROM THIS DRAWING WITHOUT THE CONSENT OF ALUMINUM COMPANY OF AMERICA.

IN CHG OF	S. C. H.	DESIGN
SCALE	1" = 1"	DATE 11-29-67
L-011614-RK		DRAWN S. GLOZIK
		CHECK
		APPR <i>[Signature]</i>

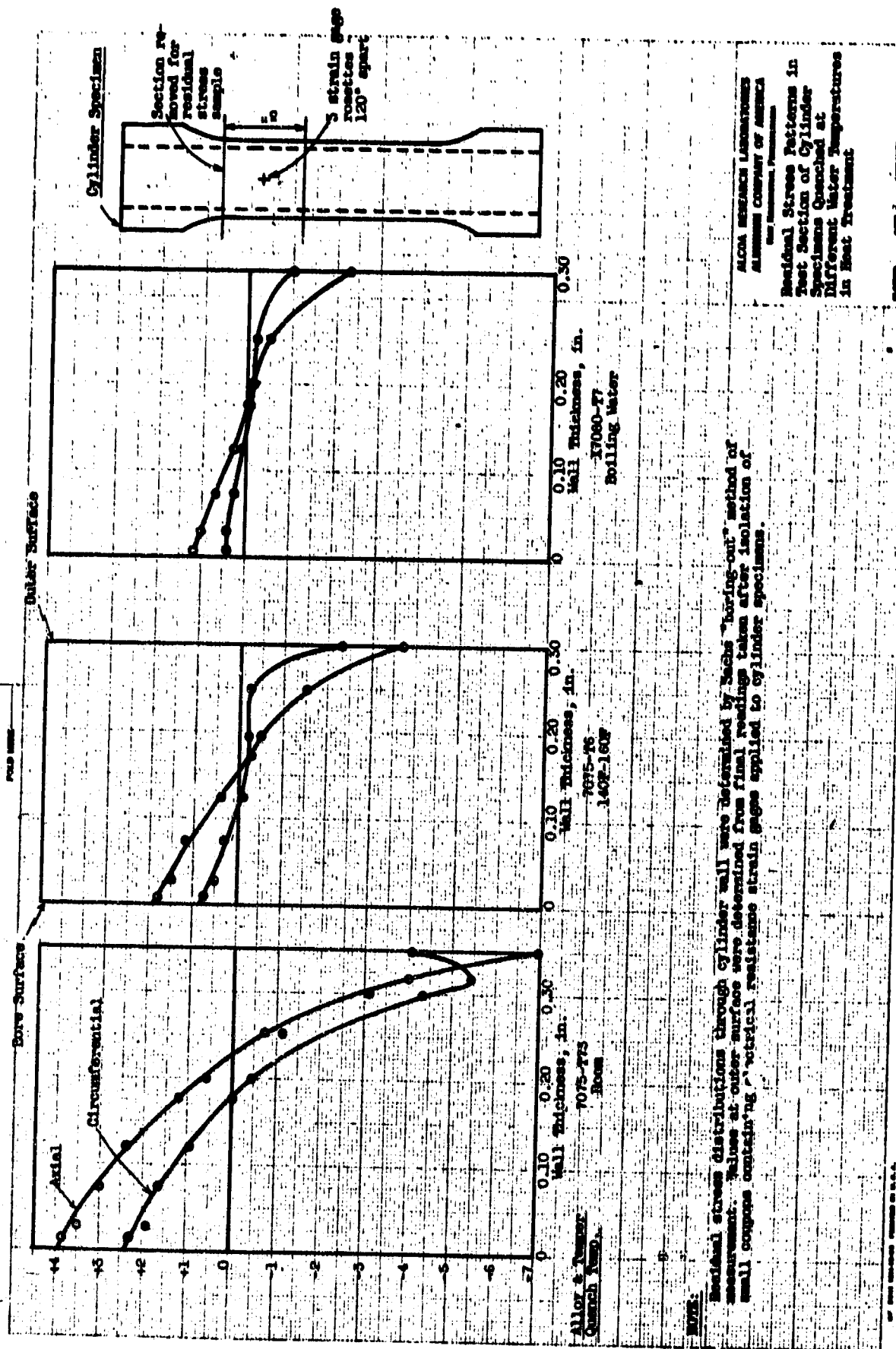
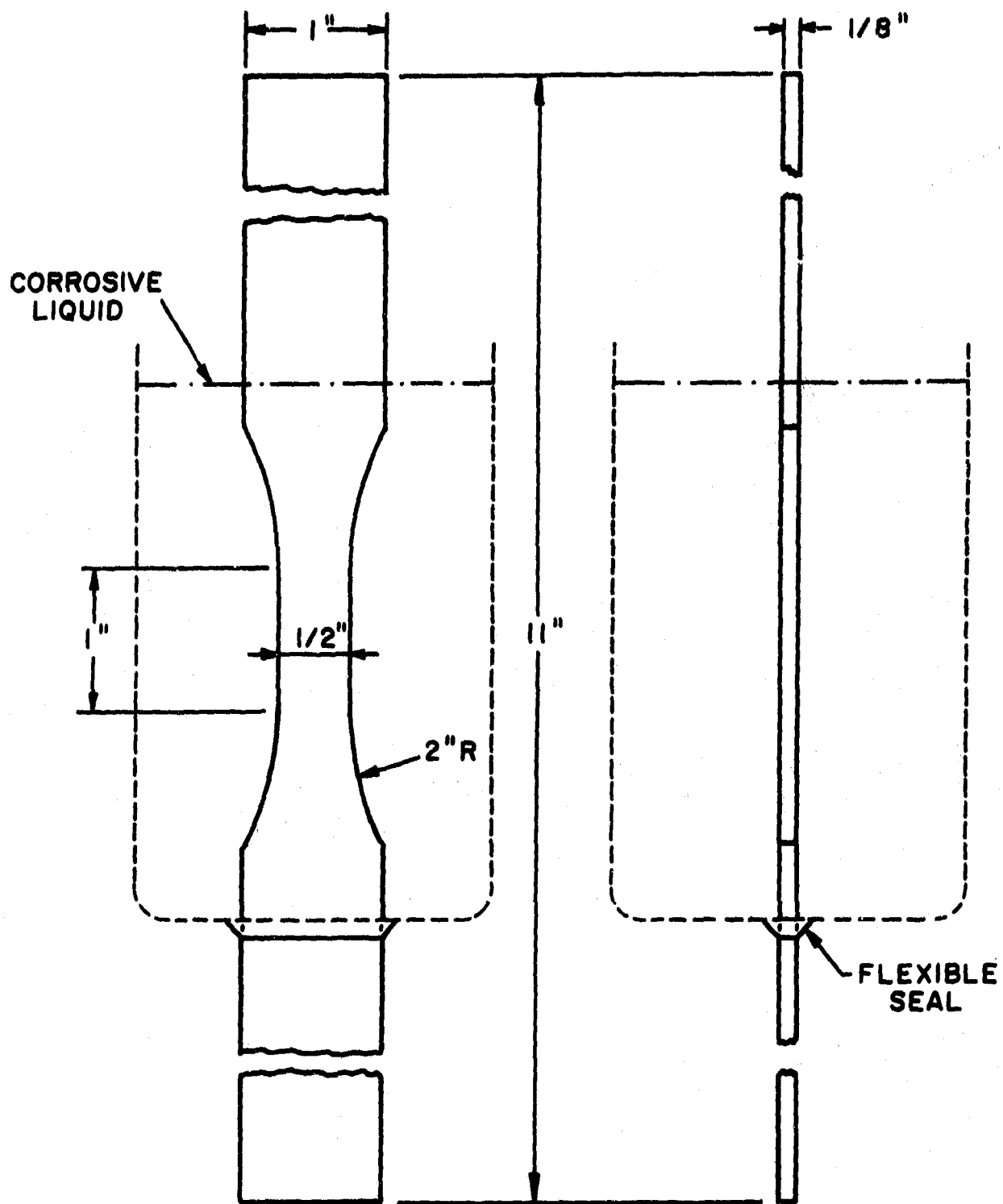


Fig. 8

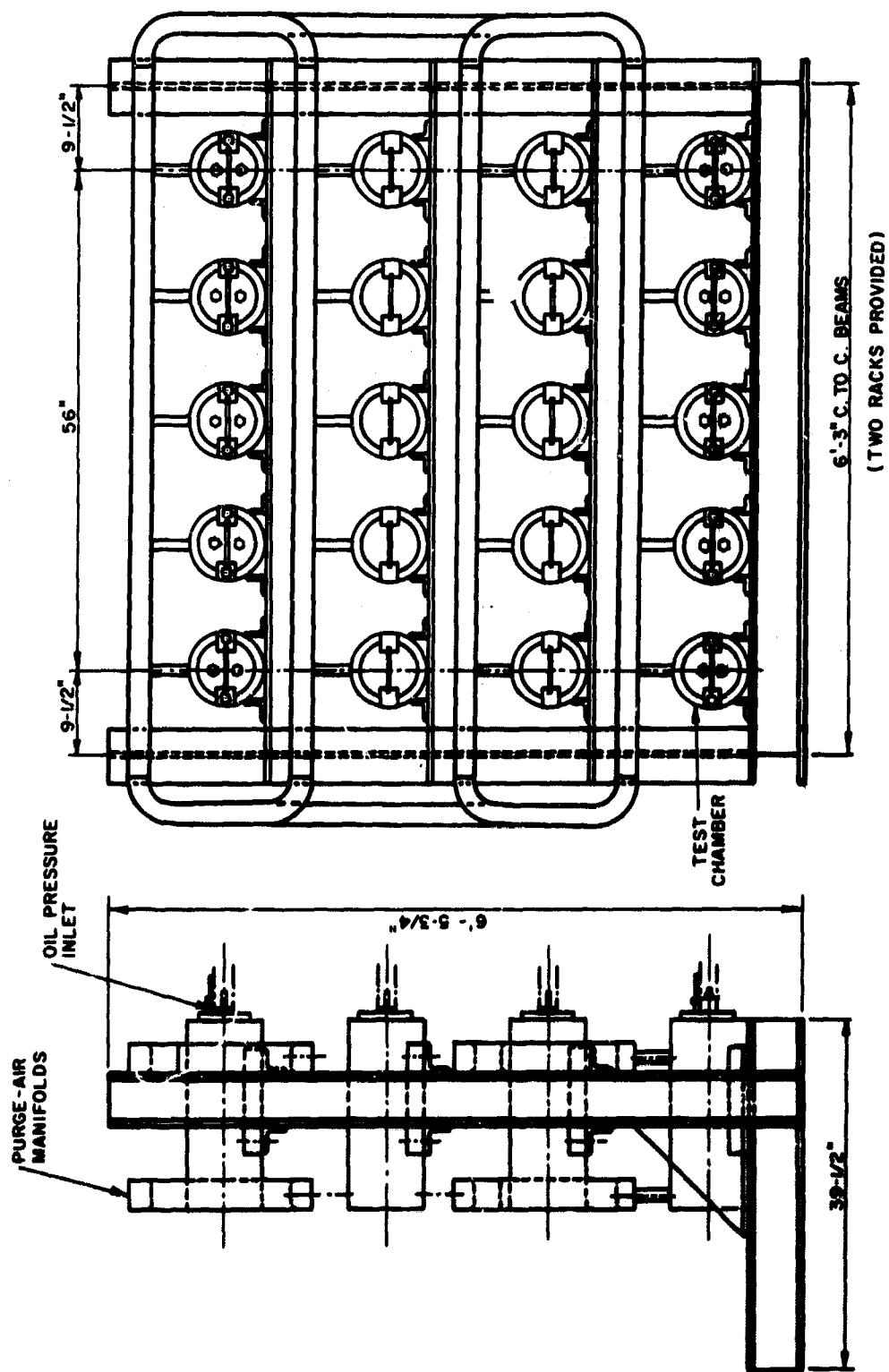




AXIAL STRESS FATIGUE SPECIMEN FOR  
TESTS IN LABORATORY ATMOSPHERE  
OR SUBMERGED IN HIGHLY CORROSIVE  
LIQUID.

FIG. 9





ASSEMBLY OF CYLINDERS ON TEST RACK

FIGURE II

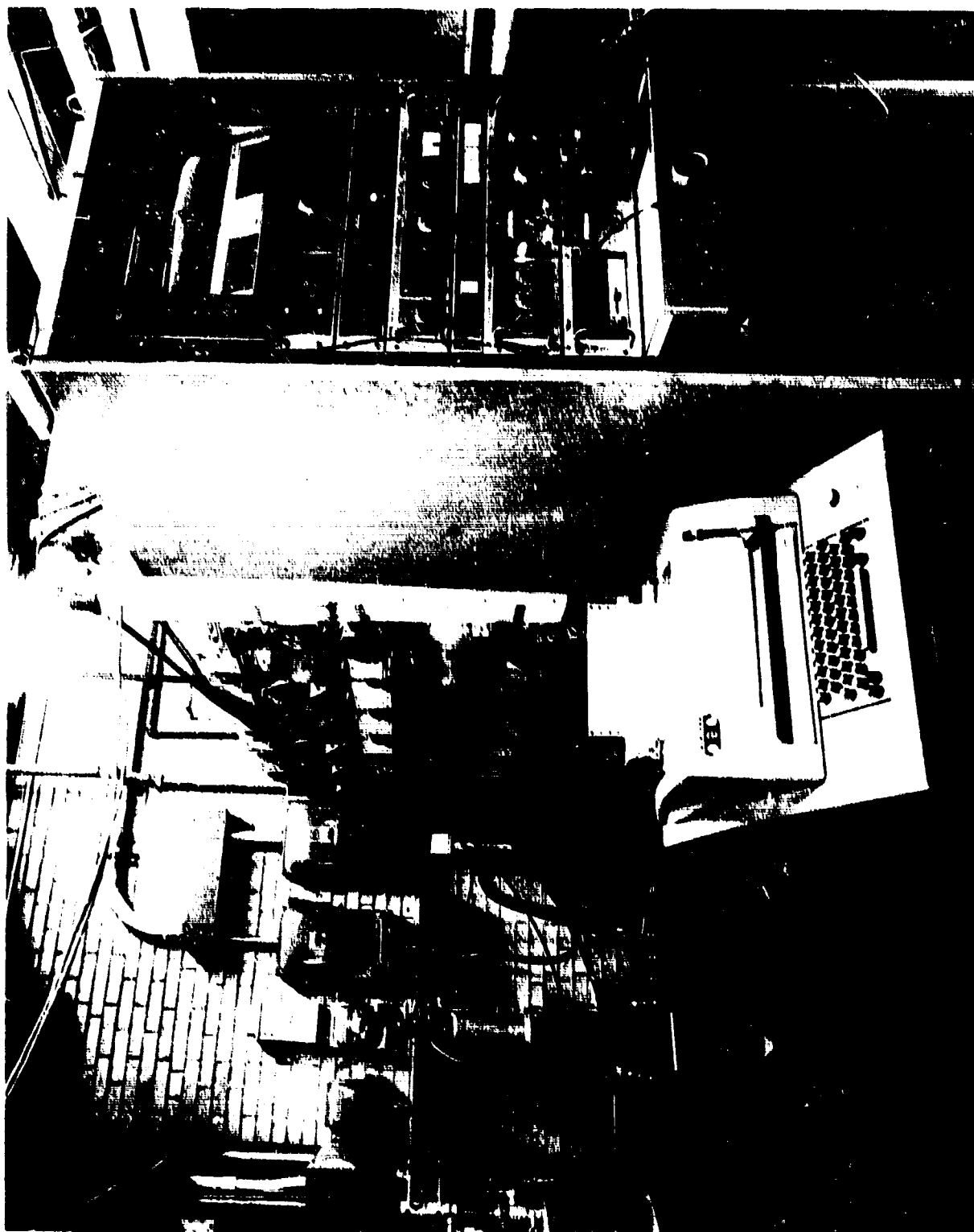
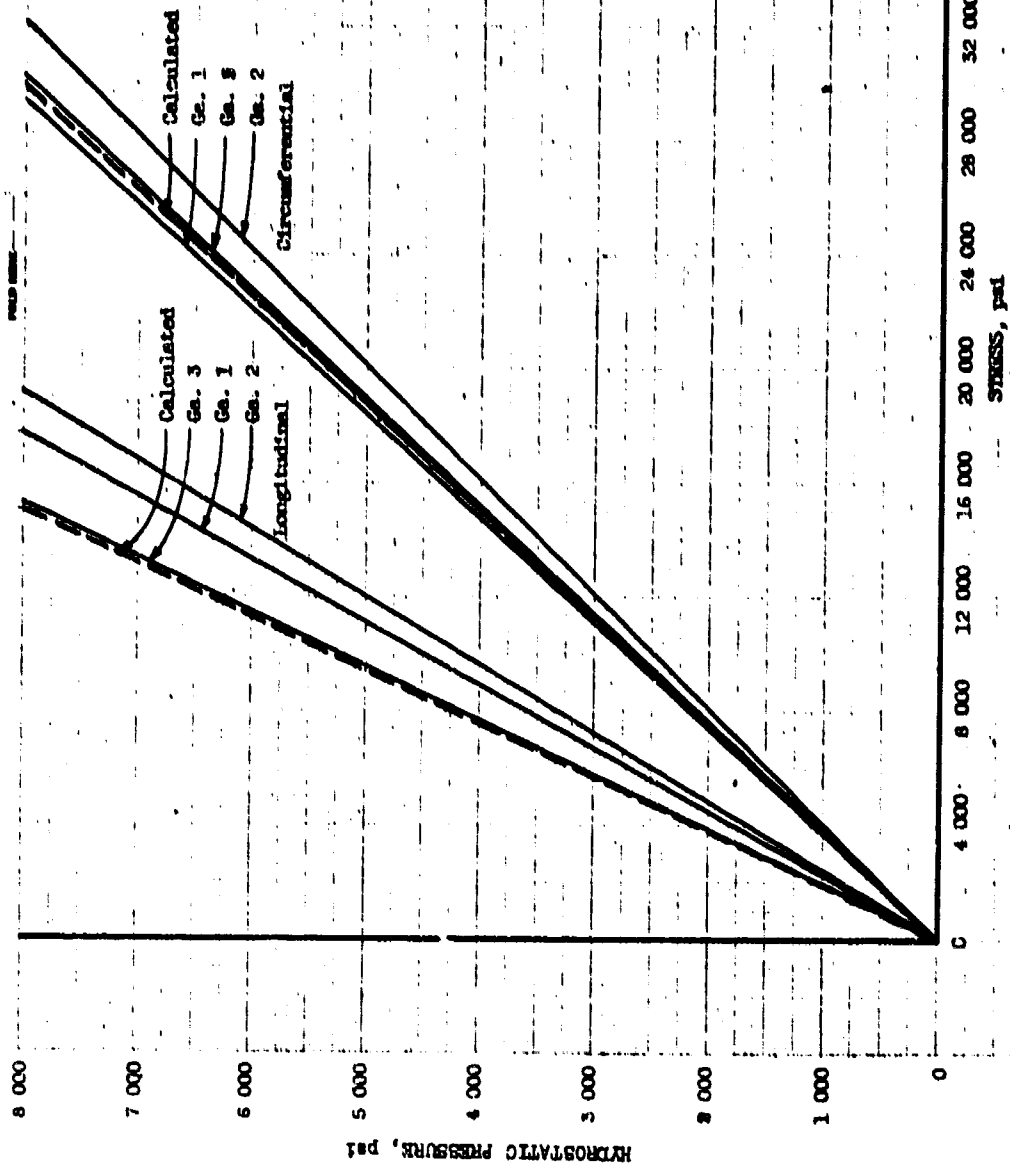
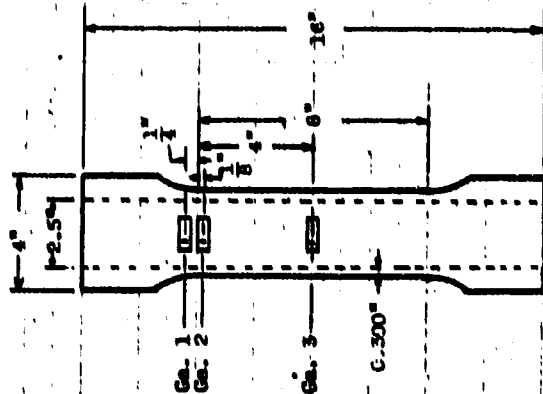


FIG. 12. FACILITIES FOR FATIGUE TESTING OF HYDRAULIC CYLINDERS



□ Radial strain gage,  
Foil Gages,  
1/8" Gage Length



ALCOA RESEARCH LABORATORIES  
ALUMINUM COMPANY OF AMERICA  
New Kensington, Pennsylvania

J. O. 12-2854

Calibration of 7075 Cylinder  
Loaded Hydrostatically

Fig. 13

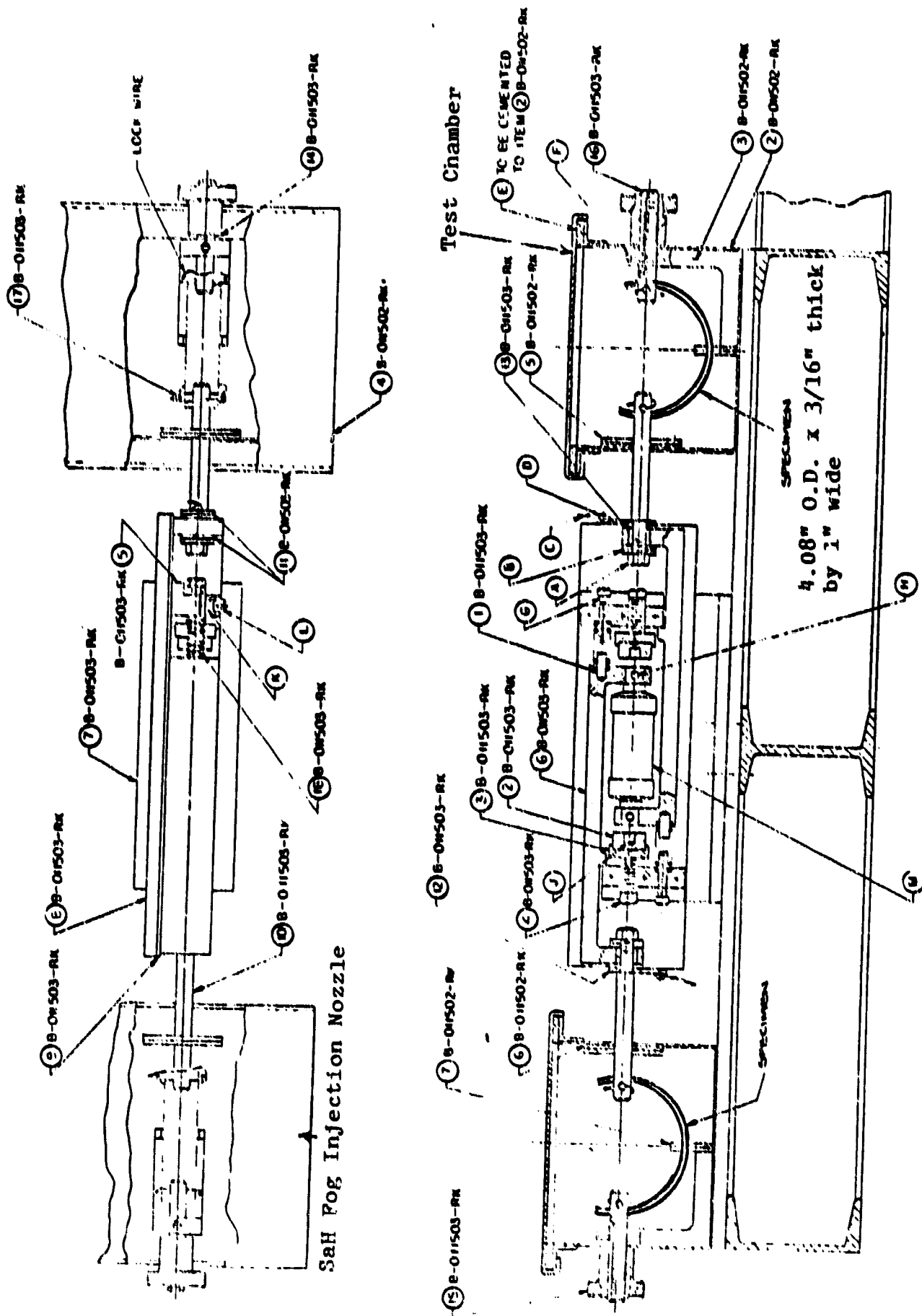
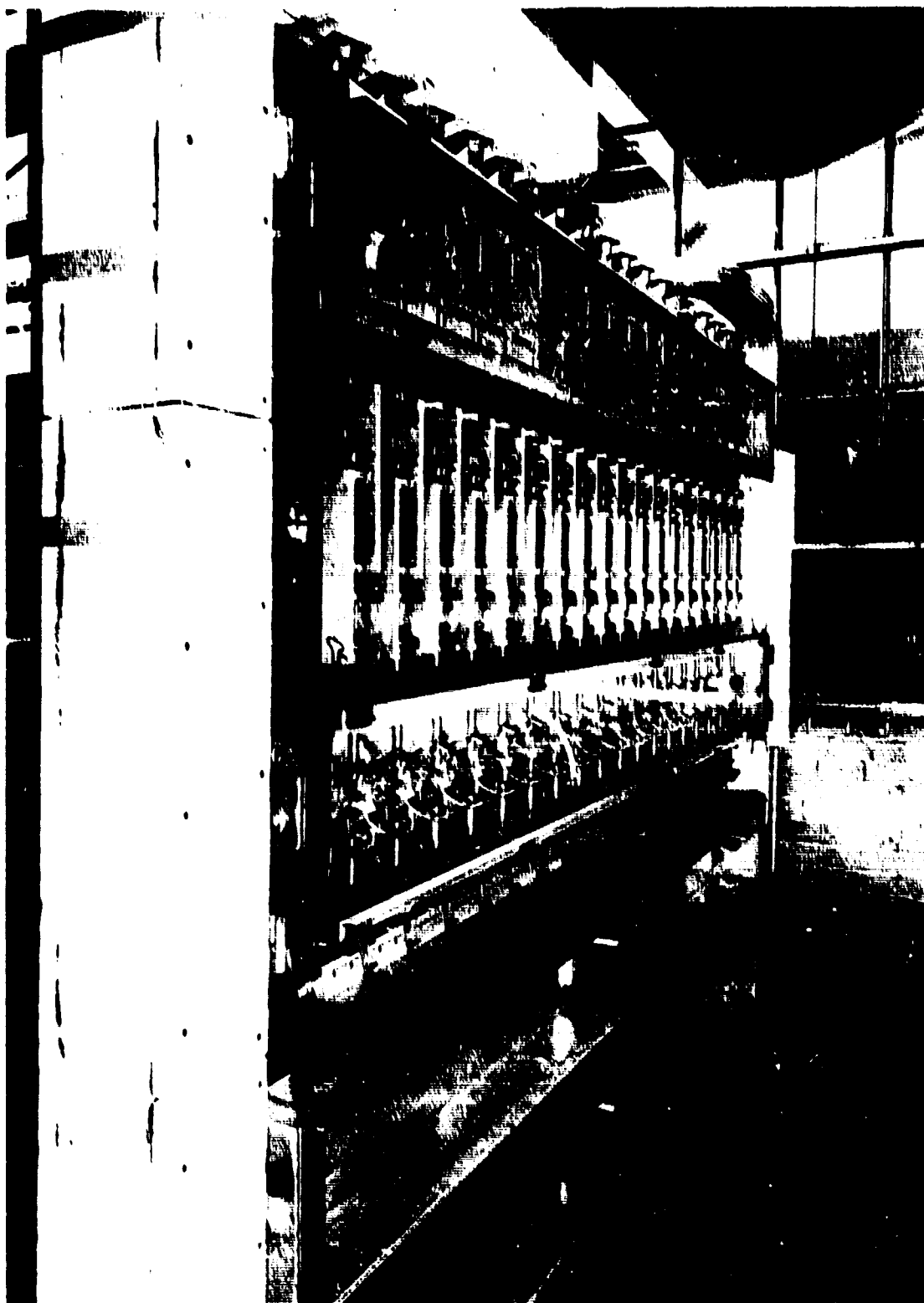
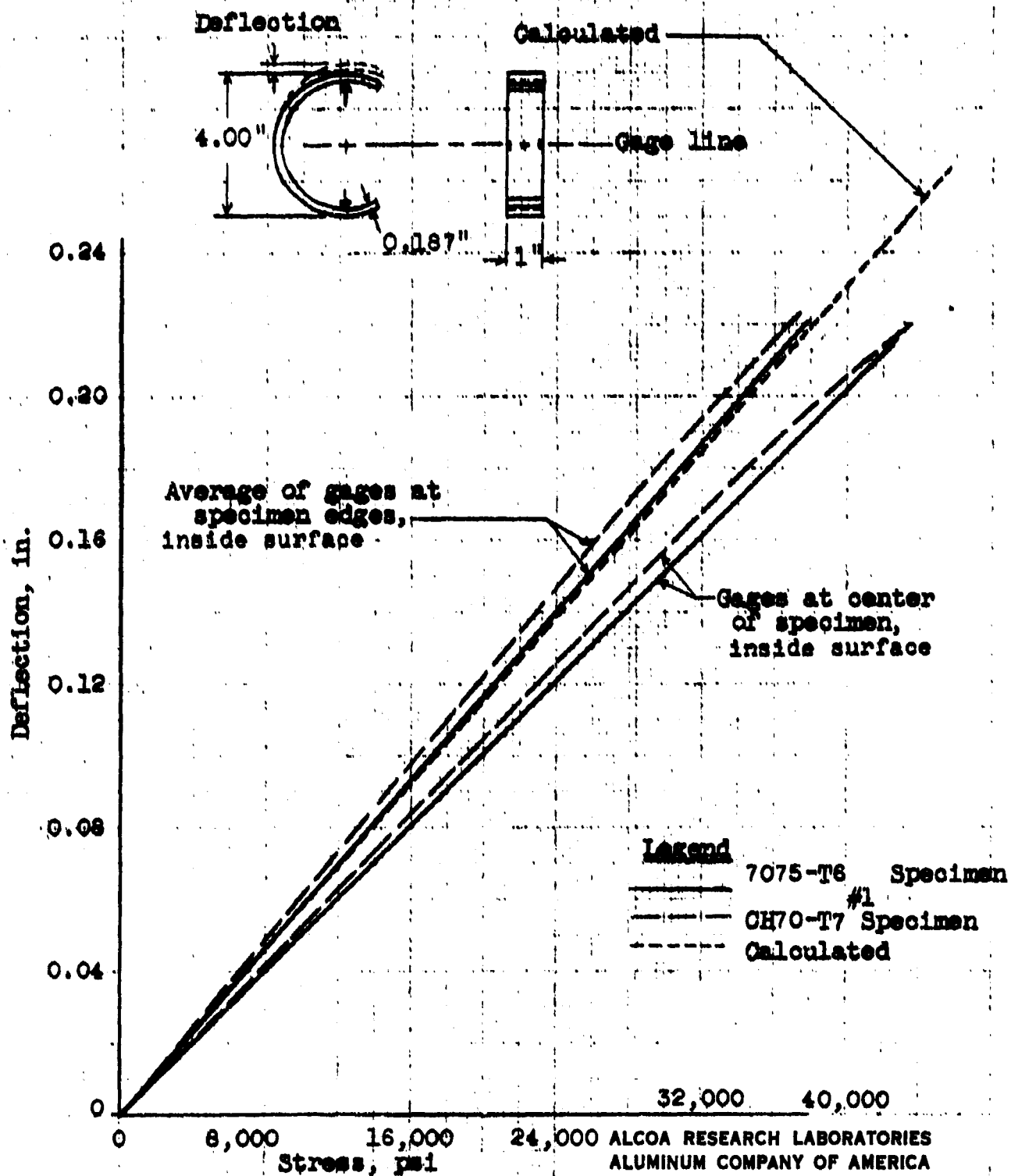


FIG. 14. APPARATUS FOR FATIGUE TESTING C-RINGS IN CONTROLLED ENVIRONMENT



MACHINE FOR FATIGUE AND CORROSION-FATIGUE TESTS OF C-RINGS  
IN CONTROLLED ENVIRONMENT  
Enclosures at bottom of rack are for stress-corrosion tests  
of C-rings in same environments.



ALCOA RESEARCH LABORATORIES  
ALUMINUM COMPANY OF AMERICA  
NEW KENSINGTON, PENNSYLVANIA

Comparison of Measured  
and Calculated Stresses  
in C-Rings

PLOTTED \_\_\_\_\_ DATE \_\_\_\_\_ APPROVED \_\_\_\_\_ DATE \_\_\_\_\_



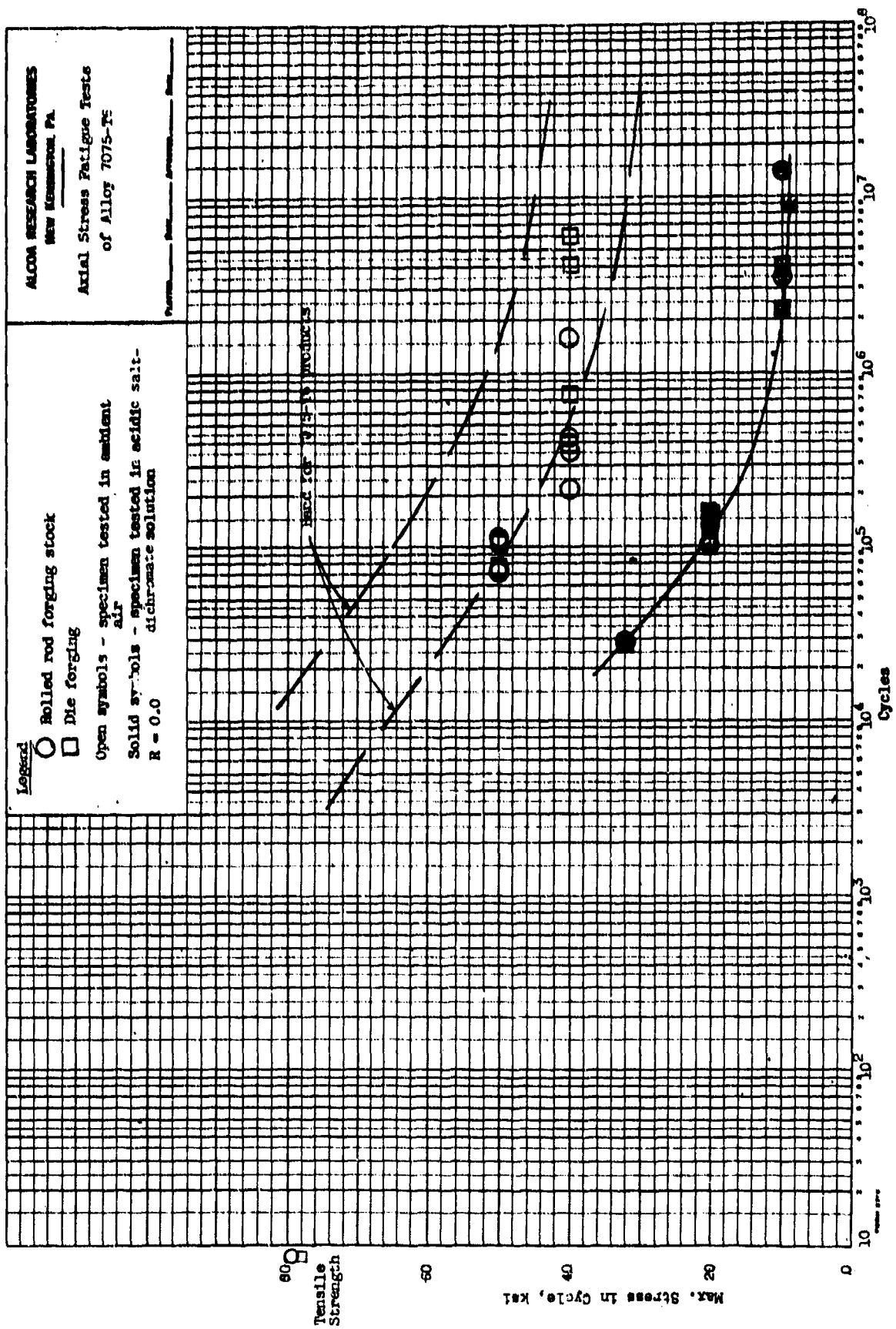


Fig. 17

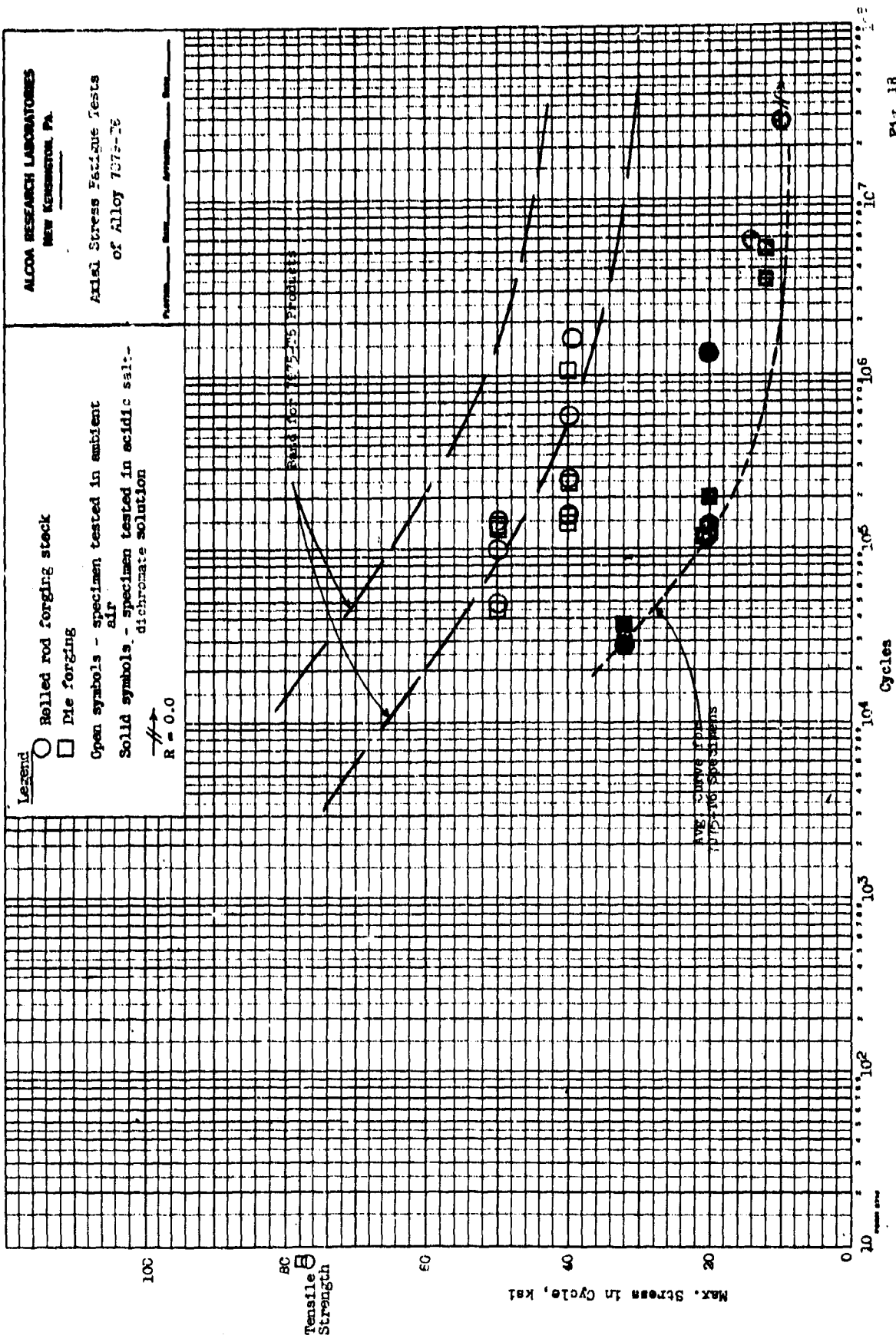


Fig. 18

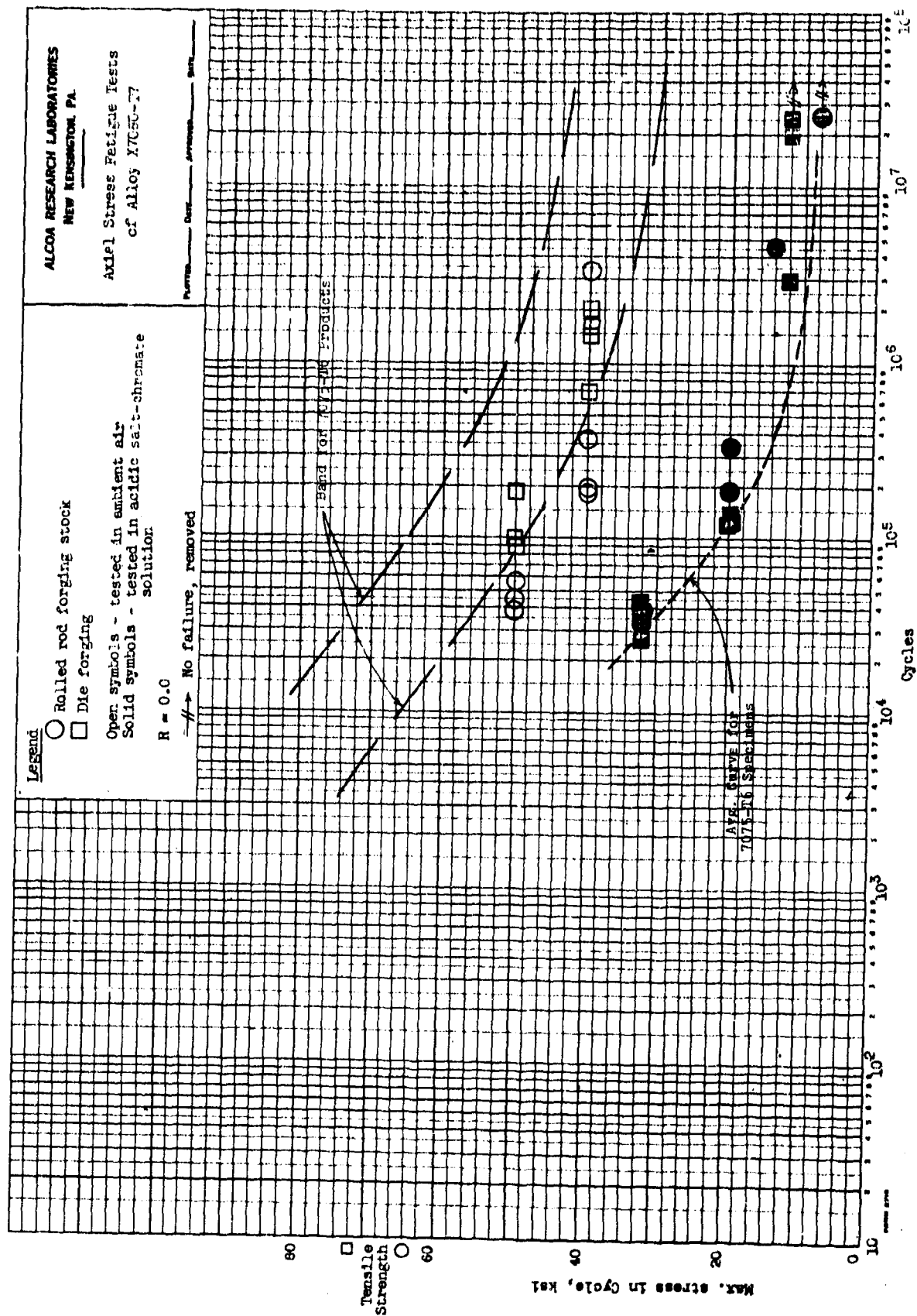


FIG. 15.19

AXIAL-STRESS Fatigue Tests  
of Alloy 2014-T6

**Plotter** — **Dyn** — **Arcweld** — **Pawl**

**Legend**

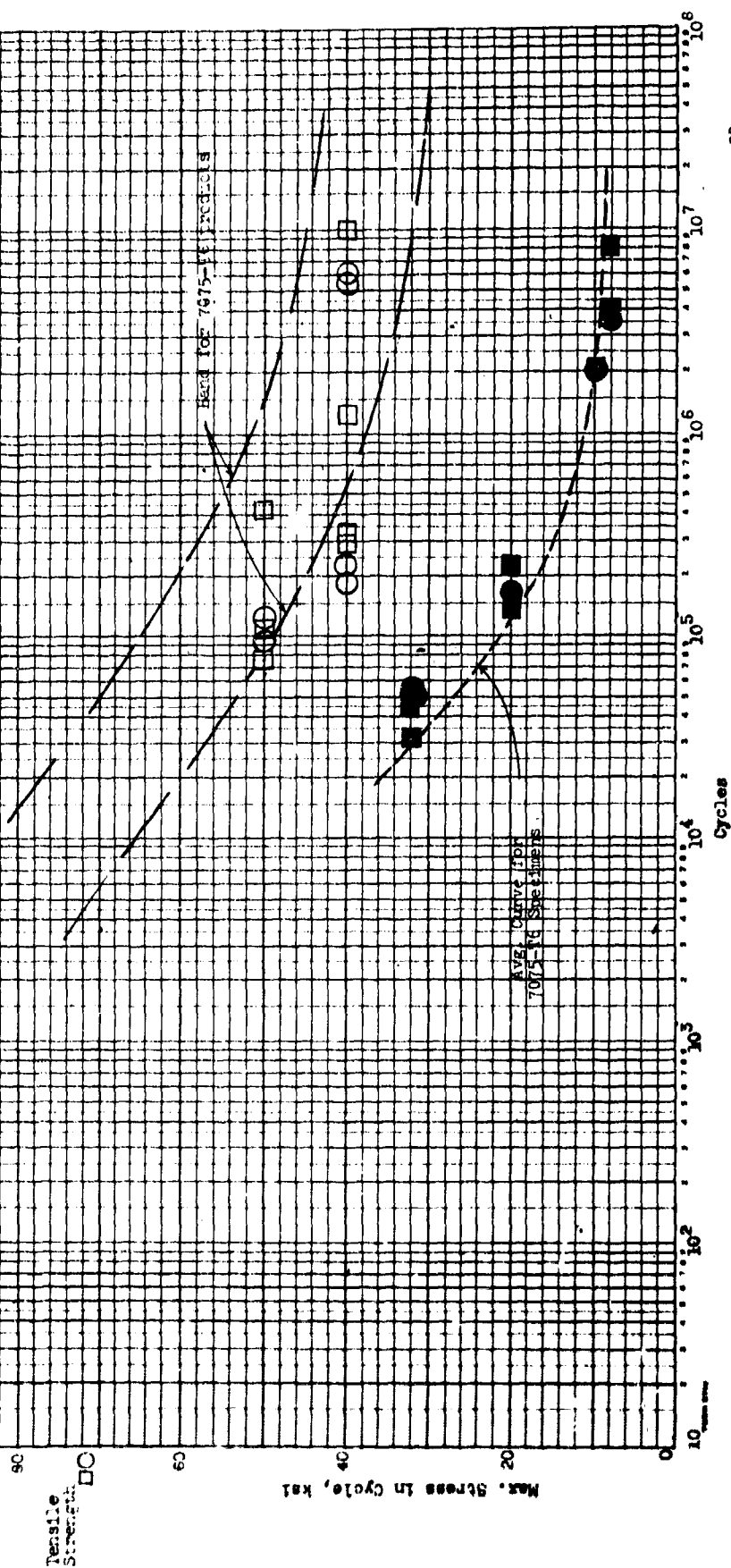
Roller rod forming stock

Die forgnngs

Open symbols - tested in ambient air

Solid symbols - tested in acidic salt-dichromate solution

○  
○  
●  
■



Max. stress in cycle, ksi

### Cycles

Hand for 7675-66 Fred:cls

AVG. CURVE TO  
7075-TH STREET

Plg. 20

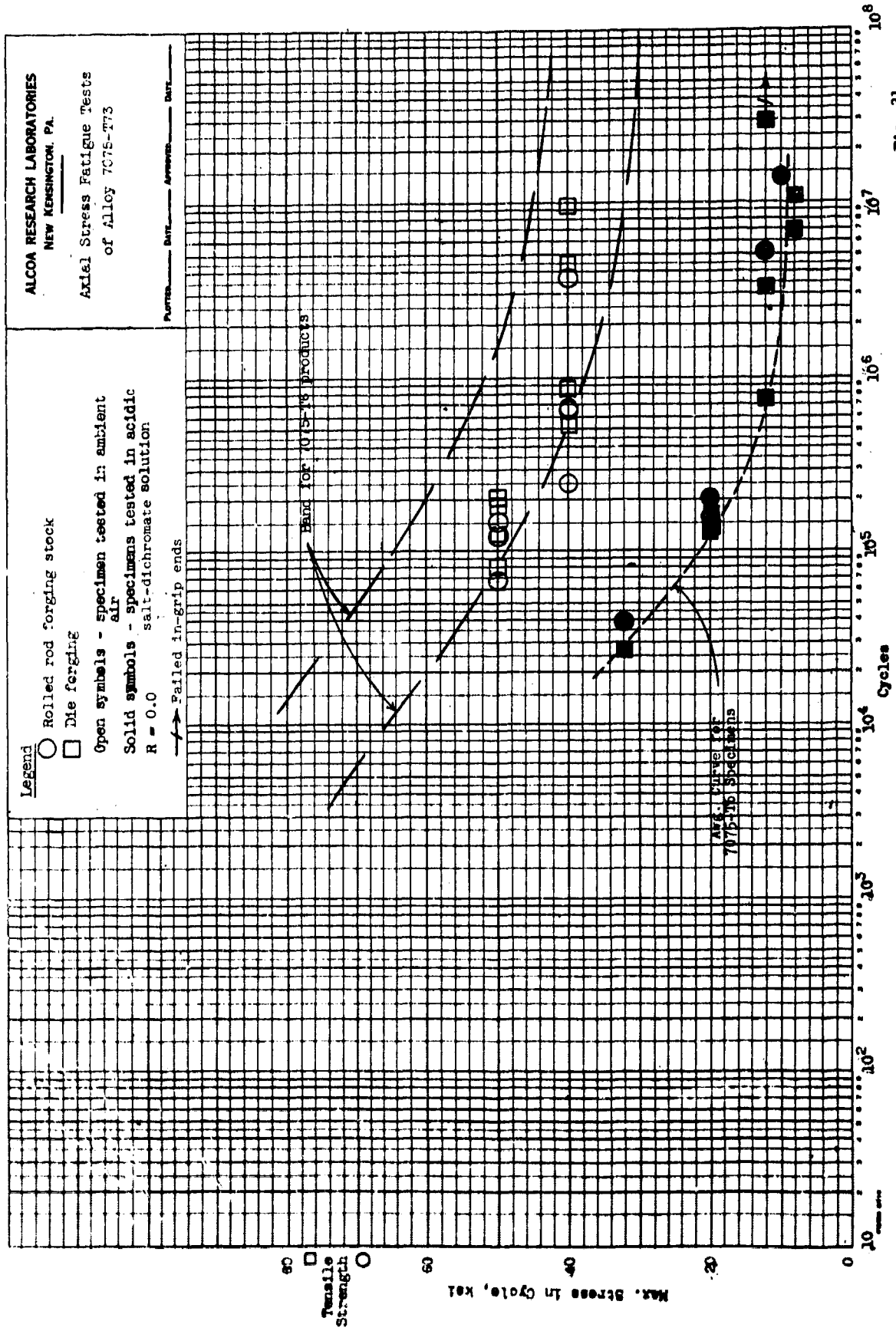


Fig. 21

STRESS-STRAIN CURVES  
 FOR ALUMINUM  
 1000-HOUR  
 100°C

1000-HOUR

100°C

1000-HOUR

100°C

1000-HOUR

100°C

1000-HOUR

100°C

1000-HOUR

100°C

1000-HOUR

100°C

1000-HOUR

100°C

1000-HOUR

100°C

1000-HOUR

100°C

1000-HOUR

100°C

1000-HOUR

100°C

1000-HOUR

100°C

1000-HOUR

100°C

1000-HOUR

100°C

1000-HOUR

100°C

1000-HOUR

100°C

1000-HOUR

100°C

1000-HOUR

100°C

1000-HOUR

100°C

1000-HOUR

100°C

1000-HOUR

100°C

1000-HOUR

100°C

1000-HOUR

100°C

1000-HOUR

100°C

1000-HOUR

100°C

1000-HOUR

100°C

1000-HOUR

100°C

1000-HOUR

100°C

1000-HOUR

100°C

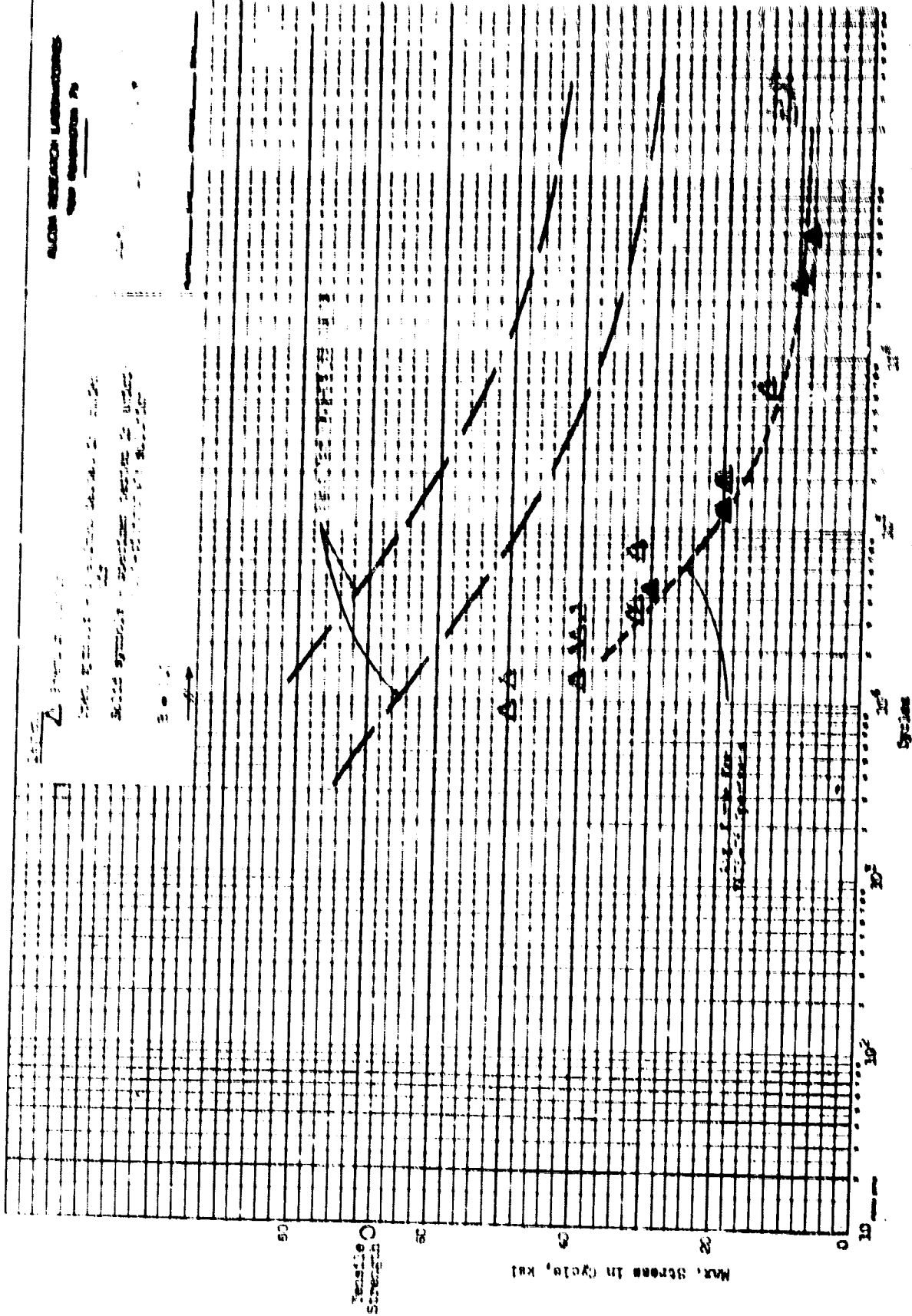
1000-HOUR

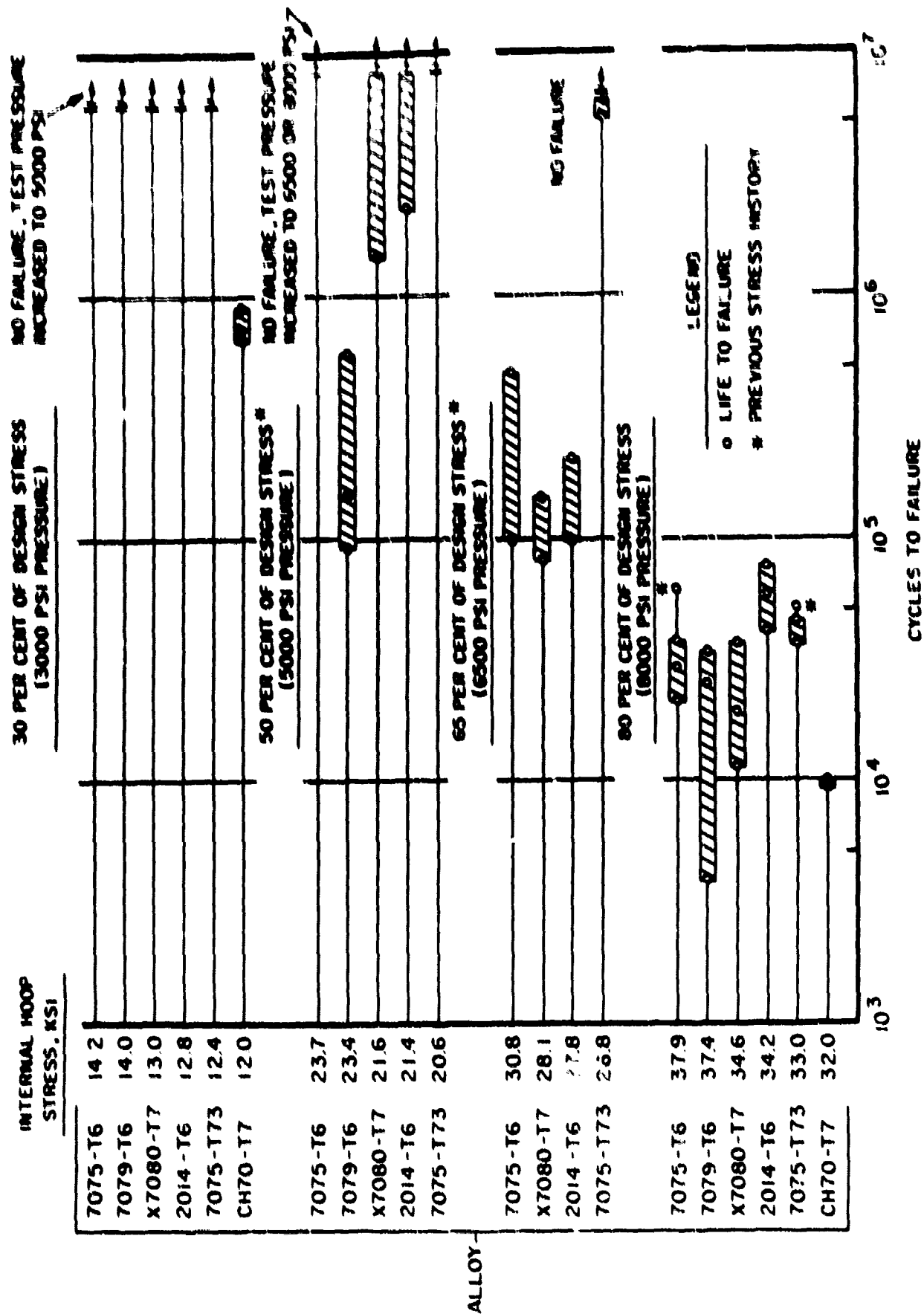
100°C

1000-HOUR

100°C

1000-HOUR





# FATIGUE LIVES OF CYLINDERS - NO CORROSIVE ENVIRONMENT

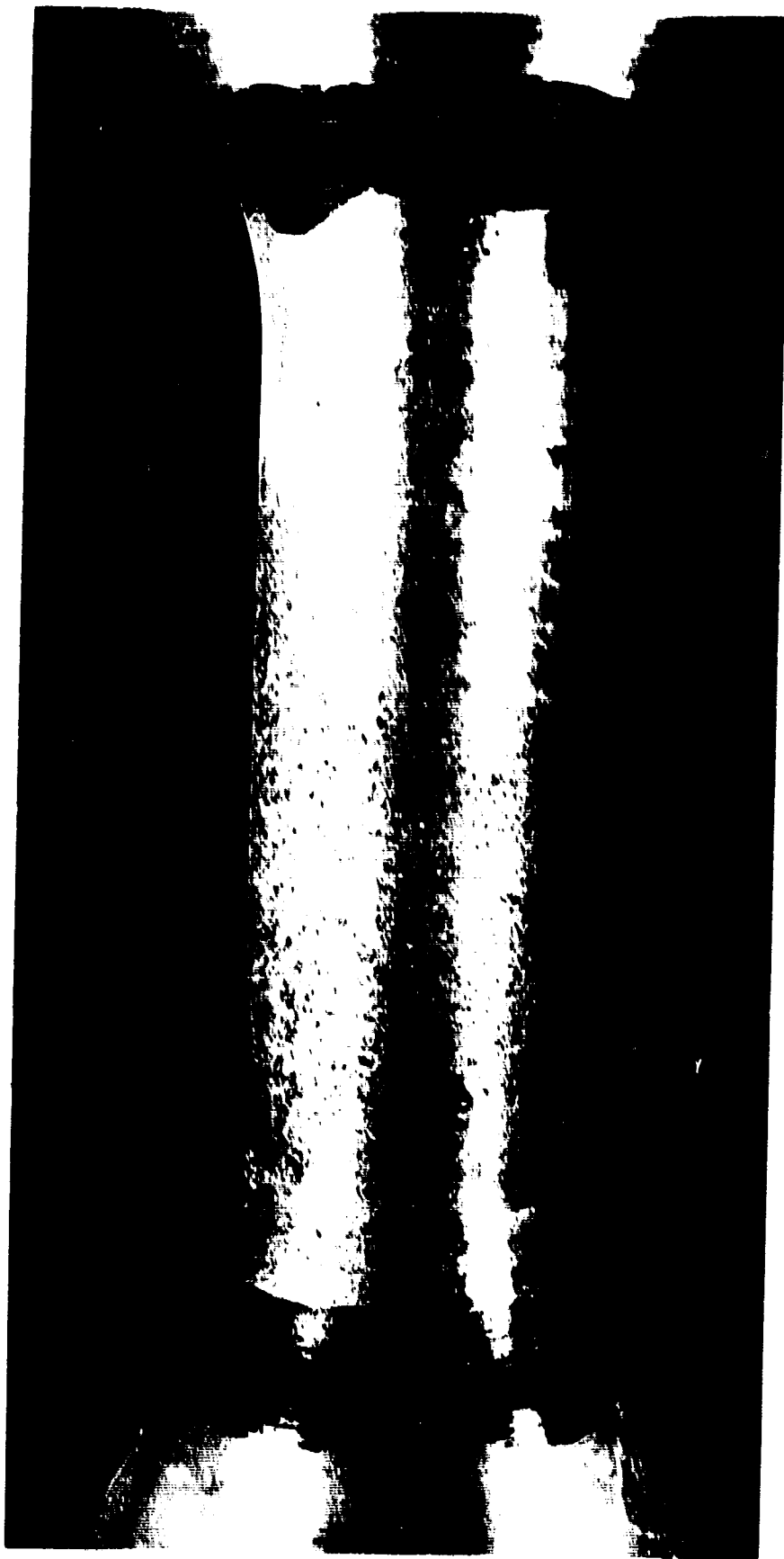
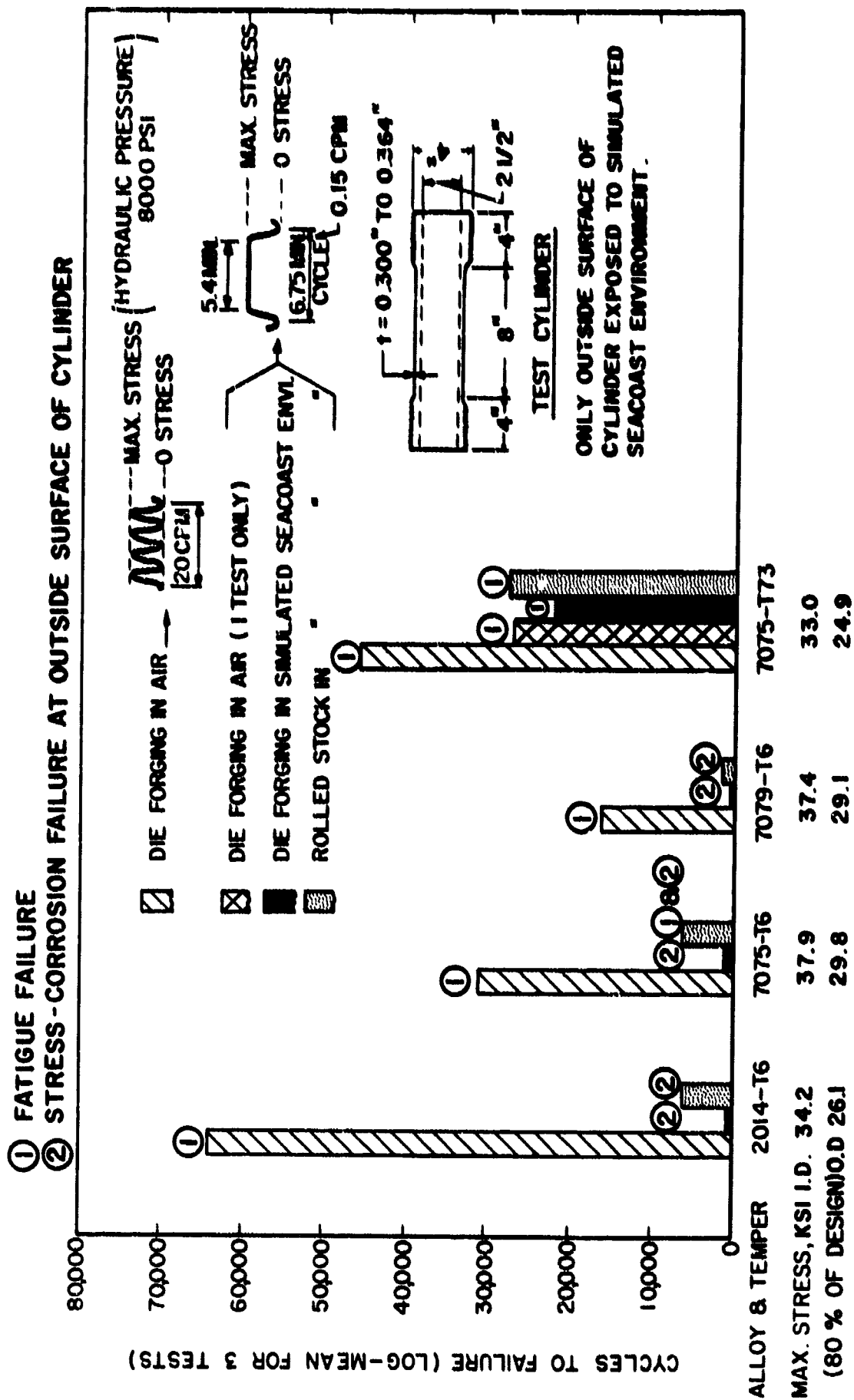


FIG. 24. FAILURE OF 7075-T6 DIE FORGED SPECIMEN #18 IN STATIC STRESS-CORROSION TESTS IN SIMULATED SEACOAST ENVIRONMENT

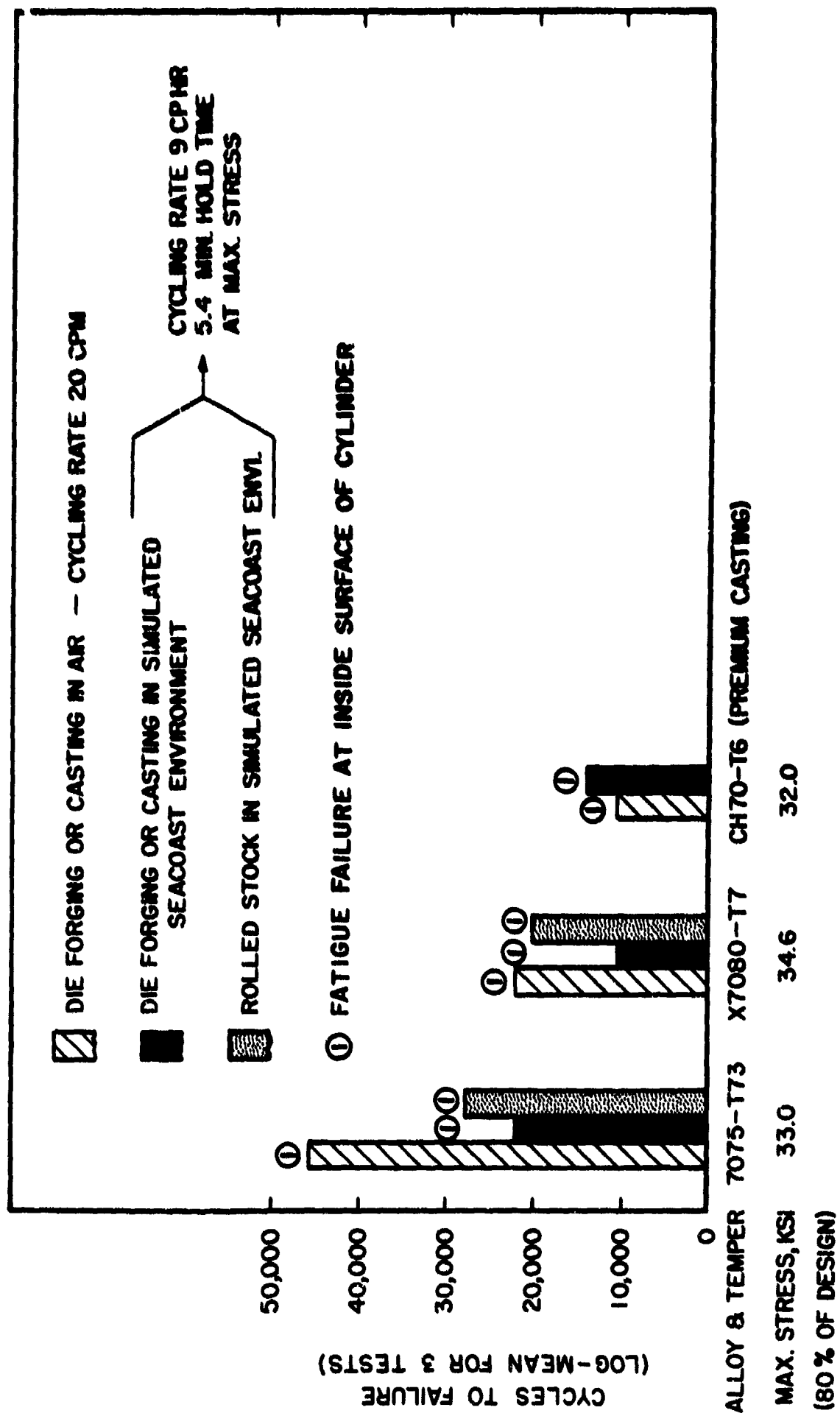
(8000 psi pressure; hoop stress on exterior = 29.8 ksi)





**EFFECT OF ENVIRONMENT ON FATIGUE LIFE OF HYDRAULIC CYLINDERS**

**FIG. 25a**



EFFECT OF ENVIRONMENT ON FATIGUE LIFE OF HYDRAULIC CYLINDERS

FIG. 25b

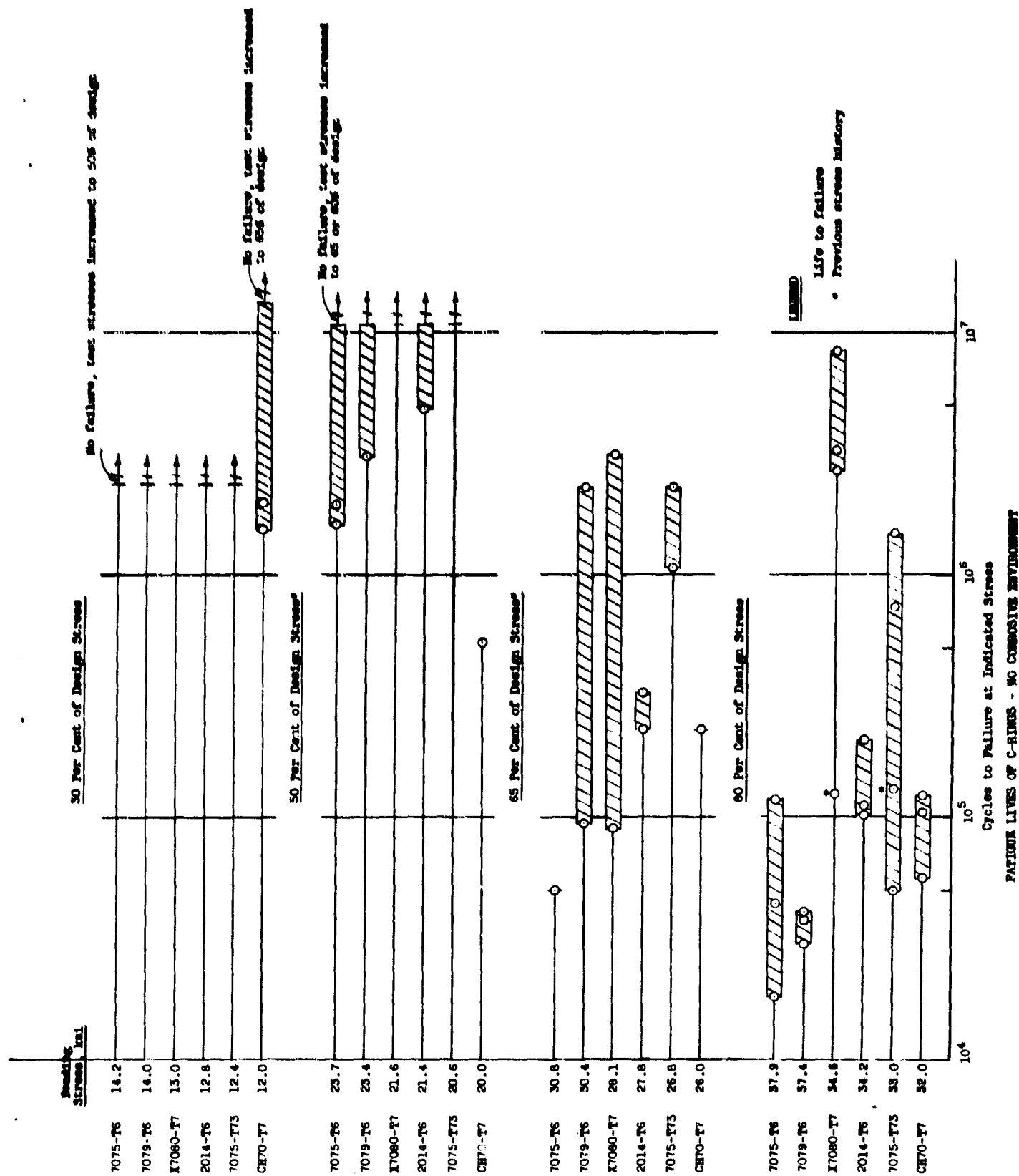
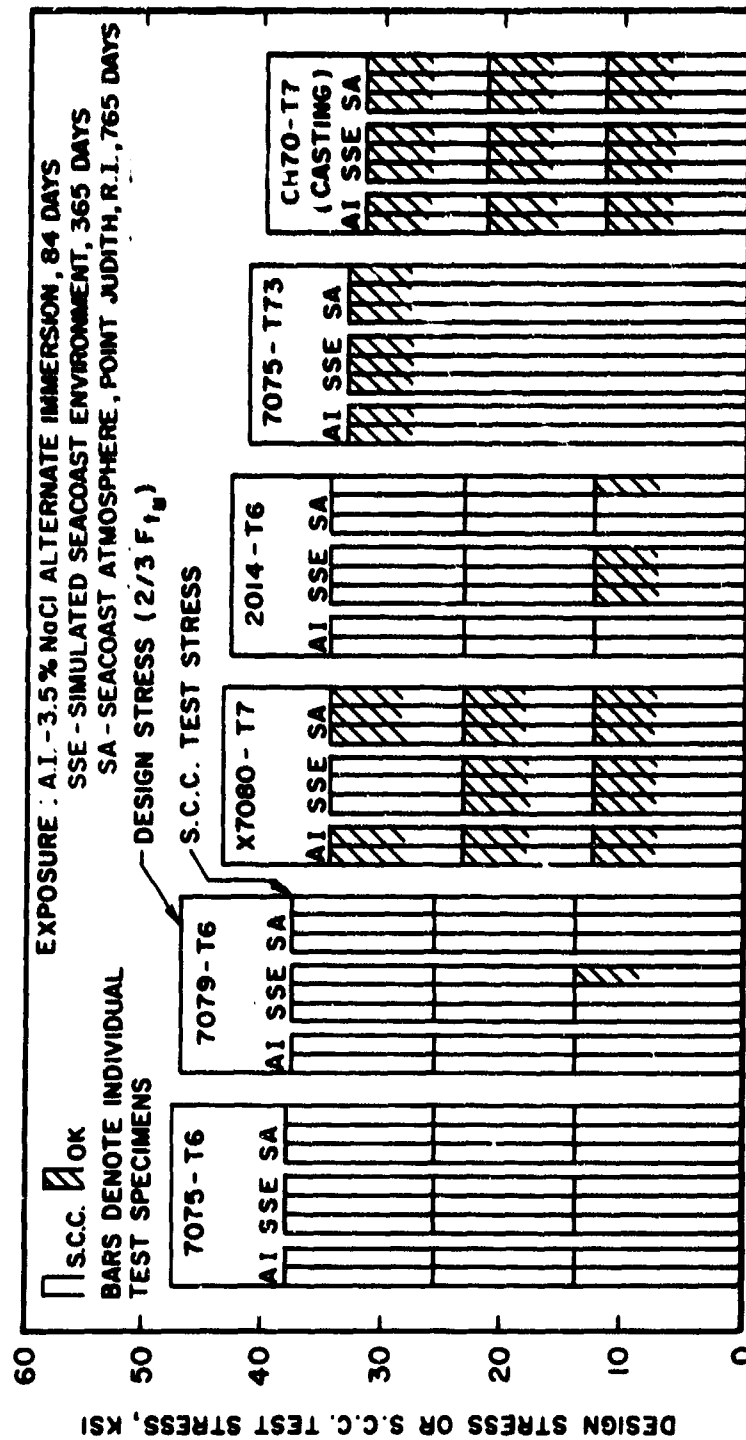


Fig. 26

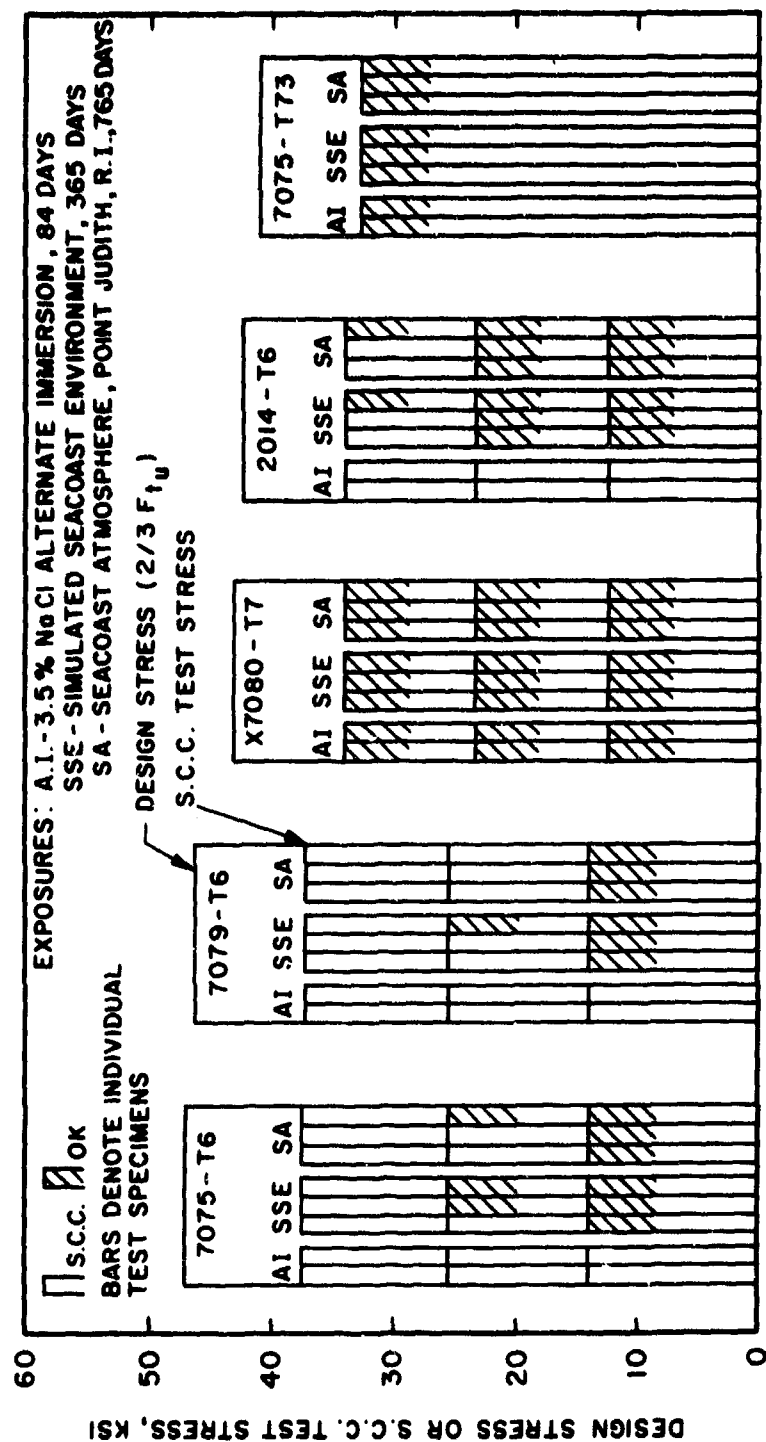
B



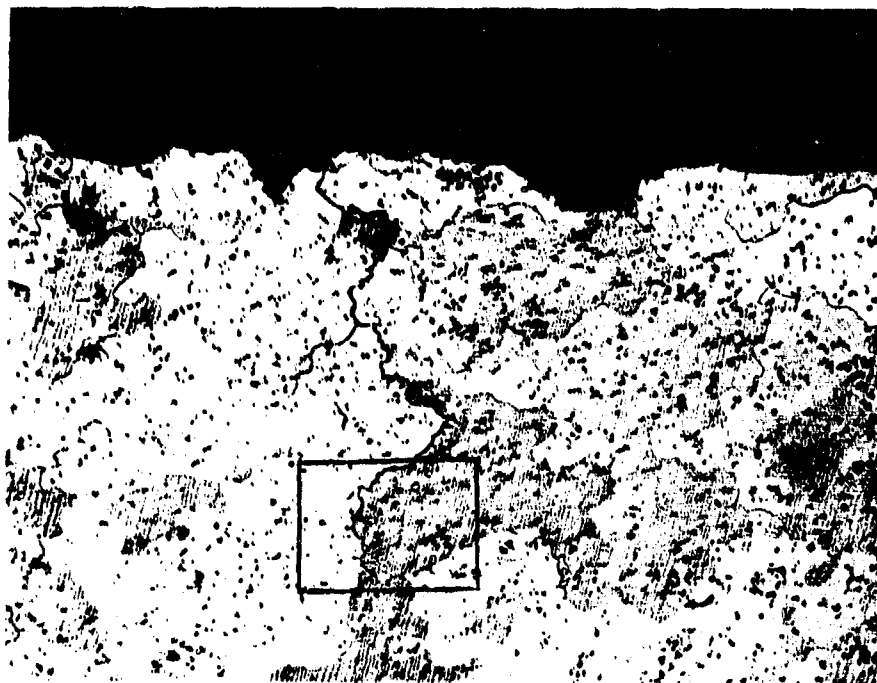
COMPARISON OF THE STRESS-CORROSION PERFORMANCE OF STATIC-LOADED C-RINGS FROM THE DIE FORGINGS AND CAST IN THREE CORROSIVE ENVIRONMENTS.

Fig. 27

62



COMPARISON OF THE STRESS-CORROSION PERFORMANCE OF STATIC-LOADED C-RINGS FROM THE ROLLED ROD STOCK IN THREE CORROSIVE ENVIRONMENTS.



- a Cross-section through C-ring from 2014-T6 rod stock, stressed to 80% of design stress after 44 days' exposure to alternate immersion. Many short stress corrosion cracks of the type illustrated were found. (X100)

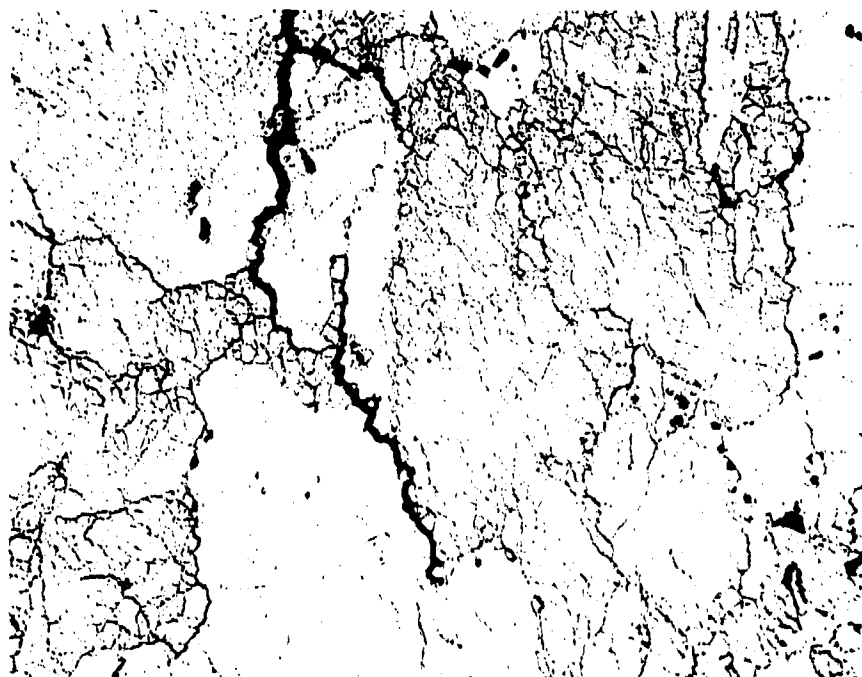


- b Higher magnification of region outlined above more clearly showing the intergranular nature of the cracking, which is typical of stress-corrosion cracking in aluminum alloys. (X500)

STATIC STRESS-CORROSION CRACKING OF C-RING FROM 2014-T6 ROLLED ROD STOCK IN ALTERNATE IMMERSION TEST

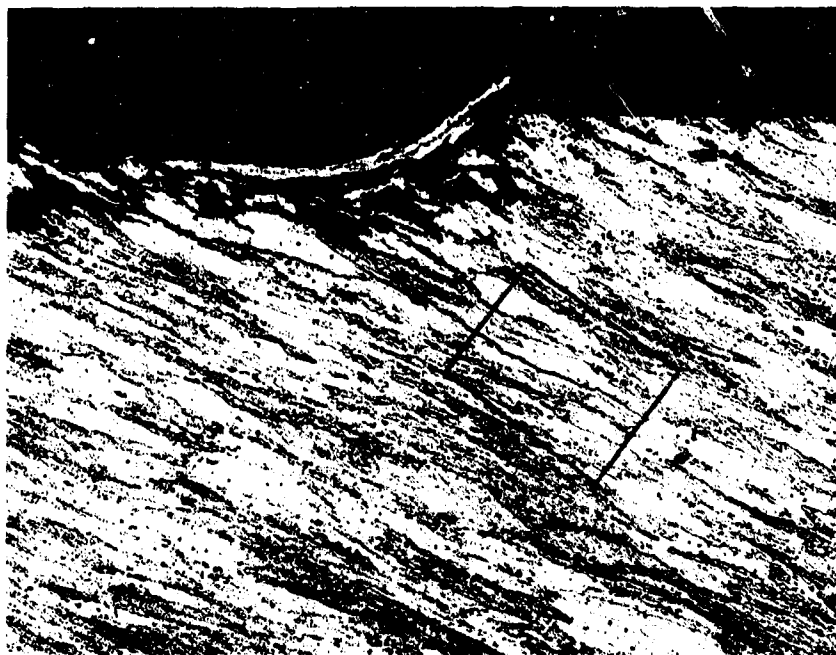


- a Cross-section through C-ring from 7075-T6 rod stock, stressed to 80% of design stress after 44 days' exposure to alternate immersion. Many short stress corrosion cracks of the type illustrated were found. (X100)



- b Higher magnification of region outlined above more clearly showing the intergranular nature of the cracking, which is typical of stress-corrosion cracking in aluminum alloys. (X500)

STATIC STRESS-CORROSION CRACKING OF C-RING FROM 7075-T6 ROLLED ROD STOCK IN ALTERNATE IMMERSION TEST



a

Cross-section through one of the C-rings from 7075-T6 die forging stressed to 30% design stress after 293 days' exposure to the simulated seacoast environment. These rings were removed from test because of exfoliation in the test region but microscopic examination showed small stress corrosion cracks were also present. (X100)



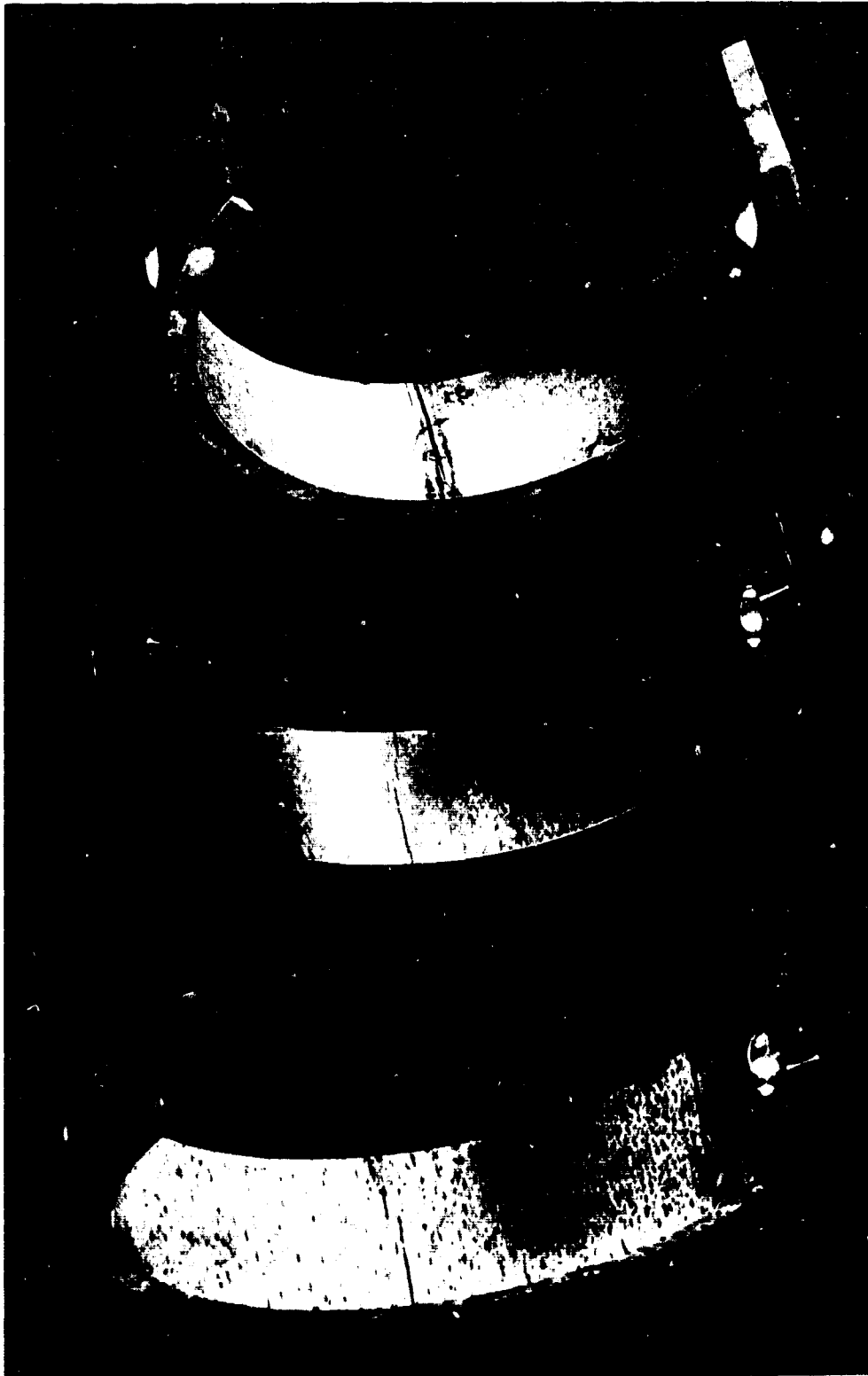
b

Higher magnification of region outlined above showing the crack is following an intergranular path, which is typical of stress-corrosion cracking in aluminum alloys. (X500)

STATIC STRESS-CORROSION CRACKING OF C-RING FROM 7075-T6 FORGING  
IN SIMULATED SEACOAST ENVIRONMENT

Fig. 31





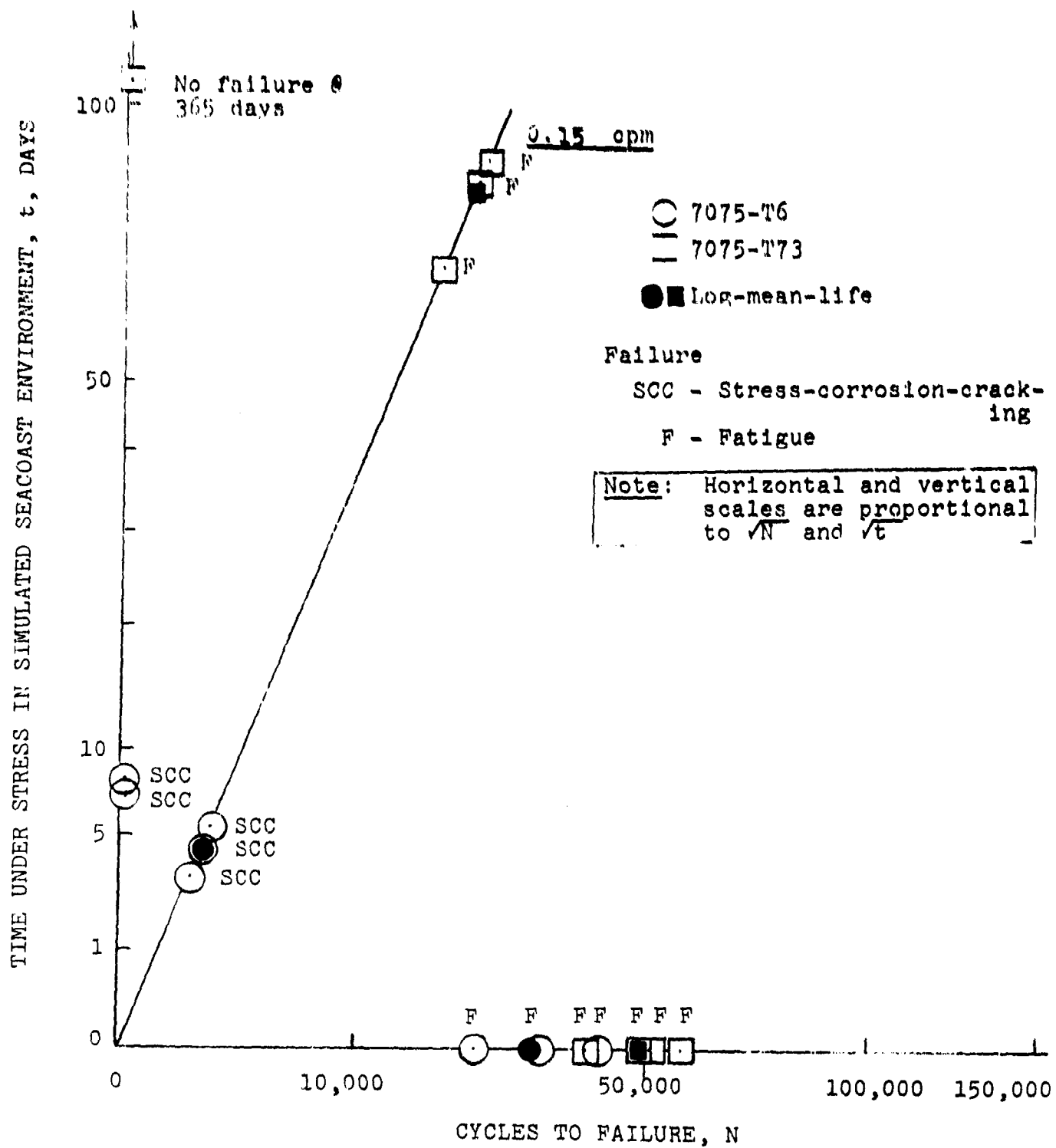
30 Days A. I.

70 Days S. S. E.

210 Days S. A.

Illustrates appearance of three C-rings from the 7075-T6 forging after exposure to 3.5% NaCl - alternate immersion, simulated seacoast environment and seacoast atmosphere at a stress of 55% design stress. Note that the corrosivity of the simulated seacoast environment is similar to the actual seacoast atmosphere causing a general roughening of the surface. In contrast, the alternate immersion test is more corrosive and develops discrete pits.

FIG. 32. TYPICAL STRESS-CORROSION FAILURES OF STATICALLY LOADED C-RINGS

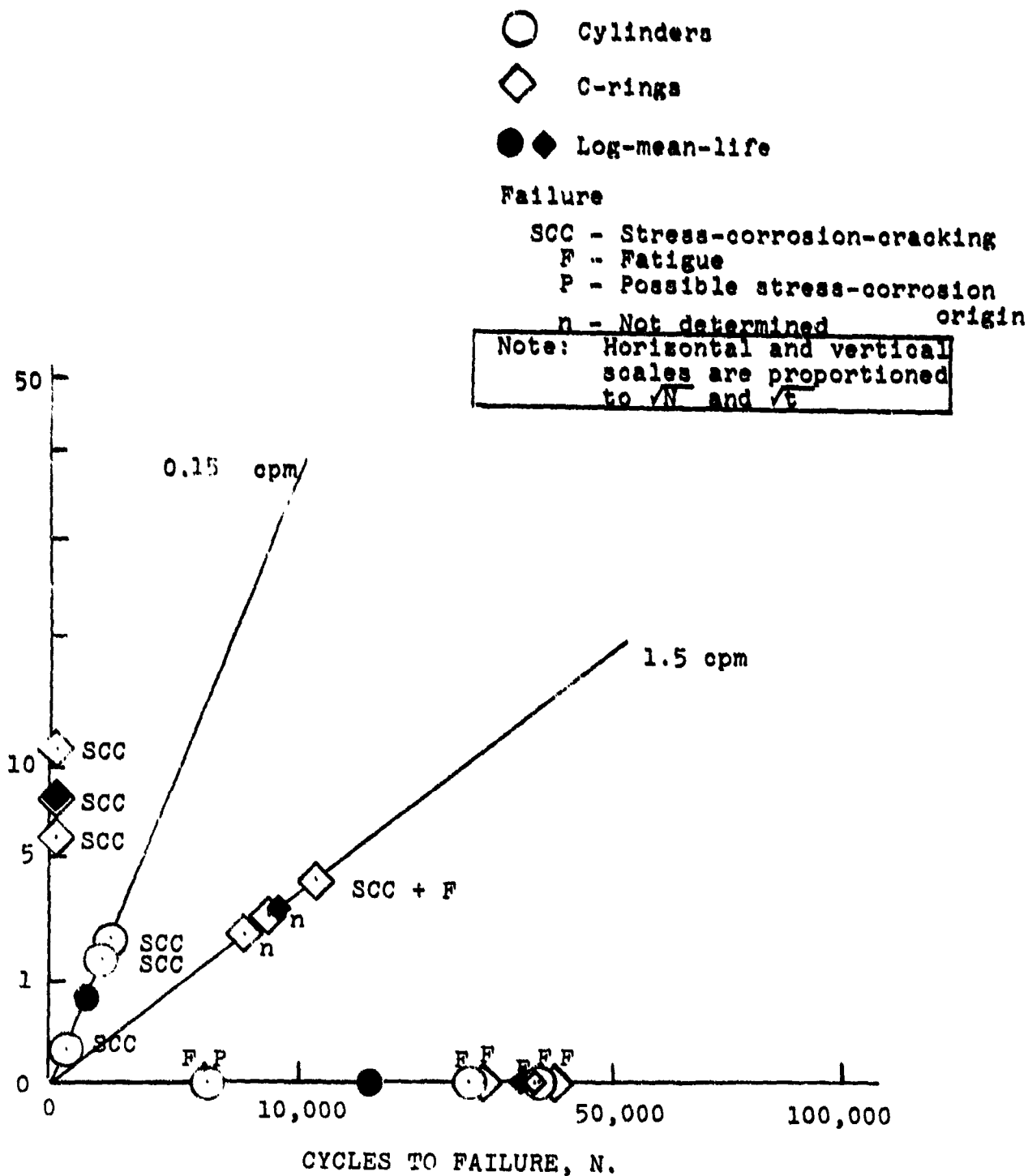


STRESS-CORROSION-FATIGUE TESTS OF 7075-T6 AND 7075-T73 CYLINDERS

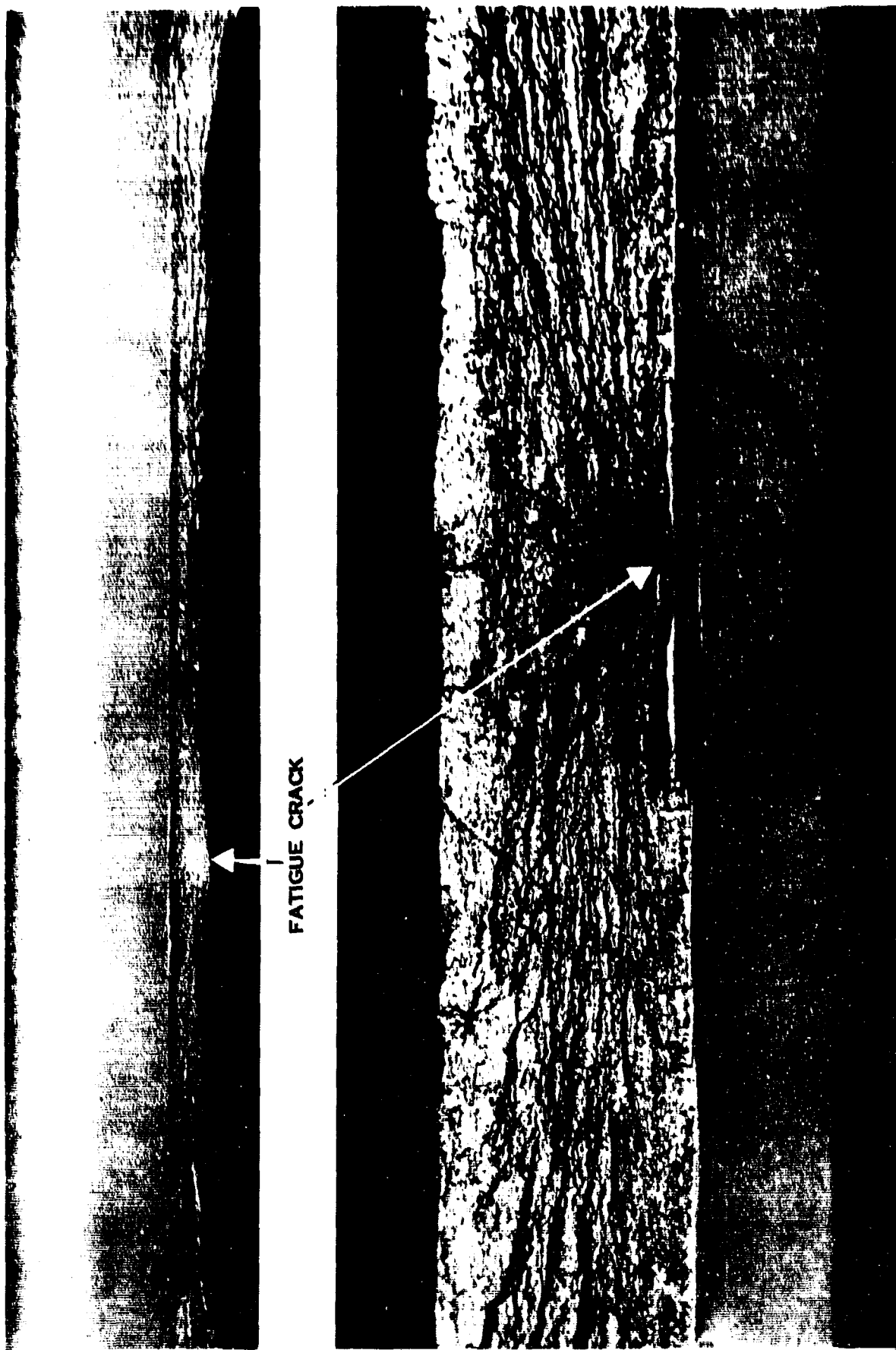
Maximum Stress = 80% of Design



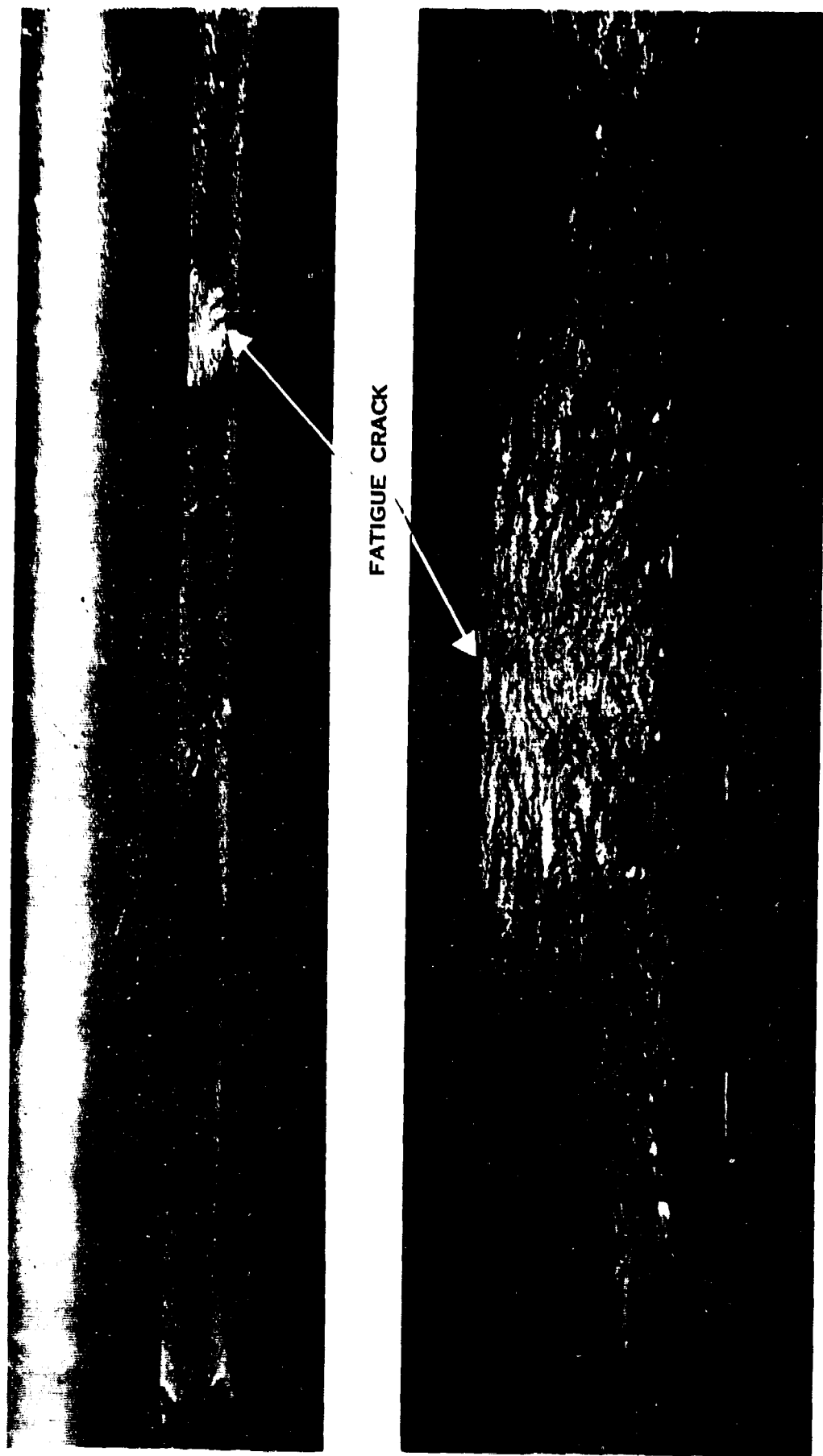
TIME UNDER STRESS IN SIMULATED SEACOAST ENVIRONMENT, t, DAYS



STRESS-CORROSION-FATIGUE TESTS OF 7079-T6 CYLINDERS AND C-RINGS  
Maximum Stress = 80% of Design



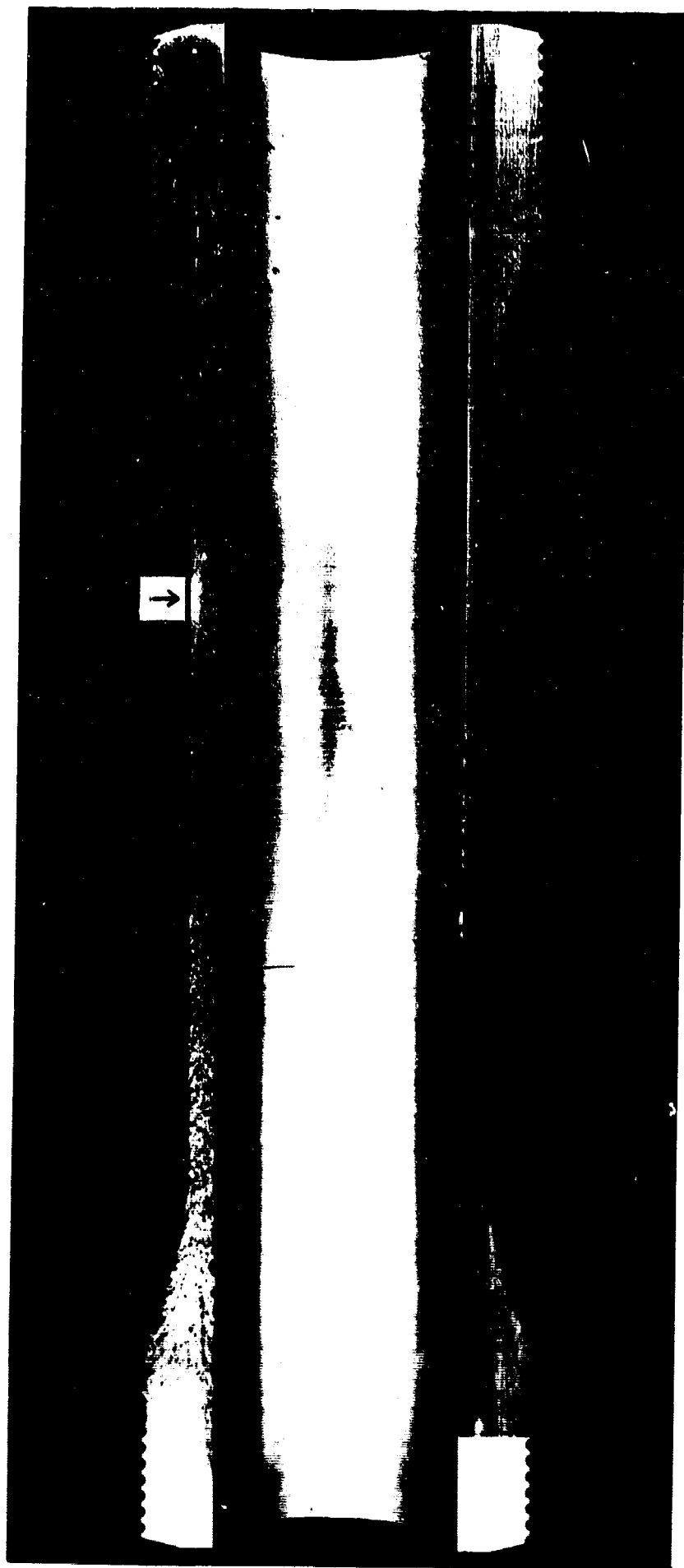
FRACTURE OF 7079 - T6 CYLINDER NO. 7 RESULTING FROM FATIGUE CRACK  
PROPAGATING FROM OUTSIDE SURFACE (WALL THICKNESS 0.306 IN.)



FRACTURE OF 7075 - T73 CYLINDER NO. 7 RESULTING FROM FATIGUE CRACK  
PROPAGATING FROM INSIDE SURFACE (WALL THICKNESS 0.350 IN.)



FAILURES OF CH70-T7 CYLINDERS RESULTING FROM FATIGUE CRACKS  
PROPAGATING FROM INSIDE SURFACE (WALL THICKNESS 0.364 IN.)

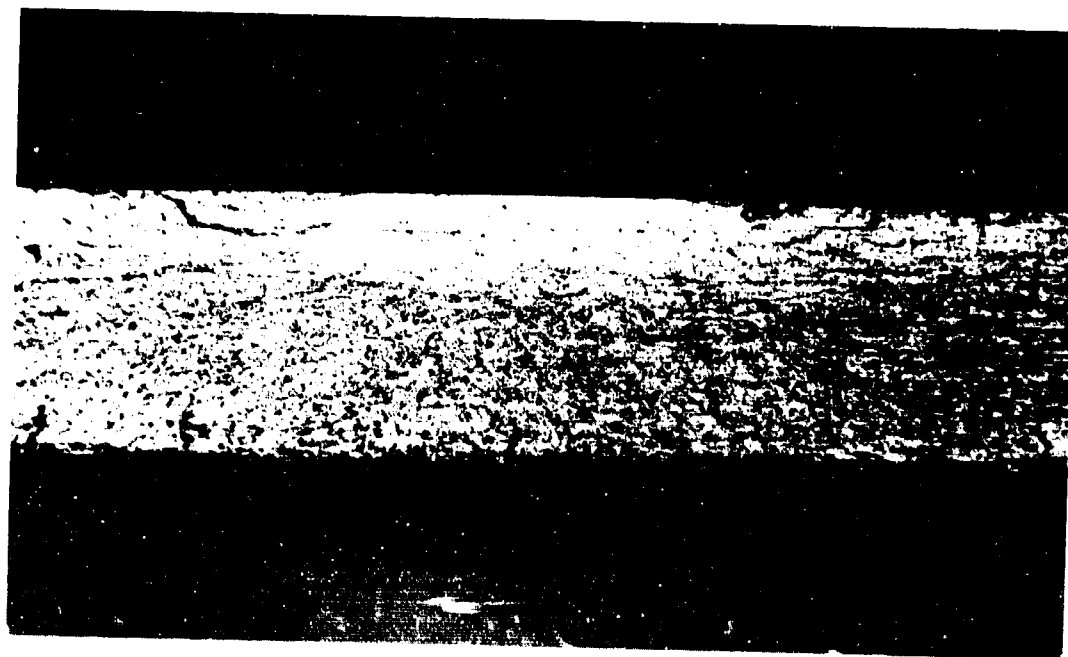


2/3 Actual Size

Longitudinal splitting of cylinder in corrosion-fatigue test. Single crack initiation site in 7079-T6 cylinder is indicated by arrow.

Figure 38





Single initiation site in Fig. 38 at higher magnification, showing gradual transition from slow-fracture to fast-fracture region (X5).

Figure 39



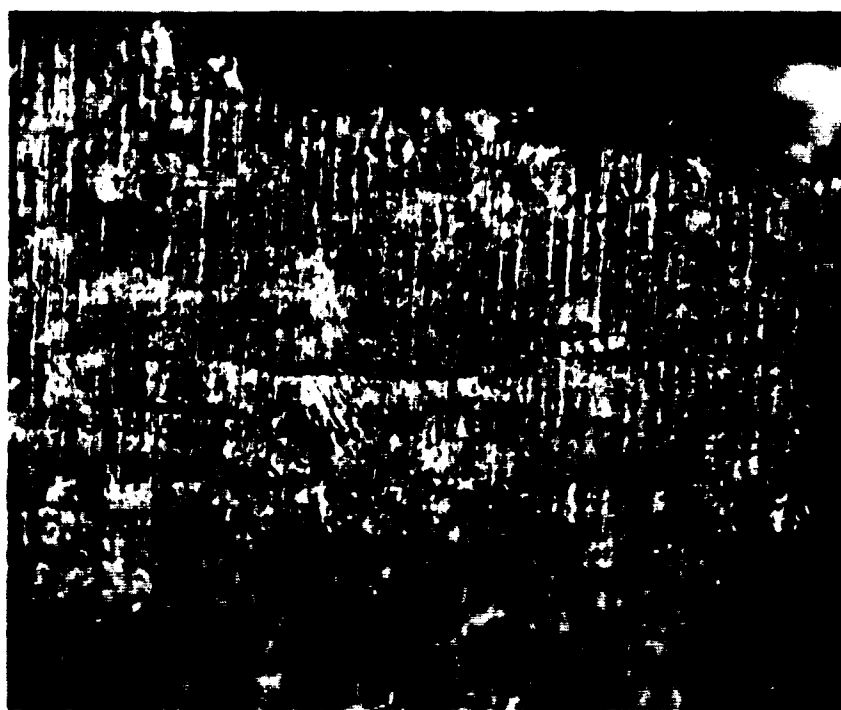
Multiple cracking sites and difference in appearance of slow and fast-fracture regions characteristic of 2014-T6 and 7075-T6 cylinders in corrosion-fatigue test (X5).

Figure 40



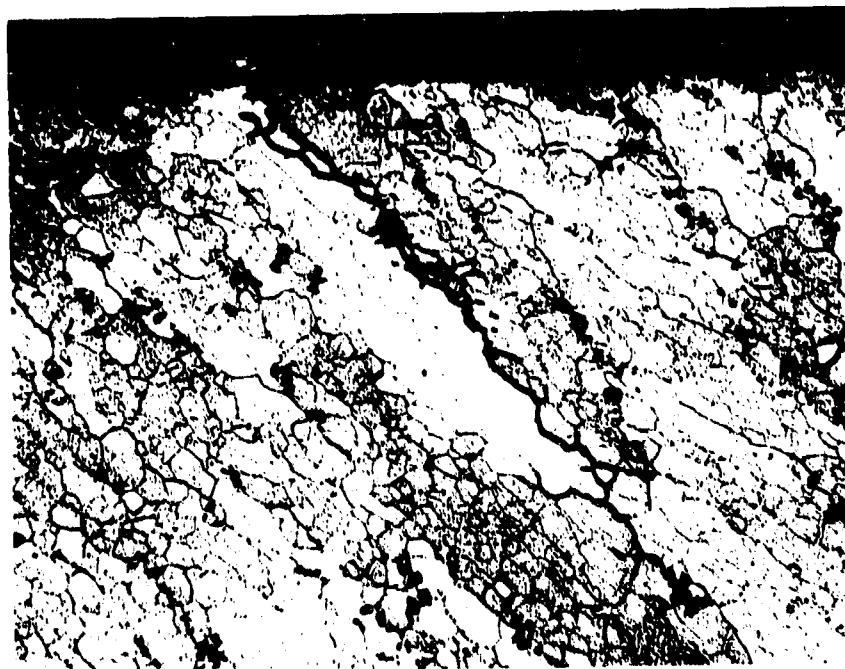
Multiple auxiliary cracks adjacent to main fracture in 7075-T6 corrosion-fatigue specimen (X30).

Figure 41



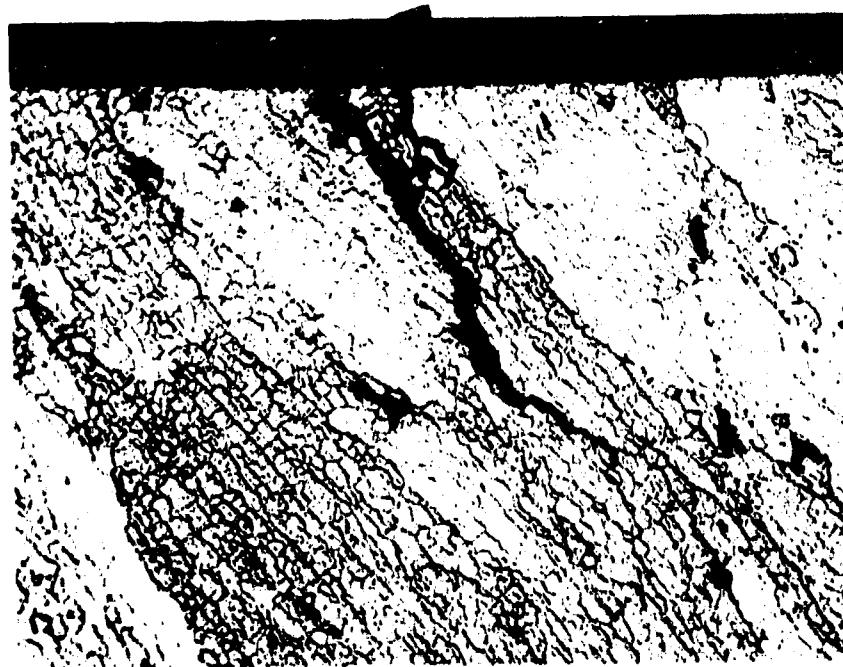
Multiple auxiliary cracks adjacent to main fracture in 2014-T6 corrosion-fatigue specimen (X30).

Figure 42



Intergranular and interfragmentary path of one of the auxiliary cracks (Fig. 42) in 2014-T6 cylinder in corrosion-fatigue test (X500).

Figure 43



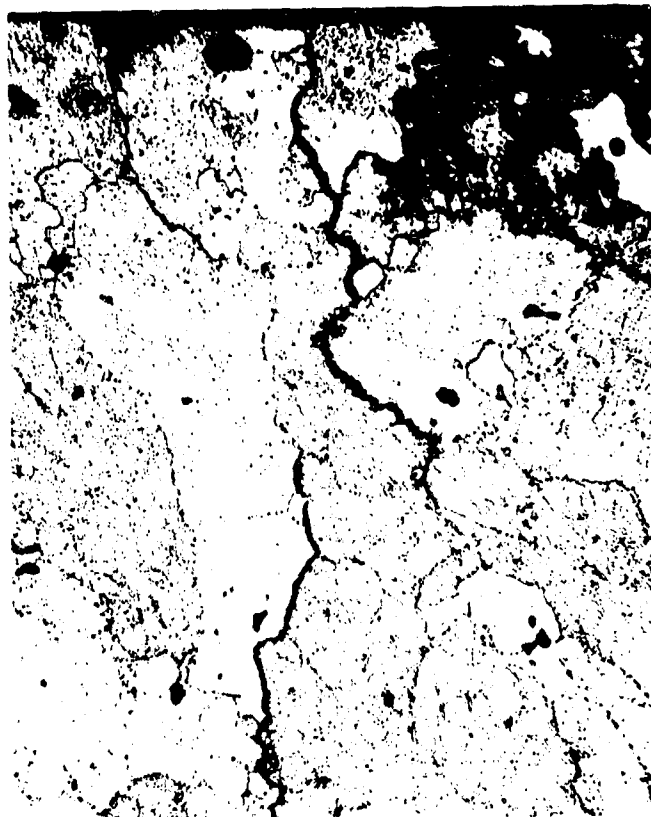
Intergranular and interfragmentary path of auxiliary crack (Fig. 41) in 7075-T6 cylinder from corrosion-fatigue test (X500).

Figure 44

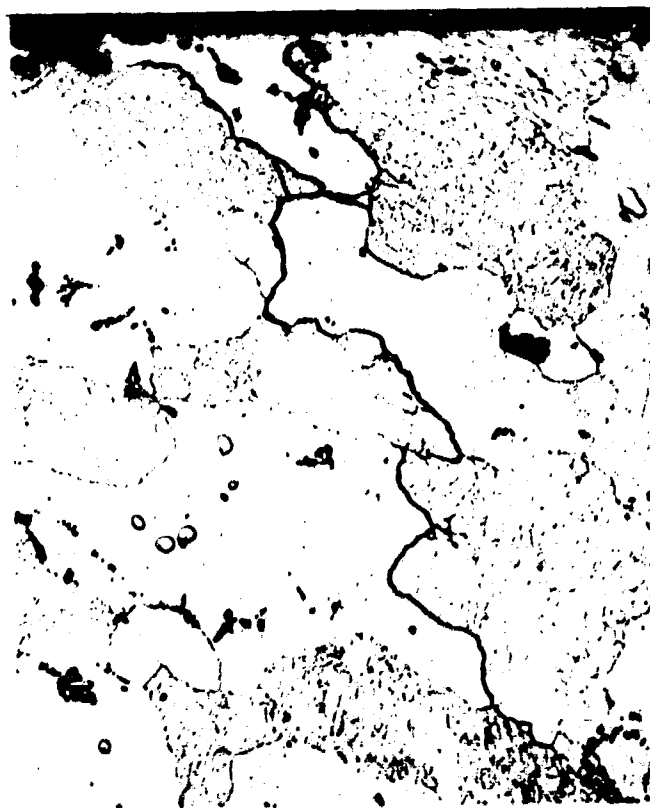


Intergranular and interfragmentary path of auxiliary crack in 7075-T6 cylinder from stress-corrosion test (X500).

Figure 45



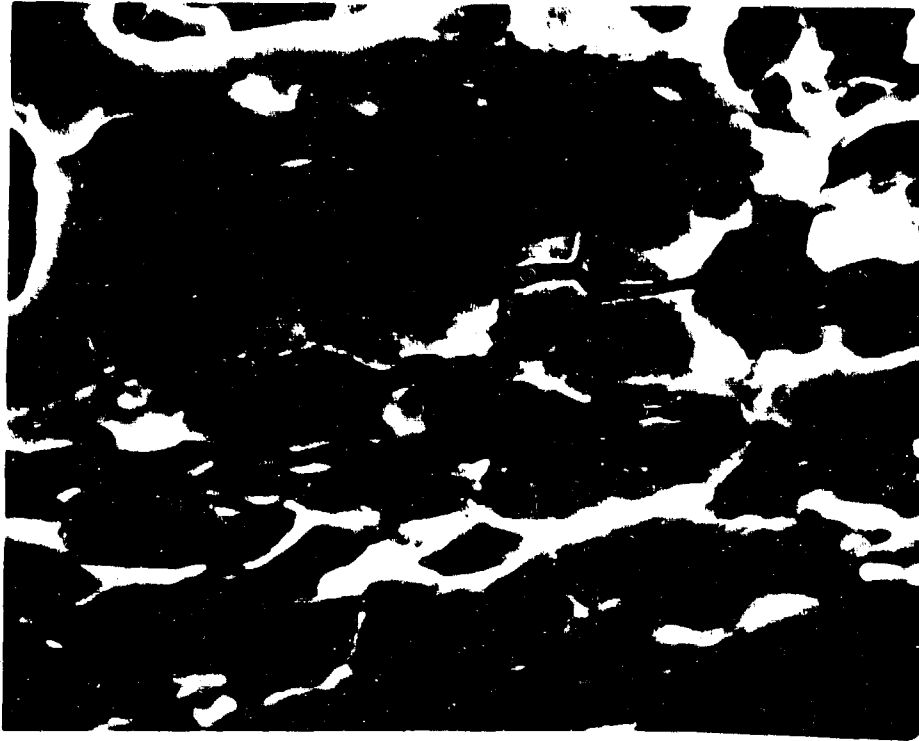
7075-T6



2014-T6

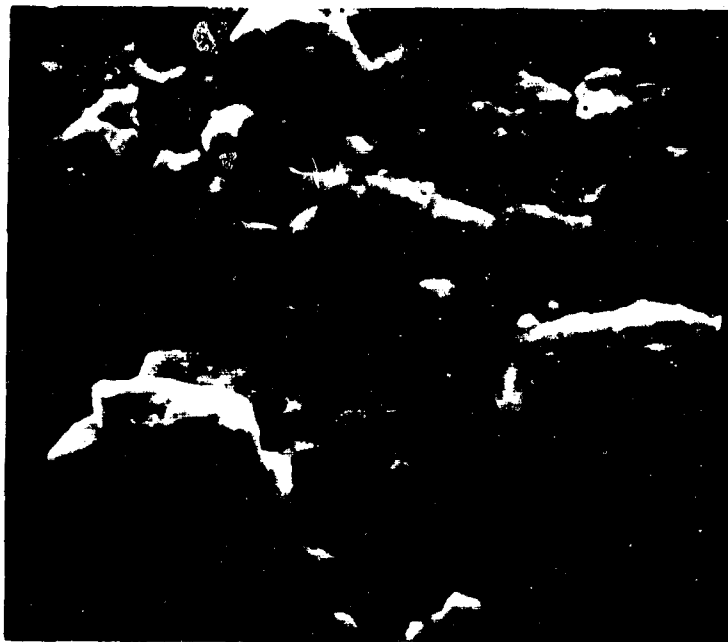
Cross sections of auxiliary cracks in cylinders  
from rod exposed to corrosion-fatigue test (X500).

Figure 46



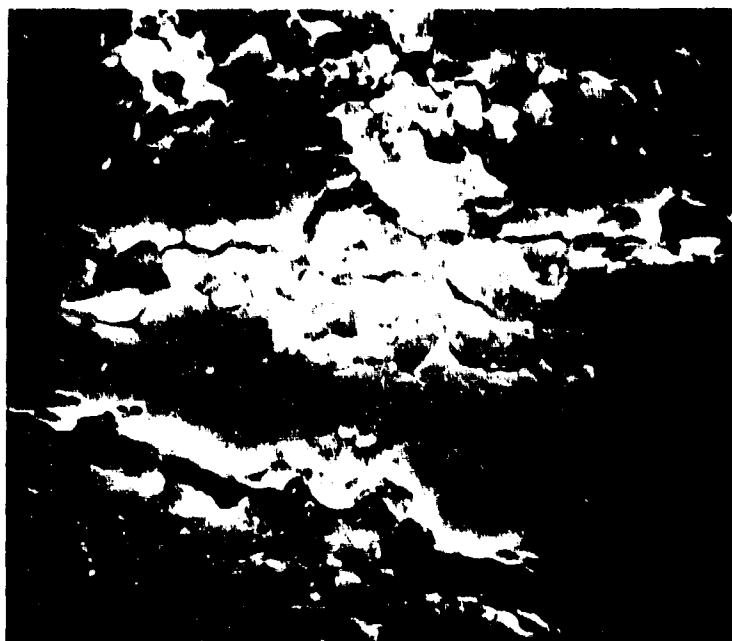
Scanning electron micrograph (SEM) of fracture surface in slow-fracture region of 7079-T6 cylinder in corrosion-fatigue test (X1000).

Figure 47



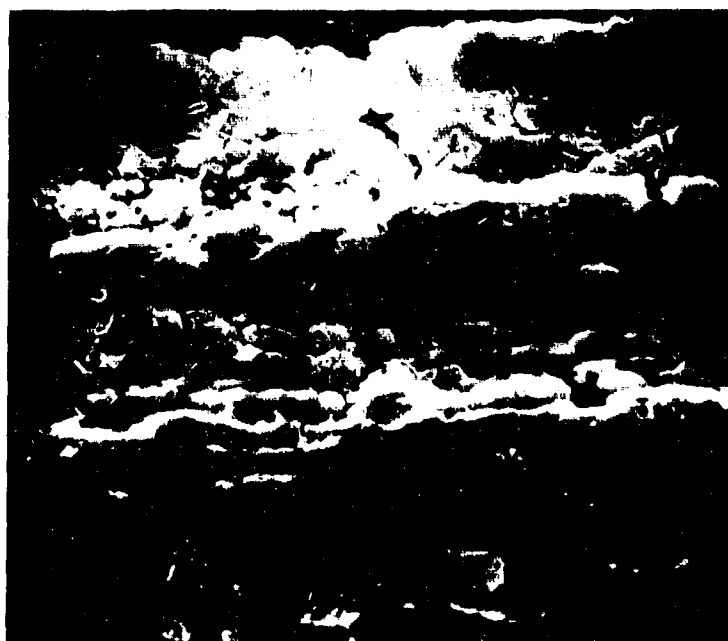
SEM of fracture surface in slow-fracture region of 2014-T6 cylinder in corrosion-fatigue test (X1600).

Figure 48



SEM of fracture surface in slow-fracture region of 7075-T6 cylinder in corrosion-fatigue test (X900).

Figure 49



SEM of fracture surface in slow-fracture region of 7075-T6 cylinder in stress-corrosion test (X1000).

Figure 50



a Ray pattern at origin (X70)

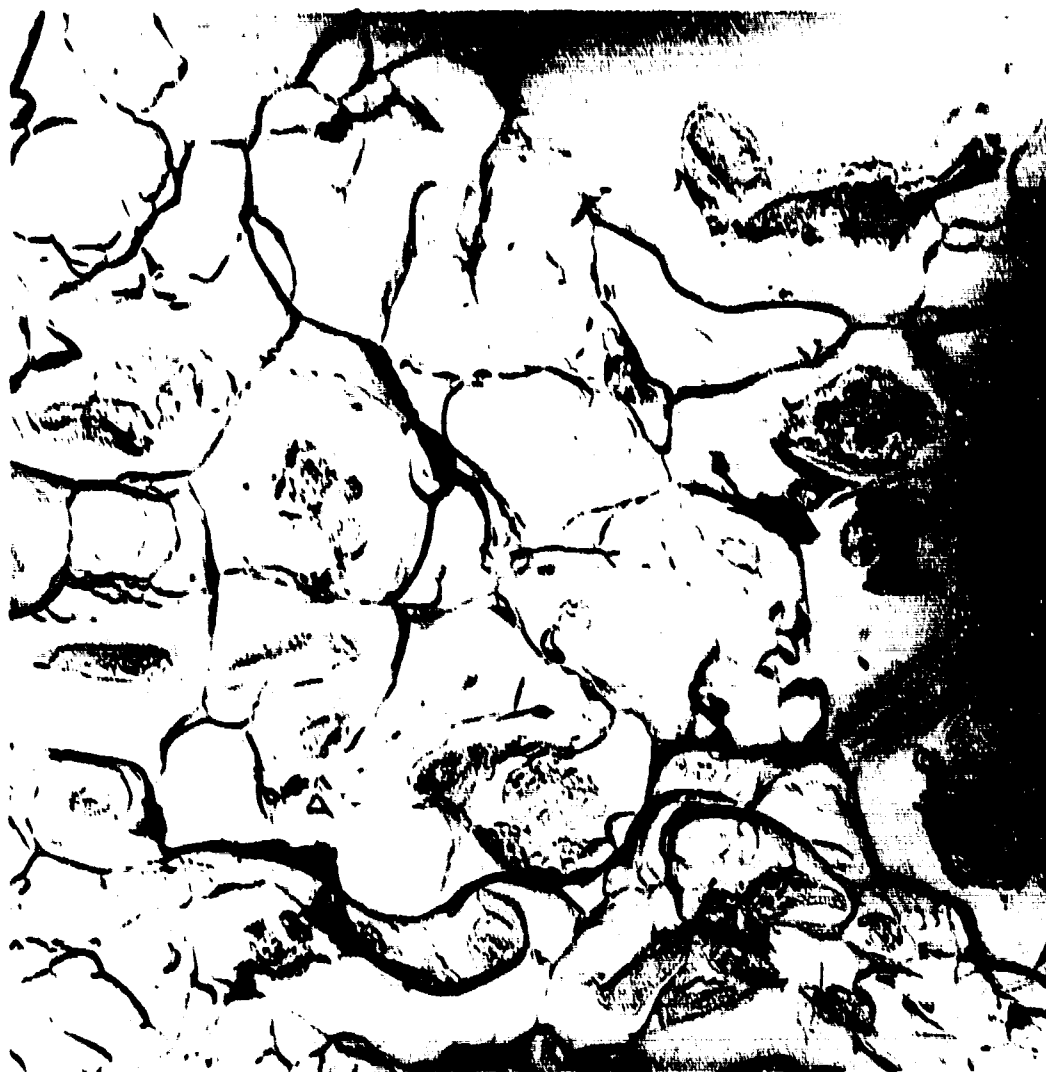


b Fatigue striations (X2600)

SEM of slow-fracture surface (inside origin) of cylinder from X7080-T7 forging in corrosion fatigue test.

Figure 51





Transmission electron micrograph typical of fracture appearance in slow-fracture region of 7079-T6, 7075-T6 and 2014-T6 cylinder in corrosion-fatigue test (X15,000).

Figure 52



TEM showing dimpled rupture characteristic of tensile failure in fast-fracture region of cylinders in corrosion-fatigue test (X15,000).

Figure 53



TEM showing striations typical of fatigue failure in slow fracture region of cylinders in corrosion fatigue test (X15,000).

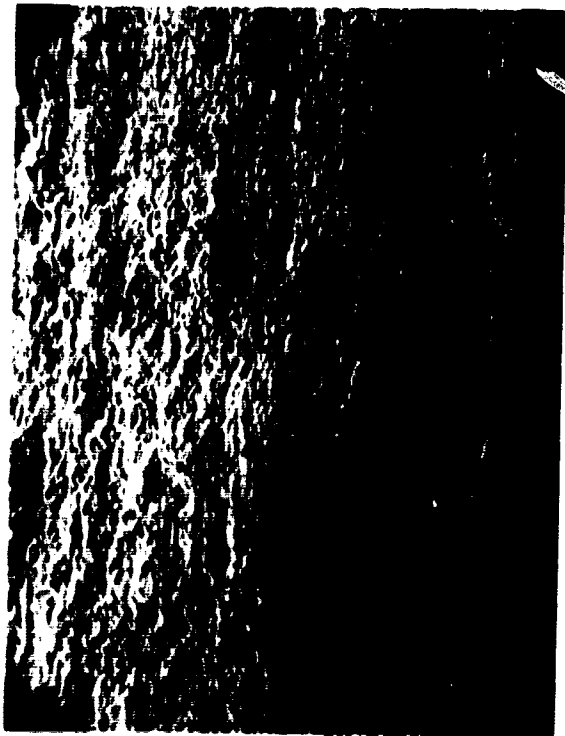
Figure 54



TEM showing faceted appearance of  
slow-fracture region of 7075-T6 cylinder  
in stress-corrosion test (X15,000).

Figure 55

S186-1  
S186-4  
180671



Fracture origin (X50)



Fracture surface (X200)



Cross section (X500)

Granular appearance of fracture and intergranular path of auxiliary crack in 2014-T6 cylinder.

Figure 56

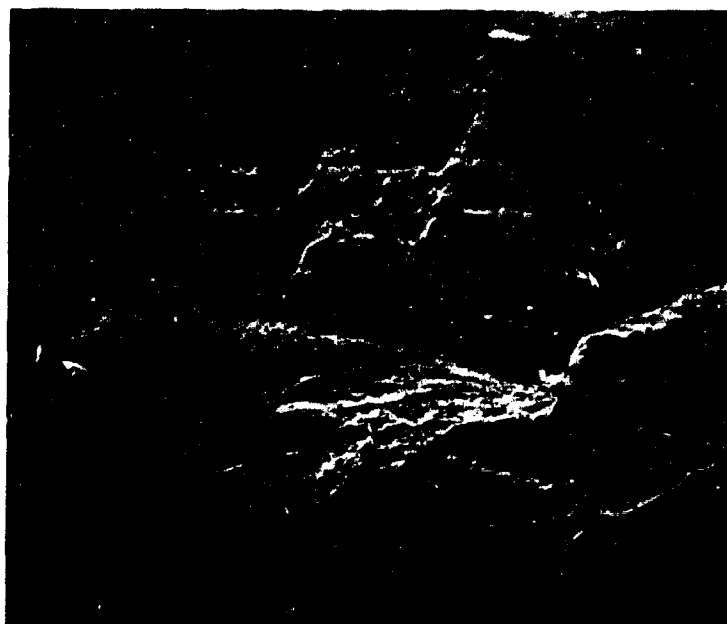


Figure 57 Granular appearance at origin and adjoining ray pattern (X50).

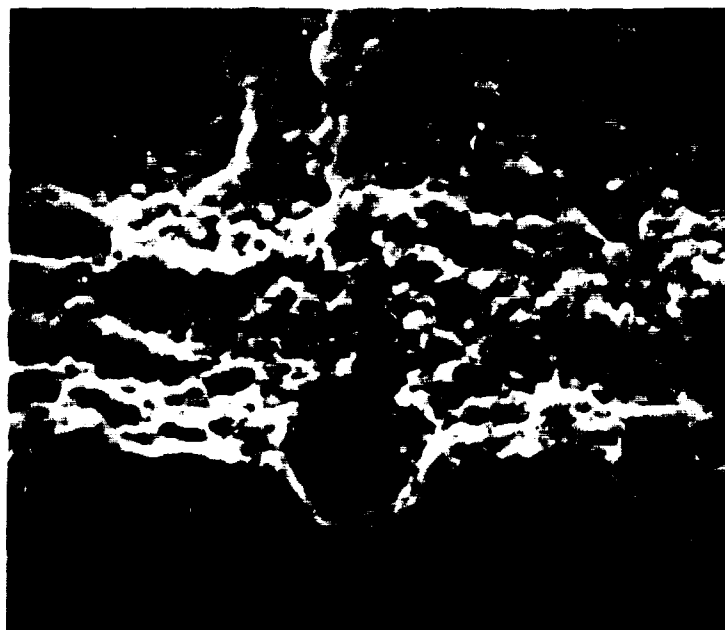
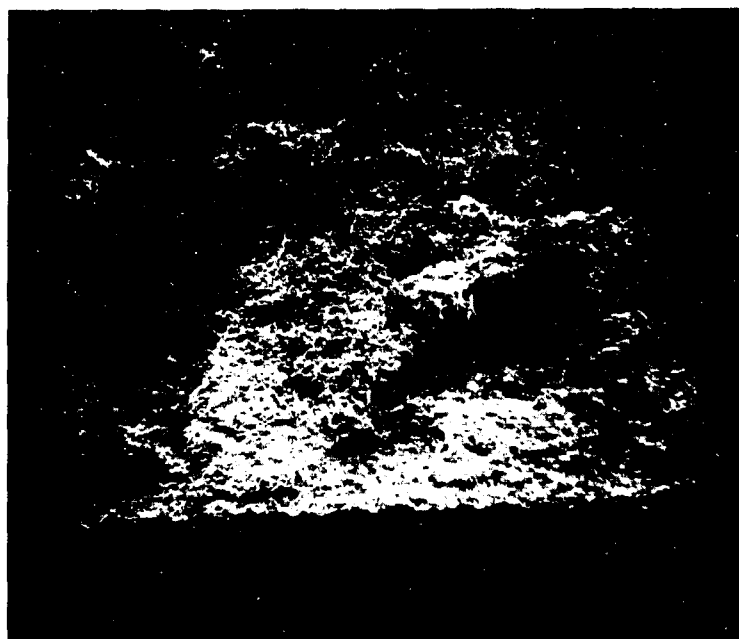
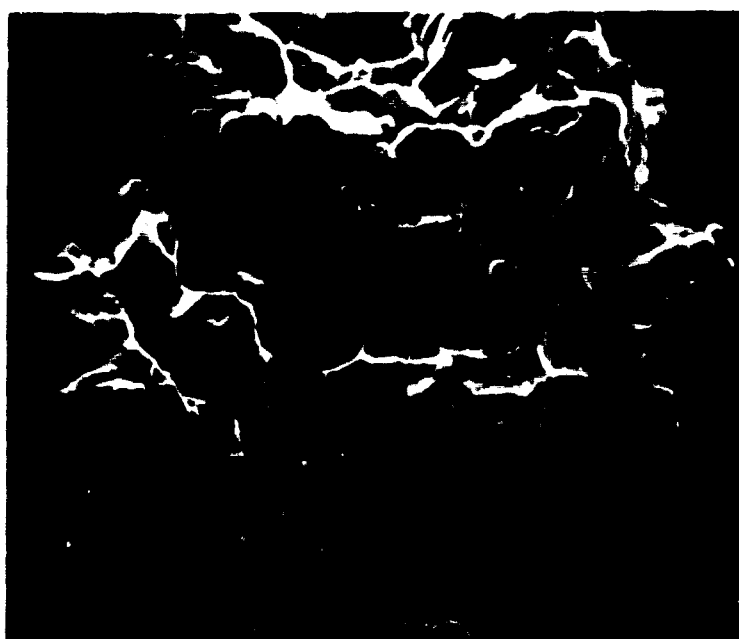


Figure 58 Granular appearance at origin (X500).

Fracture appearance typical of 7079-T6  
and 7075-T6 cylinders in corrosion fatigue  
test at 50% of design stress.



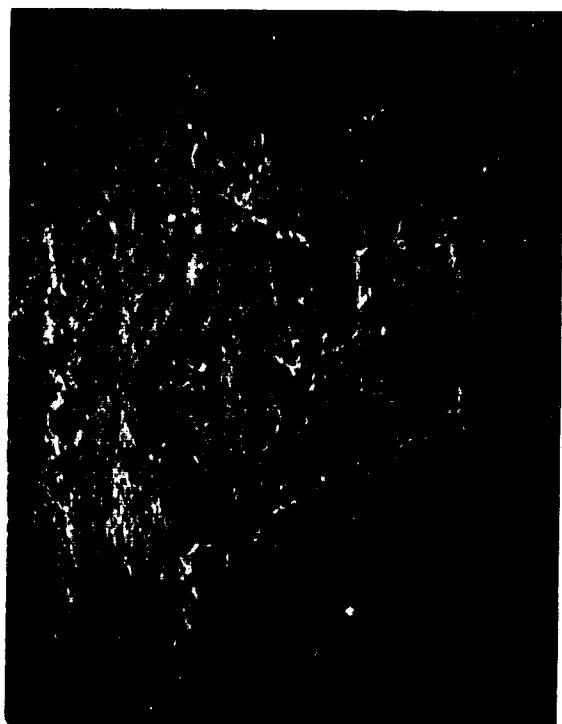
a Granular appearance at origin (X50)



b Faceted appearance and intergranular penetration (1000X).

SEM of fracture of C-Ring from 2014-T6  
forging exposed in corrosion fatigue test.

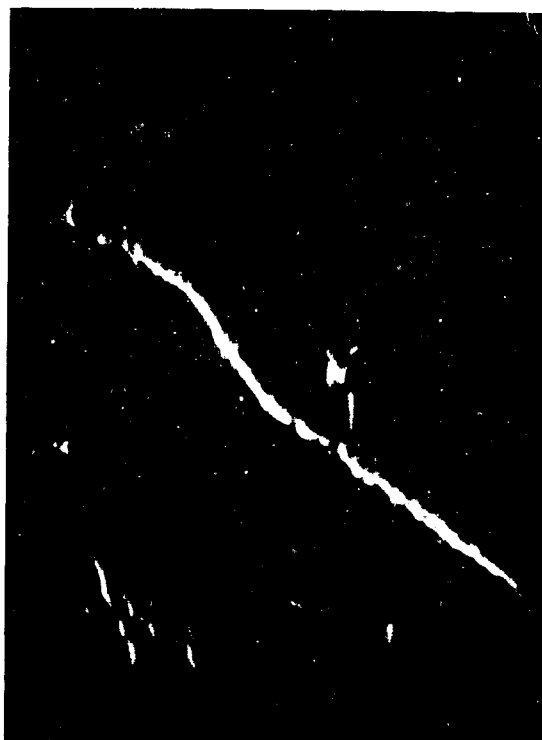
Figure 59



a Indistinct ray pattern at origin (X20)



b Faceted, intergranular fracture (X500)



c Fatigue striations (X2000)

SEM typical of C-Rings from 7079-T6, 7075-T6 and  
X7080-T7 forgings exposed to corrosion-fatigue test.

Figure 60





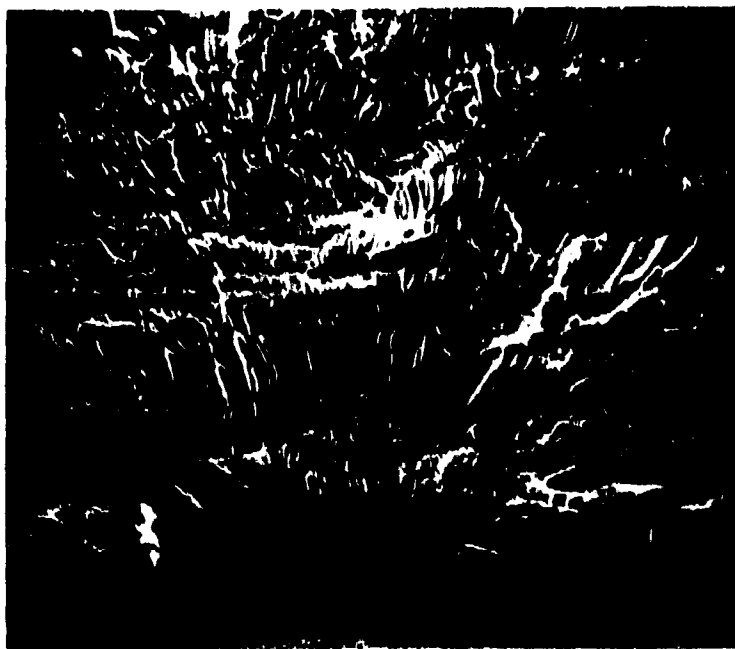
a 7075-T6



X7080-T7

- b Cross sections of auxiliary cracks in C-Rings  
indicating mixed fracture mode (X100).

Figure 61



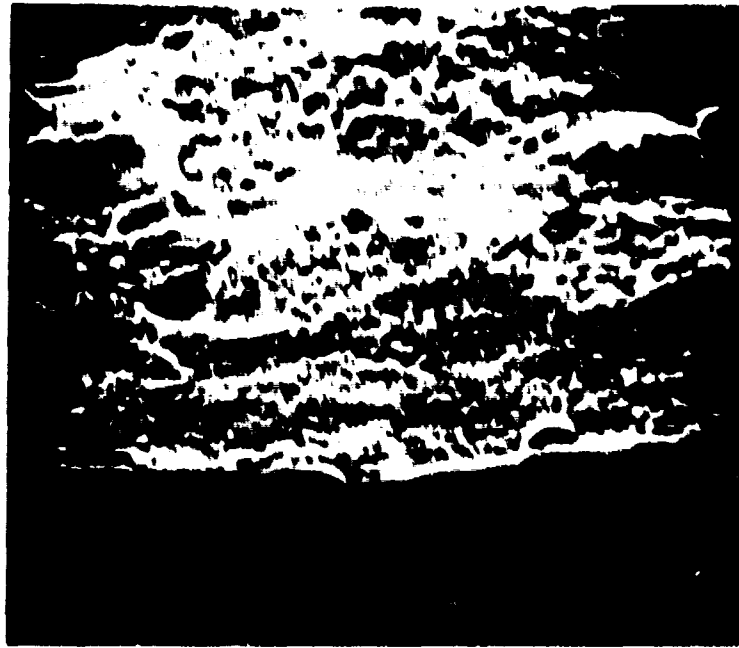
a Ray pattern at origin (X60)



b Fatigue striations (X2400)

SEM showing appearance typical of fractures  
having inside origin in cylinder  
subjected to fatigue in laboratory air.

Figure 62



a Granular appearance at origin (X280)



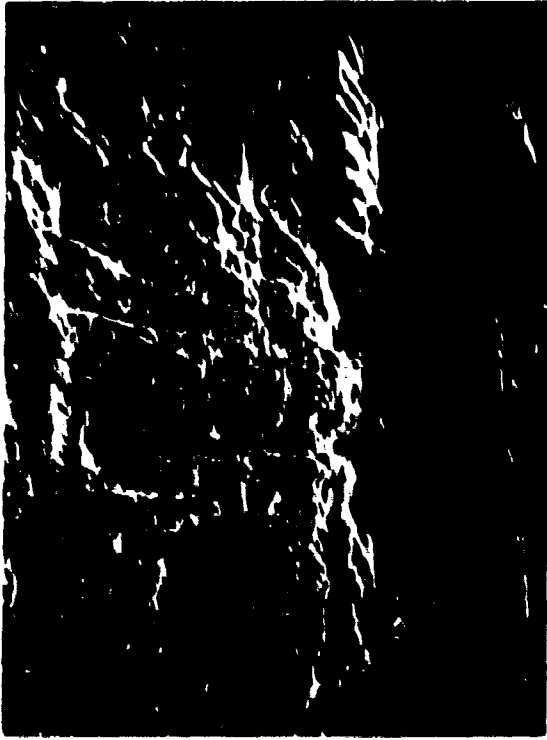
b Fatigue striations (X2400)

SEM showing appearance of fracture having  
outside origin in cylinder subjected to  
fatigue in laboratory air.

Figure 63



Origin (X150)



Origin (X150)



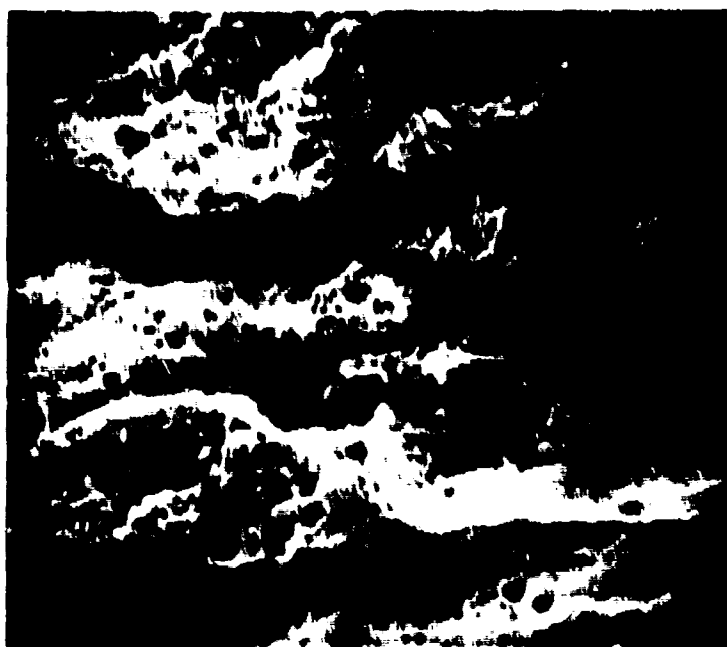
Striations (X2500)  
a 20 cycles per minute



Striations (X2500)  
b 0.148 cycles per minute

Fracture appearance as affected by cycle rate.

Figure 64



a Intergranular penetration and pitting on grain surfaces (X850).



b Fatigue striations near end of slow-fracture region (X1300).

SEM of fracture surface of cylinder from 2014-T6 rod having long life in corrosion-fatigue test.

TABLE 1  
TENSILE PROPERTIES OF MATERIALS

Alloy and Temper	Product	AISI Sample No.	Longitudinal <sup>a</sup>			Transverse <sup>b</sup>			Transverse <sup>c</sup>		
			Tensile Strength, ksi	Yield Strength <sup>a</sup> , ksi	Elong., % in 2 in.	Tensile Strength, ksi	Yield Strength <sup>a</sup> , ksi	Elong., % in 2 in.	Tensile Strength, ksi	Yield Strength <sup>a</sup> , ksi	Elong., % in 2 in.
7075-T6	Rolled rod	314975	79.6	68.0	15.0	74.8	62.8	11.0	----	----	----
			79.1	67.6	15.0	74.2	63.0	11.0	----	----	----
			78.4	67.8	15.0	74.8	63.4	11.0	----	----	----
	Die forging	315023	80.0	69.8	17.0	84.6	70.9	11.5	78.4	66.8	6.5
			79.6	69.3	17.0	84.2	69.7	11.5	78.2	67.6	6.5
			79.8	69.6	17.0	84.4	70.0	11.5	78.4	67.7	6.5
7075-T71	Rolled rod	314976	69.6	57.0	15.5	68.6	55.8	12.0	----	----	----
			69.4	56.3	15.5	68.7	55.7	11.9	----	----	----
			69.5	56.6	15.5	68.6	55.8	11.9	----	----	----
	Die forging	315024	78.2	67.7	14.0	75.9	64.5	10.0	74.0	64.3	8.0
			78.0	67.0	14.0	75.8	64.4	10.0	74.1	64.3	8.0
			78.0	66.4	14.5	75.8	64.4	10.0	74.0	64.3	8.0
7079-T6	Rolled rod	314977	77.1	68.2	15.0	77.2	67.4	10.0	----	----	----
			77.1	68.2	15.0	77.1	67.3	9.0	----	----	----
			77.1	68.2	15.0	77.2	67.4	9.0	----	----	----
	Die forging	315022	76.2	67.3	15.5	77.2	67.8	12.0	75.4	67.6	5.0
			76.1	70.0	14.0	77.1	67.4	12.0	77.0	67.8	8.5
			77.8	68.7	14.8	77.2	67.6	12.0	76.2	67.7	6.5
X7080-T7	Rolled rod	314978	63.9	52.7	15.0	62.6	51.0	10.0	----	----	----
			63.8	52.6	14.5	62.5	50.9	10.0	----	----	----
			63.9	52.6	14.8	62.6	51.0	10.0	----	----	----
	Die forging	315049	71.3	63.7	15.0	70.8	62.5	8.5	70.1	61.9	6.5
			71.8	64.8	14.5	71.3	62.6	9.5	69.9	61.8	6.5
			72.0	64.9	14.8	71.0	62.6	9.0	70.0	61.8	6.5
2014-T6	Rolled rod	314979	71.4	64.1	12.0	69.8	62.7	6.0	----	----	----
			71.5	64.3	12.0	69.7	62.2	7.0	----	----	----
			71.4	64.2	12.0	69.8	62.4	7.5	----	----	----
	Die forging	315021	71.3	63.6	12.0	70.3	63.1	7.0	70.0	62.5	5.0
			71.1	64.1	11.0	70.3	62.9	8.0	69.6	62.3	5.0
			71.3	63.8	11.5	70.3	63.0	8.5	69.8	62.4	5.0
CH70-T7	Premium casting	314944	69.0	63.3	8.0	63.8	60.1	6.0 <sup>e</sup>	----	----	----
			67.4	62.7	8.5	64.3	61.1	6.0 <sup>e</sup>	----	----	----
			69.2	63.0	8.2	64.0	60.6	5.0	----	----	----

a Offset equals 0.2 per cent.

b Tangential specimens parallel to parting plane, if any.

c Tangential specimens perpendicular to parting plane.

d Mechanical property limits from Alcoa Aluminum Handbook<sup>1</sup> (1967) where specified. Otherwise, minimums are tentative.

e Failed near end of gage length.

- \* Offset equal's 0.2 percent.
- † Diagonal fracture.
- \*\* Crack sent in direction of loading.
- \*\*\* Broke thru pin hole.
- \*\*\*\* Crack path slightly diagonal.
- \*\*\*\*\* Crack path changed direction.

TABLE III

## RESULTS OF PLANE-STRAIN FRACTURE-TOUGHNESS TESTS OF NOTCH-BEND SPECIMENS

Alloy and Temper	Product	ARL Sample Number	Specimen Number	Longitudinal (L-W; Axial)					Transverse (W-L; Tangential) 90° From Parting Plane					Transverse (W-L; Tangential) Across Parting Plane				
				Specimen Thickness, in.	Original Crack Length, in.	Span Length, in.	$K_{Q, \dagger}$ ksi $\sqrt{\text{in.}}$	Meaningful $K_{Ic}$	Specimen Thickness, in.	Original Crack Length, in.	Span Length, in.	$K_{Q, \dagger}$ ksi $\sqrt{\text{in.}}$	Meaningful $K_{Ic}$	Specimen Thickness, in.	Original Crack Length, in.	Span Length, in.	$K_{Q, \dagger}$ ksi $\sqrt{\text{in.}}$	Meaningful $K_{Ic}$
7075-T6	Rolled Rod	314975	1	0.688	0.722	6.0	36.4	No (b)	0.251	0.313	2.0	21.5	No (b)	-	-	-	-	-
			2	0.679	0.772	6.0	36.1	No (b)	0.250	0.282	2.0	22.4	No (b)	-	-	-	-	-
	Die Forging	315023	1	0.715	0.862	6.0	29.7	No (b)	0.249	0.273	2.0	24.4	No (b)	0.249	0.265	2.0	19.7	Yes
			2	0.715	0.903	6.0	35.5	No (b)	0.249	0.273	2.0	22.1	Yes	0.249	0.265	2.0	19.5	Yes (c,d)
7079-T6	Rolled Rod	314977	1	0.689	0.767	6.0	36.7	No (b)	0.250	0.277	2.0	21.0	Yes	-	-	-	-	-
			2	0.688	0.748	6.0	35.1	Yes	0.250	0.276	2.0	21.3	Yes	-	-	-	-	-
	Die Forging	315022	1	0.714	0.852	6.0	42.8	No (b)	0.249	0.266	2.0	23.9	No (b)	0.249	0.292	2.0	18.5	No (a)
			2	0.715	0.920	6.0	36.2	No (b)	0.249	0.269	2.0	22.7	No (b)	0.249	0.258	2.0	20.6	Yes
7080-T7	Rolled Rod	314978	1	0.688	0.700	6.0	38.9	No (b)	0.250	0.267	2.0	22.1	No (b)	-	-	-	-	-
			2	0.688	0.685	6.0	34.9	No (b)	0.250	0.242	2.0	21.1	No (b)	-	-	-	-	-
	Die Forging	315049	1	0.251	0.262	2.0	28.6	No (b)	0.249	0.271	2.0	20.8	No (b)	0.250	0.268	2.0	20.4	No (b)
			2	0.251	0.262	2.0	28.8	No (b)	0.249	0.267	2.0	21.3	No (b)	0.249	0.279	2.0	19.7	No (b)
2014-T6	Rolled Rod	314979	1	0.689	0.757	6.0	29.0	Yes	0.249	0.268	2.0	16.2	Yes	-	-	-	-	-
			2	0.689	0.737	6.0	28.3	Yes	0.249	0.258	2.0	17.1	Yes	-	-	-	-	-
	Die Forging	315021	1	0.714	0.798	6.0	28.5	Yes	0.249	0.266	2.0	18.2	Yes	0.249	0.266	2.0	15.5	Yes
			2	0.713	0.778	6.0	27.2	Yes	0.249	0.258	2.0	19.2	Yes	0.249	0.269	2.0	16.5	Yes
7075-T73	Rolled Rod	314976	1	0.688	0.790	6.0	41.8	No (b)	0.250	0.287	2.0	24.0	No (b)	-	-	-	-	-
			2	0.688	0.743	6.0	39.1	No (b)	0.249	0.260	2.0	24.6	No (b)	-	-	-	-	-
	Die Forging	315024	1	0.713	0.870	6.0	40.8	No (b)	0.249	0.268	2.0	20.6	Yes	0.249	0.294	2.0	21.2	No (a)
			2	0.712	0.873	6.0	41.2	No (b)	0.249	0.278	2.0	21.6	No (a,c)	0.249	0.275	2.0	19.8	No (b)
CF70-T7	Premium Casting	315044	1	0.687	0.665	6.0	33.3	No (b)	0.250	0.256	2.0	26.4	No (b)	-	-	-	-	-
			2	0.668	0.710	6.0	34.5	No (b)	0.250	0.263	2.0	25.0	No (b)	-	-	-	-	-

\* Judged from compliance with criteria in ASTM Method E399-70T, with minor deviations as covered by notes below:

- (a) Crack length slightly outside tolerance;  $a < 2.5(K_{Ic}/\sigma_{YS})^2$ .
- (b) Specimen not quite thick enough to insure plane-strain conditions;  $b < 2.5(K_{Ic}/\sigma_{YS})^2$ .
- (c) Slightly excessive yielding prior to 5% secant offset.
- (d) Fatigue crack front curvature slightly greater than specified;  $q/0.8$  B.
- (e) Stress intensity during fatigue cracking slightly higher than presently recommended;  $6.5\% K_{Ic} \leq K \leq 7.5\% K_{Ic}$ .

†  $K_Q$  is the candidate value of  $K_{Ic}$  from the fracture toughness test, which must meet certain criteria concerning achievement of cracking under plane-strain conditions before it can be assigned  $K_{Ic}$  designation.



TABLE IV

## RESULTS OF PLANE-STRAIN FRACTURE TOUGHNESS TESTS OF COMPACT TENSION SPECIMENS

Alloy and Temper	Product	ABL Sample Number	Specimen Number	Transverse (W-L, Tangential): 90° From Parting Plane Specimen Thickness, B, in. Crack Length, a, in. $K_{IC}$	Transverse (W-L, Tangential): Across Parting Plane Specimen Thickness, B, in. Crack Length, a, in. $K_{IC}$
7075-T6	Die Forging	315023	1 2	0.75 0.75 0.82 0.82 19.6 19.3	0.75 0.75 0.81 0.80 19.2 19.1
7075-T6	Die Forging	315022	1 2	0.75 0.75 0.85 0.88 20.3 20.5	0.75 0.75 0.88 0.83 16.3 16.3
X7080-T7	Die Forging	315049	1 2	0.75 0.75 0.77 0.78 18.1 19.2	0.75 0.75 0.80 0.79 20.5 19.8
2014-T6	Die Forging	315021	1 2	0.75 0.75 0.73 0.75 15.1 14.3	0.75 0.75 0.75 0.77 14.5 14.1
7075-T73	Die Forging	315024	1 2 3 4	0.75 0.75 0.75 0.75 0.84 0.79 0.82 0.80 21.1 22.1 22.0 20.6	0.75 0.75 0.75 0.75 0.81 0.81 0.82 0.83 20.4 19.2 19.6 19.9
CS70-T7	Premium Casting	314944	1 2	0.75 0.75 0.79 0.74 33.6 33.5	-- -- -- -- -- --

\* Judged from compliance with criteria in ASTM Method E399-70†, with minor deviations as covered by notes below:

- (a) Crack length slightly outside tolerance;  $a < 2.5(K_{IC}/\sigma_{YS})^2$ .
- (b) Specimens not quite thick enough to insure plane-strain conditions;  $b < 2.5(K_{IC}/\sigma_{YS})^2$ .
- (c) Slightly excessive yielding prior to 5% secant offset.
- (d) Fatigue crack front curvature slightly greater than specified;  $\phi \leq 8$ .
- (e) Stress intensity during fatigue cracking slightly higher than presently recommended;  $K_{I0} \leq K \leq 1.75 K_{I0}$ .

†  $K_{I0}$  is the candidate value of  $K_{IC}$  from the fracture toughness test, which must meet certain criteria concerning achievement of cracking under plane-strain conditions before it can be assigned  $K_{IC}$  designation.

TABLE V  
SUMMARY OF PLANE-STRAIN FRACTURE TOUGHNESS DATA

Alloy and Temper	Product	Plane-Strain Fracture Toughness, $K_{Ic}$ , $\text{ksi}\sqrt{\text{in.}}$					
		L-W		W-L		W-L (P)	
		Notch Bend	Notch Bend	Notch Bend	Compact Tension	Notch Bend	Compact Tension
7075-T6	Rolled Rod Die Forging	(36) (33)	(22) 22.1	-- 19.4	-- 19.2	-- 19.6	-- 19.2
7079-T6	Rolled Rod Die Forging	35.1 (36)	21.2 --	-- 20.4	-- 16.3	-- 20.6	-- 16.3
X7080-T7	Rolled Rod Die Forging	(>30) (>30)	(22) (21)	-- 18.6	-- 20.2	-- (20)	-- 20.2
2014-T6	Rolled Rod Die Forging	28.6 27.8	16.8 18.7	-- 14.7	-- 14.3	-- 16.0	-- 14.3
7075-T73	Rolled Rod Die Forging	(>35) (>35)	(24) 20.6	-- 21.4	-- 20.0	-- (21)	-- 20.0
CH70-T7	Premium Casting	(33)	--	(33)	--	--	--

\* Values in parentheses are best engineering estimates of  $K_{Ic}$  from tests in which entirely meaningful results were not obtained. Other values are average results of meaningful values presented in Table

TABLE VI  
CYLINDER DIMENSIONS AND CALCULATED HOOP TENSIONS  
FOR 8000 PSI TEST PRESSURE

Alloy	Tensile Strength <sup>a</sup> , Ktu, ksi	Design Stress, ksi (2/3 F <sub>tu</sub> )	Cylinder Dimensions <sup>c</sup> , in.		Hoop Tension <sup>d</sup> , ksi	
			G.D.	Wall	Interior	Exterior
<u>Die Forged</u>						
7075-T6	71 <sup>a</sup>	47.4	3.101	0.300	37.9	29.8
7075-T73	62 <sup>a</sup>	41.3	3.201	0.350	33.0	24.9
7079-T6	70 <sup>a</sup>	46.7	3.113	0.306	37.4	29.1
A7080-T7	65 <sup>b</sup>	43.3	3.161	0.330	34.6	26.7
2014-T6	64 <sup>a</sup>	42.7	3.177	0.338	34.2	26.1
<u>Premium Cast</u>						
Ch70-T7	60 <sup>b</sup>	40	3.229	0.364	32.0	24.0

- a Specified minimum values for transverse specimens, Ref. 7.  
b Tentative minimum for transverse specimens.  
c Dimensions apply to cylinders machined from rolled rod as well as from die forgings.  
d Based on formulas for thick-wall cylinders.  
e 80% of design stresses.

TABLE VII. RESULTS OF AXIAL STRESS FATIGUE TESTS

Alloy	Tests in Ambient Air			Tests in Acidified Salt			Chromate Solution		
	Die Forging			Die Forging			Rolled Rod		
	Spec. No.	Stress, ksi	Cycles to Failure	Spec. No.	Stress, ksi	Cycles to Failure	Spec. No.	Stress, ksi	Cycles to Failure
7075-T6	14(F)	50.0	27,000	14	50.0	29,700	22	32.0	28,700
	23	50.0	109,000	1	50.0	71,000			
	1	50.0	197,000	23	50.0	110,000	18	20.0	101,000
		100-mean=11Fe	9,000		100-mean=11Fe	83,000	26	20.0	135,600
								100-mean=11Fe	117,000
	16(F)	40.0	300,000	16	40.0	217,800			
	9	40.0	750,000	9	40.0	654,700			
	12(F)	40.0	4,081,000	12	40.0	433,000	28(F)	10.0	3,460,000
	4	40.0	6,029,000	4	40.0	1,610,700	19	10.0	13,156,700
		100-mean=11Fe	1,750,000		100-mean=11Fe	482,000			
7079-T6	14(F)	50.0	45,000	1	50.0	43,800	22	32.0	28,000
	23	50.0	138,000	14	50.0	37,800	27(F)	32.0	36,500
	1	50.0	140,000	23	50.0	140,000			
		100-mean=11Fe	93,000		100-mean=11Fe	80,000	30(F)	20.0	120,800
							18	20.0	123,700
	12(F)	40.0	100,000	9	40.0	160,000	26	20.0	1,378,700
	9	40.0	15,000	16	40.0	261,800		100-mean=11Fe	117,000
	16(F)	40.0	344,000	4	40.0	594,000			
	4	40.0	1,027,000	12	40.0	1,627,000	24	14.0	9,739,000
		100-mean=11Fe	774,000		100-mean=11Fe	517,000			
7080-T7	1	50.0	88,000	1	50.0	27,800	22	32.0	33,200
	23	50.0	98,000	14	50.0	45,100	27(F)	32.0	37,700
	14(F)	50.0	147,000	23	50.0	55,500		32.0	39,500
		100-mean=11Fe	117,700		100-mean=11Fe	45,500		100-mean=11Fe	36,700
	9	40.0	692,000	16	40.0	183,500	18	20.0	188,600
	16(F)	40.0	1,481,400	9	40.0	196,800	26	20.0	326,600
	12(F)	40.0	1,622,000	4	40.0	346,000		100-mean=11Fe	262,600
	4	40.0	2,000,000	12	40.0	3,327,000			
		100-mean=11Fe	1,366,000		100-mean=11Fe	450,000	24	14.0	4,534,000
2014-T6	1	50.0	79,700	23	50.0	91,000	22	32.0	51,700
	14(F)	50.0	105,700	1	50.0	122,000	27(F)	32.0	44,000
	23	50.0	818,500		100-mean=11Fe	105,400		32.0	37,400
		100-mean=11Fe	109,600					100-mean=11Fe	54,000
	16(F)	40.0	293,300	16	40.0	184,400	18	20.0	149,200
	9	40.0	323,500	9	40.0	226,500	30(F)	20.0	228,600
	12(F)	40.0	1,080,700	4	40.0	5,400,700	19	10.0	2,090,500
	4	40.0	10,001,800	12	40.0	6,176,100		10.0	2,053,500
		100-mean=11Fe	1,948,000		100-mean=11Fe	1,987,000	24	8.0	3,535,300
								8.0	7,965,800
7075-T73	14(F)	50.0	79,100	23	50.0	66,000	22	32.0	27,400
	23	50.0	124,100	1	50.0	121,000		32.0	39,400
	4	50.0	134,800	14	50.0	122,300	18	20.0	128,300
	1	50.0	200,400		100-mean=11Fe	106,800	30(F)	20.0	136,400
		100-mean=11Fe	138,000				26	20.0	165,200
								100-mean=11Fe	171,000
	16(F)	40.0	527,700	16	40.0	350,700	14	10.0	756,600
	12(F)	40.0	967,300	9	40.0	650,000	27(F)	10.0	3,248,500
	9	40.0	4,008,000	4	40.0	779,000	17	10.0	29,188,800 <sup>c</sup>
	4	40.0	2,676,000	12	40.0	2,000,000		8.0	6,815,000
		100-mean=11Fe	3,105,000		100-mean=11Fe	705,700	24	8.0	10,491,700

CONTINUED

Alloy	Tests in Ambient Air			Tests in Acidified Salt			Chromate Solution		
	Spec. No.	Stress, ksi	Cycles to Failure	Spec. No.	Stress, ksi	Cycles to Failure	Spec. No.	Stress, ksi	Cycles to Failure
7079-T7	1	50.0	8,000				22	32.0	49,800
	24	50.0	14,100				26	20.0	131,500
	14	50.0	15,000				19	20.0	142,000
		100-mean=11Fe	11,500						
	9	40.0	13,000				18	10.0	2,559,300
	3	40.0	19,000						
	16	40.0	24,000				26	0.0	2,980,100
	12	40.0	32,000						
		100-mean=11Fe	21,800				24	8.0	4,021,700
7080-T7	2	50.0	60,000						
	11	50.0	60,000						
	9	50.0	70,000						
		100-mean=11Fe	46,000						
	2	40.0	100,000						
	19	40.0	111,000						
		100-mean=11Fe	108,000						
	9	40.0	2,008,000						
	7	40.0	2,000,000						
	1	40.0	2,000,000						

TABLE VIII. RESULTS OF FATIGUE TESTS OF HYDRAULIC CYLINDERS  
Alloy 7075-T6

Environment	Cylinder Stock	Spec. No.	Fatigue Loading <sup>(3)</sup>		Max. Stress, ksi	No. of Cycles	Description of Failure			
			Pressure, psi	Freq. cpm			Type	Initiation	Position <sup>(4)</sup>	Parting Plane
Maximum Stress = 80% of Design Value										
Lab Air <sup>(1)</sup>	Die forged	6	8,000	20	37.9	22,800	Fatigue	Inside	-	No
		8	"	"	"	31,800	Fatigue	"	-	Yes
		9	"	"	"	40,800	Fatigue	"	-	Yes
		5*	"	"	"	68,300 <sup>(5)</sup>	Fatigue	"	-	Yes
				log-mean-life		31,100				
Seacoast <sup>(2)</sup>	Die forged	1	8,000	0.148	37.9	889	SCC <sup>(6)</sup>	Outside	2:00	Yes
		2	"	"	"	1,169	SCC	"	2:00	Yes
		3	"	"	"	1,457	SCC	"	10:00	Yes
				log-mean-life		1,150				
Seacoast	Rolled	A	8,000	0.148	37.9	2,760	SCC <sup>(6)</sup>	Outside	1:00	-
		B	"	"	"	6,570	SCC	"	10:30	-
		C	"	"	"	14,490	Fatigue	Inside	11:00	-
				log-mean-life		6,410				
Maximum Stress = 65% of Design Value										
Lab Air	Die forged	4*	6,500	48	30.8	505,100	Fatigue <sup>(6)</sup>	Outside	-	Yes
		7*	"	"	"	88,300	Fatigue	Inside	-	No
				log-mean-life		211,000				
Maximum Stress = 50% of Design Value										
Lab Air	Die forged	4*	5,000	48	23.7	8,000,000	None	-	-	-
		5*	"	"	"	"	"	-	-	-
		7*	"	"	"	"	"	-	-	-
Seacoast	Die forged	10	5,000	3	23.7	213,590	SCC-Fatigue <sup>(6)</sup>	Outside	8:30	Yes
		11	"	"	"	60,500	Fatigue <sup>(6)</sup>	Inside	1:00	Yes
		12	"	"	"	51,300	Fatigue <sup>(6)</sup>	Inside	9:30	Yes
				log-mean-life		87,100				
Seacoast	Rolled	D	5,000	3	23.7	931,400	Fatigue <sup>(6)</sup>	Outside <sup>(9)</sup>	7:30	-
		E	"	"	"	115,900	Fatigue	Inside	5:00	-
		F	"	"	"	76,200	Fatigue	"	10:30	-
				log-mean-life		202,000				
Maximum Stress = 30% of Design Value										
Lab Air	Die forged	4	3,000	60	14.2	6,059,610	None	-	-	-
		5	"	"	"	"	"	-	-	-
		7	"	"	"	"	"	-	-	-

(1) Circulating laboratory air at 50 ±5% relative humidity.

(2) Specimen enclosures subjected to 1-min. injections of warm salt mist at 12-hr intervals. For balance of time specimens were exposed to circulating laboratory air as in (1).

(3) For tests in laboratory air hydraulic pressure cycled sinusoidally between minimum pressure of 200 to 400 psi and maximum indicated. For tests in seacoast environment pressure held at maximum indicated for 80% of cycle time, then dropped sinusoidally to minimum of 200 to 400 psi.

(4) For tests in seacoast environment, salt buildup and corrosion product was heaviest on top side of specimen (9 o'clock position).

(5) Not included in log mean life.

(6) Based on metallographic examination, others on visual appearance.

(9) Origin at corrosion pit

\*Specimens had prior loading history, as indicated.

TABLE 1A. RESULTS OF FATIGUE TESTS OF HYDRAULIC CYLINDERS  
ALUMINUM 7075-T6

Environment	Cylinder Stock	Spec. No.	Pressure, psi	Max. Stress, ksi	No. of Cycles	Type	Initiation of Failure	Failure Mode	
Maximum Stress = 80% of Design Value									
Lab Air <sup>(1)</sup>	Die forged	7	8,000	17.4	1,380	Fatigue(6)	Outside(7)	Yes	
		8	"	"	27,860	Fatigue(6)	Inside	"	
		9	"	"	38,110	Fatigue	Outside	No	
log-mean-life					16,700				
Seacoast <sup>(2)</sup>	Die forged	3	8,000	17.4	40	SCC	Outside	Yes	
		1	"	"	44	SCC	"	"	
		2	"	"	112	SCC	"	No	
log-mean-life					220				
Seacoast	Rolled	A	8,000	17.4	703	SCC(6)	Outside	Yes	
		C	"	"	167	SCC(6)	"	"	
		B	"	"	1,100	SCC	"	"	
log-mean-life					1,100				
Maximum Stress = 50% of Design Value									
Lab Air	Die forged	40	5,000	23.4	80,590	Fatigue	Outside(7)	Yes	
		48	"	"	149,920	Fatigue	Inside	No	
		60	"	"	387,100	Fatigue	Outside	Yes	
log-mean-life					199,000				
Seacoast	Die forged	10	5,000	"	20,910	Fatigue(6)	Inside	No	
		11	"	"	34,110	Fatigue	"	No	
		12	"	"	58,000	Fatigue	"	No	
log-mean-life					55,700				
Seacoast	Rolled	K	5,000	"	9,560	Fatigue(6)	Outside(7)	"	
		P	"	"	55,340	Fatigue(7)	Outside(7)	"	
		D	"	"	12,300	Fatigue	Inside	"	
log-mean-life					32,710				
Maximum Stress = 30% of Design Value									
Lab Air	Die forged	4	3,000	14.0	6,050	None	"	"	
		5	"	"	"	"	"	"	
		6	"	"	"	"	"	"	

(1) Circulating laboratory air at 50 ±5% relative humidity.

(2) Specimen enclosures subjected to 1-min. injections of warm salt mist at 12-hr intervals. For balance of time specimens were exposed to circulating laboratory air as in (1).

(3) For tests in laboratory air hydraulic pressure cycled sinusoidally between minimum pressure of 200 to 400 psi and maximum indicated. For tests in seacoast environment pressure held at maximum indicated for 80% of cycle time, then dropped sinusoidally to minimum of 200 to 400 psi.

(4) For tests in seacoast environment, salt buildup and corrosion product was heaviest on top side of specimen (9 to 3 o'clock position).

(6) Based on metallographic examination.

(7) Initiation possibly from stress-corrosion crack.

\*Specimens had prior loading history, as indicated.

TABLE I. RESULTS OF SECTION TESTS OF HYDRAULIC CYLINDERS  
 ALLY 8700-27

Environment	Cylinder Stock	Spec. No.	Section Location (3)		Max. Stress, ksi	No. of Specimens	Investigation of Specimen		Parting Plane
			Pressure, psi	Temp, °F			Type	Location	
Lab Air (1)	Die Forged	1	5000	20	34.5	22, 1770	Package 1	Inside	Yes
		2	-	-	-	21, 1840	Package 2	-	No
		3	Log-mean-1100	-	-	21, 1840	Package 3	-	Yes
Seacoast (2)	Die Forged	1	3000	1100	34.5	8, 1650	Package 4	Inside	Yes
		2	-	-	-	11, 1700	Package 5	-	No
		3	Log-mean-1100	-	-	11, 1700	Package 6	-	No
Seacoast	Rolled	1	5000	1100	34.5	11, 1610	Package 7	Inside	-
		2	-	-	-	11, 1610	Package 8	-	-
		3	Log-mean-1100	-	-	11, 1610	Package 9	-	-
Lab Air	Die Forged	10	5000	20	26.5	50, 1430	Package 10	Inside	Yes
		11	-	-	-	50, 1430	Package 11	Inside	-
		12	Log-mean-1100	-	-	50, 1430	Package 12	Inside	-
Lab Air	Die Forged	10	5000	20	26.5	50, 1430	Package 13	Inside	Yes
		11	-	-	-	50, 1430	Package 14	Inside	-
		12	Log-mean-1100	-	-	50, 1430	Package 15	Inside	-
Seacoast	Die Forged	10	5000	20	26.5	50, 1430	Package 16	Inside	Yes
		11	-	-	-	50, 1430	Package 17	Inside	-
		12	Log-mean-1100	-	-	50, 1430	Package 18	Inside	-
Seacoast	Rolled	7	5000	20	26.5	17, 1450	Package 19	Inside	-
		8	-	-	-	17, 1450	Package 20	Inside	-
		9	Log-mean-1100	-	-	17, 1450	Package 21	Inside	-
Lab Air	Die Forged	4	5000	60	13.0	4, 2500	None	-	-
		5	-	-	-	4, 2500	-	-	-
		6	-	-	-	4, 2500	-	-	-

- (1) Circulation laboratory air at 50 ± 5% relative humidity.  
 (2) Specimen enclosures subjected to 1-sec. injections of water salt water at 11-12 hr. intervals. For balance of time specimens were exposed to circulating laboratory air at 11-12 hr.  
 (3) For tests in laboratory air hydraulic pressure varied sinusoidally between minimum pressure of 700 to 1000 psi and maximum indicated. For tests in seacoast environment pressure held at maximum indicated for 100 to 1500 psi, then dropped sinusoidally to minimum of 700 to 1000 psi.  
 (4) For tests in seacoast environment, salt buildup and corrosion product was heaviest in the side of specimen (9 to 3 o'clock position).  
 (5) Based on metallographic examination.  
 (6) Origin at corrosion pit.  
 (7) Specimens had prior loading history, as indicated.

TABLE VI. RESULTS OF PREDICTION TESTS BY MECHANICAL TESTING  
 JULY 28-31-56

Environment	Cylinder Stock	Spec. No.	Pressure, psi	Pressure, psi	Max. Pressure, psi	No. of Cycles	Type	Intermittent Prediction			
								Intermittent	Final	Final	
Maximum Stress = 80% of Design Value											
Lab Air	Die Purged	8	8000	28	36.2	46,350	Particular	Intermittent	-	Yes	
		10	-	-	-	65,500	Particular	-	-	Yes	
Seacoast	Die Purged	1	8000	3.148	31.2	649	Log-mean-1150	Intermittent	-	Yes	
		2	-	-	-	645	Log-mean-1150	-	-	-	
Seacoast	Rolled	4	8000	3.148	36.2	1,573	Log-mean-1150	Intermittent	-	-	
		5	-	-	-	1,700	Log-mean-1150	-	-	-	
Maximum Stress = 60% of Design Value											
Lab Air	Die Purged	70	6500	40	27.8	97,400	Particular	Intermittent	-	Yes	
		71	-	-	-	219,240	Particular	-	-	Yes	
Maximum Stress = 90% of Design Value											
Lab Air	Die Purged	50	5000	40	21.8	2,135,790	Particular	Intermittent	-	Yes	
		51	-	-	-	8,400,470	Particular	-	-	Yes	
Seacoast	Die Purged	12	5000	3	21.8	67,000	Log-mean-1150	Intermittent	-	Yes	
		13	-	-	-	708,000	Log-mean-1150	-	-	Yes	
Seacoast	Rolled	9	5000	3	21.8	960,000	Log-mean-1150	Intermittent	-	Yes	
		10	-	-	-	1,357,000	Log-mean-1150	-	-	Yes	
Maximum Stress = 30% of Design Value											
Lab Air	Die Purged	5	3000	60	12.8	6,079,610	Log-mean-1150	Intermittent	-	-	
		6	-	-	-	-	Log-mean-1150	-	-	-	

- (1) Circulating laboratory air at 50 ± 5% relative humidity.  
 (2) Specimen enclosures subjected to 1-atm. injections of sea salt mist at 12-hr. intervals. For balance of time specimens were exposed to circulating laboratory air as in (1).  
 (3) For tests in laboratory air specimens were cycled alternately between minimum pressure of 200 to 400 psi and maximum indicated. For tests in seacoast environment specimens held at minimum indicated for 80% of cycle time, then dropped immediately to minimum of 200 to 400 psi.  
 (4) For tests in seacoast environment, salt buildup and corrosion product was heaviest on top side of specimen.  
 (5) Based on metallographic examination.  
 (6) Origin at corrosion pit.  
 (7) Specimens had prior loading history, as indicated.



TABLE 1. SUMMARY OF RESULTS OF AIR HYDRAULIC TESTING  
OF ALUMINUM TUBES

Test Result	Tested Specimen	No.	Min. Stress	Max. Stress	No. of Cycles	Type of Failure	Location of Failure	Time	Remarks
Maximum Stress = 80% of Design Value									
Fat. Air	Std. T-1000	10	8,000	10,000	27,100	Fatigue	Inside	"	Yes
		11	"	"	27,100	Fatigue	"	"	"
		12	"	"	27,100	Fatigue	"	"	"
		13	"	"	27,100	Fatigue	"	"	"
Log-mean-life					27,100				
Fat. Air	Std. T-1000	14	8,000	10,000	27,100	Fatigue	Inside	7:00	Yes
		15	"	"	27,100	Fatigue	"	7:00	"
		16	"	"	27,100	Fatigue	"	7:00	"
Log-mean-life					27,100				
Fat. Air	Std. T-1000	17	8,000	10,000	27,100	Fatigue	Inside	7:00	"
		18	"	"	27,100	Fatigue	"	7:00	"
		19	"	"	27,100	Fatigue	"	7:00	"
Log-mean-life					27,100				
Maximum Stress = 100% of Design Value									
Fat. Air	Std. T-1000	20	8,000	10,000	27,100	Fatigue	Inside	"	Yes
		21	"	"	27,100	Fatigue	"	"	"
Maximum Stress = 80% of Design Value									
Fat. Air	Std. T-1000	22	8,000	10,000	27,100	None	"	"	"
		23	"	"	27,100	"	"	"	"
		24	"	"	27,100	"	"	"	"
Fat. Air	Std. T-1000	25	8,000	10,000	27,100	Fatigue	Inside	7:00	Yes
		26	"	"	27,100	None	"	"	"
		27	"	"	27,100	Fatigue (1)	Outside (9)	7:00	Yes
Log-mean-life					27,100				
Fat. Air	Std. T-1000	28	8,000	10,000	27,100	None	"	"	"
		29	"	"	27,100	Fatigue	Inside	7:00	"
		30	"	"	27,100	Fatigue	Inside	7:00	"
Log-mean-life					27,100				
Maximum Stress = 100% of Design Value									
Fat. Air	Std. T-1000	31	8,000	10,000	27,100	None	"	"	"
		32	"	"	27,100	"	"	"	"
		33	"	"	27,100	"	"	"	"

(1) Circulating laboratory air at 50-55% relative humidity.

(2) Specimen enclosures subjected to 1-min. injections of warm salt mist at 12-hr intervals. For balance of time specimens were exposed to circulating laboratory air as in (1).

(3) For tests in laboratory air hydraulic pressure cycled sinusoidally between minimum pressure of 200 to 400 psi and maximum indicated. For tests in sea-coast environment pressure held at maximum indicated for 80% of cycle time, then dropped sinusoidally to minimum of 200 to 400 psi.

(4) For tests in sea-coast environment, salt buildup and corrosion product was heaviest on top side of specimen (9 to 1 o'clock position).

(5) Not included in log mean life.

(6) Specimen subjected to same load cycle as specimens tested in sea-coast environment.

(7) Origin at corrosion pit.

• Specimens had prior loading history, as indicated.

TABLE XIII. RESULTS OF FATIGUE TESTS OF HYDRAULIC CYLINDERS  
Alloy CH70-37

Environment	Cylinder Stock	Spec. No.	Fatigue Loading (3)		Max. Stress, ksi	No. of Cycles	Type	Description of Failure	
			Pressure, psi	Freq. cpm				Initiation Position	Parting Plane
<u>Maximum Stress = 80% of Design Value</u>									
Lab Air (1)	Cast	7	8,000	20	32.0	10,170	Fatigue	Inside	-
		8	"	"	"	10,370	"	"	-
		9	"	Log-mean-life	"	10,970	"	"	-
Seacoast (2)	Cast	12	8,000	9 1/8	32.0	12,290	Fatigue	Inside	4:00
		13	"	"	"	14,590	"	"	3:00
		2	"	Log-mean-life	"	15,260	"	"	3:15
<u>Maximum Stress = 50% of Design Value</u>									
Seacoast	Cast	1	5,000	3	20.0	82,330			7:00
		10	"	"	"	92,660			5:00
		11	"	Log-mean-life	"	99,100			7:00
<u>Maximum Stress = 30% of Design Value</u>									
Lab Air	Cast	5	3,000	60	12.0	649,800	Fatigue	Inside	-
		6	"	60	"	714,100	"	"	-
		4	"	Log-mean-life	"	903,990	"	"	-
<u>710,000</u>									

- (1) Circulating laboratory air at 50 ±5% relative humidity.
- (2) Specimen enclosures subjected to 1-min. injections of warm salt mist at 12-hr intervals. For balance of time specimens were exposed to circulating laboratory air as in (1).
- (3) For tests in laboratory air hydraulic pressure cycled sinusoidally between minimum pressure of 200 to 420 psi and maximum indicated. For tests in seacoast environment, pressure held at maximum indicated for 80% of cycle time, then dropped sinusoidally to minimum of 200 to 400 psi.
- (4) For tests in seacoast environment, salt buildup and corrosion product was heaviest on top side of specimen (9 to 3 o'clock position).

TABLE III. SUMMARY OF FATIGUE TEST RESULTS OF FORGED AND ROLLED CYLINDERS

Alloy & Temper (Max. Test Stress, ksi)	Cylinder Stock	Fatigue Lives for Individual Specimens, Cycles			
		Tests in Laboratory Environment (1)		Tests in Simulated Aircraft Environment (2)	
7075-T6 (37.3)	Die forged Rolled	22,800 31,000 No tests	20,000; 12,100; 10,000 No tests	100 1,000 1,000 1,000 1,000 1,000 1,000 1,000	1,000 1,000 1,000 1,000
7075-T6 (37.4)	Die forged Rolled	4,000 27,000 No tests	10,000; 12,100; 10,000 No tests	100 1,000 1,000 1,000 1,000 1,000 1,000 1,000	1,000 1,000 1,000 1,000
X7080-T7 (34.6)	Die forged Rolled	11,100 20,700 No tests	10,000; 12,100; 10,000 No tests	100 1,000 1,000 1,000 1,000 1,000 1,000 1,000	1,000 1,000 1,000 1,000
2014-T6 (34.2)	Die forged Rolled	46,100 55,600 No tests	57,200; 12,100; 10,000 No tests	100 1,000 1,000 1,000 1,000 1,000 1,000 1,000	1,000 1,000 1,000 1,000
7075-T73 (33.0)	Die forged Rolled	39,300 48,600 No tests	49,600; 12,100; 10,000 No tests	100 1,000 1,000 1,000 1,000 1,000 1,000 1,000	1,000 1,000 1,000 1,000
CH70-T7 (32.0)	Premium cast	10,200 10,400 No tests	11,000; 12,100; 10,000 No tests	100 1,000 1,000 1,000 1,000 1,000 1,000 1,000	1,000 1,000 1,000 1,000

(1) Cylinders cycled at approximately 20 cps in circulating laboratory air at 50% relative humidity.

(2) Cylinders cycled at approximately 9 cps, with 0.4-min hold time at maximum stress for each cycle. Specimen enclosures subjected to 1-min. injections of warm salt mist at 12-hr intervals. For balance of time specimens are exposed to circulating laboratory air at 50% relative humidity.

# 12,100 indicates log-mean-fatigue life.

TABLE XV. SUMMARY OF FATIGUE TEST RESULTS OF HYDRAULIC CYLINDERS UNDER HOOP STRESS EQUAL TO 1% OF DESIGN STRESS

Alloy & Temper. Max. Test Stress, ksi	Cylinder Stock	Fatigue Lives for Triplicate Specimens, Cycles	
		Tests in Laboratory Environment (1)	Tests in Simulated Seawater Environment (2)
7075-T6 (23.7)	Die forged Rolled	3 @ 8,000,000 without failure No tests	51,340; 60,480; 213,592 L.M.I. = 37,110 76,240; 115,920; 931,930 = 222,520
7079-T6 (23.4)	Die forged Rolled	2 @ 600; 150,000; 583,000; L.M.I. = 193,000 No tests	29,650; 35,110; 49,035 = 37,190 9,580; 52,940; 69,900 = 32,730
X7080-T7 (21.6)	Die forged Rolled	1 @ 1,361,000; 2 @ 8,000,000 without failure No tests	33,795; 304,050; 705,600 = 222,520 130,450; 127,620; 120,940 = 115,330
2014-T6 (21.4)	Die forged Rolled	1 @ 2,177,000; 2 @ 8,000,000 without failure No tests	67,980; 680,400; 705,400 = 313,110 848,100; 969,900; 1,157,400 = 938,200
7075-T73 (20.6)	Die forged Rolled	3 @ 8,000,000 without failure No tests	636,400; 1,002,700; (4) = 517,000 270,320; 1,145,570; (4) = 720,200
CH70-T7 (20.0)	Premium cast	All failed at 30% of design stress (12.3 ksi) L.M.I. = 749,000 @ 60 cpm	82,330; 92,660; 99,695 = 31,110

(1) Cylinders cycled at approximately 48 cpm in circulating laboratory air at 50% relative humidity. All die forged cylinders had previously withstood 6,060,000 cycles at 30% of design stress without failure @ 60 cpm.

(2) Cylinders cycled at approximately 3 cpm with 16-sec hold time at maximum stress for each cycle. Specimen enclosures subjected to 1-min. injections of warm salt mist at 12-hr intervals. For balance of time specimens are exposed to circulating laboratory air at 50% relative humidity.

(3) L.M.I. indicates log-mean-fatigue life.

(4) Did not fail in 1,200,000 loadings.

TABLE XVI. RESULTS OF FATIGUE TESTS OF C-RINGS  
ALLOY 7075-T6

Environment	Stock	Spec. No.	Fatigue Loading		No. of Cycles	Fracture Location		Remarks
			Max. Stress ksi	Freq. cpm		Distance from Maximum Moment, Degrees	Position <sup>a</sup>	
Maximum Stress = 80% of Design Value								
Lab Air	Die Forged	1	37.9	Approx 36	18,000	5		
		6	"	"	20,800	5		
		19	"	"	43,600	20		
		8	Log-mean-life		119,000	0	Edge	
Maximum Stress = 65% of Design Value								
Seacoast	Die Forged	2	37.9	1-1/2	32,900	5		Mixed SCC and fatigue
		9	"	"	41,300	0		
		3	Log-mean-life		47,800	20		
					40,100			
Seacoast	Rolled	B	37.9	1-1/2	30,500	10		
		C	"	"	66,300	15		
		A	Log-mean-life		81,300	5		
					54,900			
Maximum Stress = 65% of Design Value								
Lab Air	Die Forged	5*	30.8	Approx 26	49,600	0		
Maximum Stress = 50% of Design Value								
Lab Air	Die Forged	4*	23.7	Approx 36	1,617,800	0		Mixed SCC and fatigue
		7*	"	"	1,928,600	5	0.2" from Edge	
		5*	"	"	10,788,000		None	
Seacoast	Die Forged	10	23.7	10	256,500	5		
		17	"	"	1,736,200	10		
		11	Log-mean-life		1,788,800	5	0.1" from edge	
					927,000			
Seacoast	Rolled	E	23.7	10	1,801,700	15		
		F	"	"	1,836,100	5		
		D	Log-mean-life		2,048,400			
					1,930,000			
Maximum Stress = 30% of Design Value								
Lab Air	Die Forged	4	14.2	Approx 36	2,462,600		None	
		5	"	"	"		"	
		7	"	"	"		"	

Notes

- (1) Circulating laboratory air at 50 ± 5% relative humidity.
- (2) Specimen enclosures subjected to 1-min. injections of warm salt mist at 12-hr. intervals. For balance of time specimens were exposed to circulating laboratory air as in (1).
- (3) Minimum stress in cycle approximately 0.4 ksi.
- (4) Failure origins within central half of specimen unless noted otherwise.

\*Specimen had prior stress history as indicated.

TABLE XVII. RESULTS OF FATIGUE TESTS OF C-RINGS  
ALLOY 7079-T6

Environment	Stock	Spec. No.	Fatigue Loading		No. of Cycles	Fracture Location		Remarks
			Max. Stress ksi	Freq. cpm		Distance from Maximum Moment, Degrees	Position <sup>4</sup>	
Maximum Stress = 80% of Design Value								
Lab Air	Die Forged	9	37.4	Approx 36	29,800	0		
		7	"	"	37,400	5		
		8	"	"	40,400	10		
Log-mean-life								
Seacoast	Die Forged	1	37.4	1-1/2	6,030	5		
		3	"	"	7,560	5		
		2	"	"	11,370	15		0.2" from edge
Log-mean-life								
Seacoast	Rolled	A	37.4	1-1/2	9,800	15		
		B	"	"	15,500	20		
		C	"	"	19,900	25		
Log-mean-life								
Maximum Stress = 65% of Design Value								
Lab Air	Die Forged	4*	30.4	Approx 26	93,500	5		
		6*	"	"	2,298,100	10		
Log-mean-life								
Maximum Stress = 50% of Design Value								
Lab Air	Die Forged	5*	23.4	Approx 36	3,100,800	40		
		4*	"	"	10,788,000			None
		6*	"	"				
Seacoast	Die Forged	12	23.4	10	1,831,600	0		
		11	"	"	1,879,700	10		
		10	"	"	2,273,400	0		
Log-mean-life								
Seacoast	Rolled	D	23.4	10	79,600	15		
		E	"	"	359,100	20		
		F	"	"	395,000	15		
Log-mean-life								
Maximum Stress = 30% of Design Value								
Lab Air	Die Forged	4	14.0	Approx 36	2,462,600			None
		5	"	"	"			"
		6	"	"	"			"

Notes

- (1) Circulating laboratory air at 50 ± 5% relative humidity.
- (2) Specimen enclosures subjected to 1-min. injections of warm salt mist at 12-hr. intervals. For balance of time specimens were exposed to circulating laboratory air as in (1).
- (3) Minimum stress in cycle approximately 0.4 ksi.
- (4) Failure origins within central half of specimen unless noted otherwise.

\*Specimen had prior stress history as indicated.

TABLE XVIII. RESULTS OF FATIGUE TESTS OF C-RINGS  
ALLOY X7080-T7

Environment	Stock	Spec. No.	Fatigue Loading		No. of Cycles	Fracture Location		Remarks
			Max. Stress ksi	Freq. cpm		Distance from Maximum Moment, Degrees	Position <sup>4</sup>	
<u>Maximum Stress = 80% of Design Value</u>								
Lab Air	Die Forged	34*	34.6	Approx 36	125,500	0	0.2" from edge	
		38	"	"	2,681,800	5		
		37	"	"	3,263,300	0		
		39	"	"	8,838,400	0		
			Log-mean-life *		4,261,000			
Seacoast	Die Forged	32	34.6	1-1/2	34,800	5		Mixed SCC and fatigue
		31	"	"	35,500	0		
		33	"	"	74,400	0		
			Log-mean-life		45,100			
Seacoast	Rolled	B	34.6	1-1/2	100,800	20		
		A	"	"	116,300	5		
		C	"	"	171,200	5		
			Log-mean-life		126,000			
<u>Maximum Stress = 65% of Design Value</u>								
Lab Air	Die Forged	36*	28.1	Approx 26	88,800	0		
		35*	"	"	3,128,100	0		
			Log-mean-life					
<u>Maximum Stress = 50% of Design Value</u>								
Lab Air	Die Forged	34*	21.6	Approx 36	10,788,000		None	
		35*	"	"	"			
		36*	"	"	"			
Seacoast	Die Forged	40	21.6	10	1,879,700	0		
		42	"	"	1,965,900	0		
		41	"	"	2,233,800	5		
			Log-mean-life		2,020,000			
Seacoast	Rolled	D	21.6	10	2,327,100	0	None	
		E	"	"	3,353,400	15		
		F	"	"	4,100,000			
			Log-mean-life		2,820,000			
<u>Maximum Stress = 30% of Design Value</u>								
Lab Air	Die Forged	34	13.0	Approx 36	2,462,600		None	
		35	"	"	"			
		36	"	"	"			

Notes

- (1) Circulating laboratory air at 50 ± 5% relative humidity.
- (2) Specimen enclosures subjected to 1-min. injections of warm salt mist at 12-hr. intervals. For balance of time specimens were exposed to circulating laboratory air as in (1).
- (3) Minimum stress in cycle approximately 0.4 ksi.
- (4) Failure origins within central half of specimen unless noted otherwise.

\* Specimen had prior stress history as indicated.

TABLE XIX. RESULTS OF FATIGUE TESTS OF C-RINGS  
ALLOY 2014-T6

Environment	Stock	Spec. No.	Fatigue Loading		No. of Cycles	Fracture Location		Remarks
			Max. Stress ksi	Freq. cpm		Distance from Maximum Moment, Degrees	Position	
Maximum Stress = 80% of Design Value								
Lab Air	Die Forged	10	34.2	Approx 36	103,200	0		
		8	"	"	109,300	0		
		9	"	"	209,790	5		
Log-mean-life								
Seacoast	Die Forged	1	34.2	1-1/2	14,100	5		
		3	"	"	41,200	5		
		2	"	"	149,600	5	Edge	Stress-corrosion cracking SCC, small areas of fatigue
Log-mean-life								
Seacoast	Rolled	C	34.2	1-1/2	97,600	10		
		B	"	"	137,700	25		
		A	"	"	196,400	15	0.2" from edge	
Log-mean-life								
Maximum Stress = 65% of Design Value								
Lab Air	Die Forged	5*	27.8	Approx 26	230,500	0		
		6*	"	"	326,800	25	0.1" from edge	
Log-mean-life								
Maximum Stress = 50% of Design Value								
Lab Air	Die Forged	4*	21.4	Approx 36	4,883,400	0	Edge	
		5*	"	"	13,788,000		None	
		6*	"	"			"	
Seacoast	Die Forged	20	21.4	10	1,593,400	0		
		11	"	"	1,996,100	5		
		12	"	"	2,698,400	0		
Log-mean-life								
Seacoast	Rolled	D	21.4	10	4,100,000		None	
		E	"	"	2,146,100	5		
		F	"	"	4,081,600	5		
Log-mean-life								
Maximum Stress = 30% of Design Value								
Lab Air	Die Forged	4	12.8	Approx 36	2,462,600		None	
		5	"	"			"	
		6	"	"			"	

Notes

- (1) Circulating laboratory air at 50 ± 5% relative humidity.
- (2) Specimen enclosures subjected to 1-min. injections of warm salt mist at 12-hr. intervals. For balance of time specimens were exposed to circulating laboratory air as in (1).
- (3) Minimum stress in cycle approximately 0.4 ksi.
- (4) Failure origins within central half of specimen unless noted otherwise.

\* Specimen had prior stress history as indicated.



TABLE XX. RESULTS OF FATIGUE TESTS OF C-RINGS  
ALLOY 7075-T73

Environment	Stock	Spec. No.	Fatigue Loading Max. Stress ksi	Freq. cpm	No. of Cycles	Distance from Maximum Moment, Degrees	Fracture Location Position <sup>4</sup>	Remarks
Maximum Stress = 80% of Design Value								
Lab Air	Die Forged	8	33.0	Approx 36	49,400	0		
		4*	"	"	130,700	0		
		9	"	"	741,700	0	Edge	
		7	"	"	1,482,800	0		
Log-mean-life				378,800				
Seacoast	Die Forged	2	33.0	1-1/2	63,900	5	0.1" from edge	
		3	"	"	166,100	5	0.2" from edge	
		1	"	"	2,132,000	5		
			"	"	224,000			
Log-mean-life				277,000				
Seacoast	Rolled	C	33.0	1-1/2	206,900	10		
		B	"	"	239,400	30		
		A	"	"	430,200	30		
			"	"	277,000			
Log-mean-life				277,000				
Maximum Stress = 65% of Design Value								
Lab Air	Die Forged	5*	26.8	Approx 26	1,076,800	2		
		6*	"	"	2,302,900	5		
			"	"				
			"	"				
Log-mean-life				277,000				
Maximum Stress = 50% of Design Value								
Lab Air	Die Forged	4*	20.6	Approx 36	10,788,000		None	
		5*	"	"	"		"	
		6*	"	"	"		"	
			"	"	"		"	
Seacoast	Die Forged	12	20.6	10	1,793,300	5		
		10	"	"	2,185,500	5		
		11	"	"	4,100,000		None	
			"	"	2,520,000			
Log-mean-life				277,000				
Seacoast	Rolled	D	20.6	10	2,607,200	5		
		E	"	"	4,100,000		None	
		F	"	"	3,269,300	10		
			"	"	3,270,800			
Log-mean-life				277,000				
Maximum Stress = 30% of Design Value								
Lab Air	Die Forged	4	12.4	Approx 36	2,462,600		None	
		5	"	"	"		"	
		6	"	"	"		"	
			"	"	"		"	

Notes

- (1) Circulating laboratory air at 50 ± 5% relative humidity.
  - (2) Specimen enclosures subjected to 1-min. injections of warm salt mist at 12-hr. intervals. For balance of time specimens were exposed to circulating laboratory air as in (1).
  - (3) Minimum stress in cycle approximately 0.4 ksi.
  - (4) Failure origins within central half of specimen unless noted otherwise.
- \* Specimen had prior stress history as indicated.

TABLE III. RESULTS OF FATIGUE TESTS OF C-RINGS  
ALLOY CM70-37

Environment	Stock	Spec. No.	Fatigue Loading		No. of Cycles	Fracture Location		Remarks
			Max. Stress ksi	Freq. cpm		Distance from Maximum Moment, Degrees	Position <sup>1</sup>	
<u>Maximum Stress = 80% of Design Value</u>								
Lab Air	Cast	37	22.0	Approx 36	56,200	15		
		39	"	"	103,700	15		
		38	"	"	121,900	5		
				Log-mean-life	69,200			
Seacoast	Cast	32	32.0	1-1/2	62,200	10		
		33	"	"	287,500	0		
		31	"	"	418,700	0		
				Log-mean-life	196,000			
<u>Maximum Stress = 65% of Design Value</u>								
Lab Air	Cast	35*	26.0	Approx 26	227,200	15		
<u>Maximum Stress = 50% of Design Value</u>								
Lab Air	Cast	43	20.0	Approx 36	530,600	15		
Seacoast	Cast	42	20.0	10	340,000	10		
		40	"	"	388,200	5		
		41	"	"	413,100	5		
				Log-mean-life	380,300			
<u>Maximum Stress = 30% of Design Value</u>								
Lab Air	Cast	36	12.0	Approx 36	1,569,200	5		
		34	"	"	2,025,047	10		
		35	"	"	13,250,530			None

Notes

- (1) Circulating laboratory air at 50 ± 5% relative humidity.
- (2) Specimen enclosures subjected to 1-min. injections of warm salt mist at 12-hr. intervals. For balance of time specimens were exposed to circulating laboratory air as in (1).
- (3) Minimum stress in cycle approximately 0.4 ksi.
- (4) Failure origins within central half of specimen unless noted otherwise.

\*Specimen had prior stress history as indicated.

TABLE XXII. RESULTS OF STRESS-CORROSION TESTS ON STATIC-LOADED C-RINGS  
EXPOSED FOR 84 DAYS TO ALTERNATE-IMMERSION TEST IN 3.5%  
NaCl SOLUTION

Alloy & Temper	Max Stress, ksi	Number Failures (F)/Number Exposed (N) and Time to Failure		
		Die Forged or Cast	F/N	Time in Days (I)
7075-T6	37.9	2/2	2/2	44(a), 84(a)
	26.1	2/2	2/2	44(a), 84(a)
	14.2	2/2	2/2	45(a), 84(a)
7079-T6	37.4	2/2	2/2	7, 14
	25.7	2/2	2/2	18, 21
	14.0	2/2	2/2	30(a), 78
X7080-T7	34.6	0/2	0/2	2 OK 84
	23.8	0/2	0/2	" " "
	13.0	0/2	0/2	" " "
2014-T6	34.2	2/2	2/2	44(a), 84(a)
	23.5	2/2	2/2	45(a), 84(a)
	12.8	2/2	2/2	45(a), 84(a)
7075-T73	33.0	0/2	0/2	2 OK 84
CH70-T7 (cast)	32.0	0/2		
	22.0	0/2		
	12.3	0/2		

Specimens 4.08" O.D. by 3/16" thick by 1" wide. Parting plane in rings from die forgings located at section of maximum bending stress. Ring opened up to develop tensile stresses on inside surface.

Exposure cycle consisted of 10-min immersion in solution and 50-min exposure in air at 80°F and 45% relative humidity.

(1) OK 84 means specimens survived 84-day test period with no evidence of stress-corrosion cracking as determined by visual or metallographic examination. Suffix (a) means that specimens were removed from test at time indicated and the presence of stress-corrosion cracks confirmed by metallographic examination.

TABLE XXIII.- RESULTS OF STRESS-CORROSION TESTS ON STATIC-LOADED C-RINGS  
EXPOSED IN LABORATORY TO SIMULATED SEACOAST ENVIRONMENT

Alloy & Temper	Max. Stress, ksi	Number Failures (F)/Number Exposed (N)			and Time to Failure	
		Die Forged or Cast		P/N	Rolled Rod Stock	
		F/N	Time in Days		F/N	Time in Days
7075-T6	37.9	3/3	19, 20, 26		2/3	152, 160, 172
	26.1	3/3	59, 67, 70		2/3	249, 2 OK <sup>b</sup> 365
	14.2	3/3	3 at 293(a)		0/3	1 OK 293(*), 2 OK <sup>b</sup> 365
7079-T6	37.4	3/3	6, 8, 11		3/3	40, 40, 54
	25.7	3/3	40, 95, 95		2/3	267, 278, OK <sup>b</sup> 365
	14.0	2/3	104, 109, 1 OK <sup>b</sup> 365		0/3	1 OK 293(*), 2 OK <sup>b</sup> 365
X7080-T7	34.6	3/3	173, 179, 193		0/3	1 OK 293(*), 2 OK <sup>b</sup> 365
	23.8	0/3	1 OK 293(*), 2 OK <sup>b</sup> 365		0/3	" " " " " " " "
	13.0	0/3	" " " " " " " "		0/3	" " " " " " " "
2014-T6	34.2	3/3	8, 12, 32		2/3	249, 249, OK <sup>b</sup> 365
	23.5	3/3	92, 99, 249		0/3	1 OK 293(*), 2 OK <sup>b</sup> 365
	12.8	0/3	1 OK 293(*), 2 OK <sup>b</sup> 365		0/3	" " " " " " " "
7075-T73	33.0	0/3	1 OK 293(*), 2 OK <sup>b</sup> 365		0/3	1 OK 293 (*), 2 OK <sup>b</sup> 365
CH70-T7 (cast)	32.0	0/3	1 OK 293(*), 2 OK <sup>b</sup> 365			
	22.0	0/3	" " " " " " " "			
	12.0	0/3	" " " " " " " "			

Specimens 4.08" O.D. by 3/16" thick by 1" wide. Parting plane in rings from die forgings located at section of maximum bending stress. Ring opened up to develop tensile stresses on inside surface.

Environment provided by saturating specimen enclosures with warm salt mist at 12-hr intervals. For balance of time specimens were exposed to circulating laboratory air at 50% relative humidity.

<sup>b</sup> Removed after 1 year's exposure

(\*) Removed from test at 293 days for metallographic examination which confirmed that the specimen was free from any stress-corrosion cracking.

(a) All three specimens removed from test at 293 days because of exfoliation in the test area. Metallographic examination showed incipient stress-corrosion cracking was also present.

TABLE XXIV. RESULTS OF STRESS-CORROSION TESTS ON STATIC-LOADED C-RINGS EXPOSED TO SEACOAST ATMOSPHERE AT POINT JUDITH, R. I.

Alloy & Temper	Max. Stress, ksi	Number Failures (F)/Number Exposed (N) and Time to Failure			
		Die Forged or Cast		Rolled Rod Stock	
		F/N	Time in Days (1)	P/N	Time in Days (1)
7075-T6	37.9	3/3	All A	3/3	All A
	26.1	3/3	" "	2/3	2A; 1 OK 765
	14.2	3/3	" "	1/3	730b, 2 OK 765
7079-T6	37.4	3/3	All A	3/3	1 in 4; 2A
	25.7	3/3	" "	3/3	All B
	14.0	3/3	All C	0/3	3 OK 765
X7080-T7	34.6	0/3	1 OK <sup>a</sup> 730, 20K 765	0/3	3 OK 765
	23.8	0/3	3 OK 765	0/3	" "
	13.0	0/3	" "	0/3	" "
2014-T6	34.2	3/3	All A	2/3	2A; 1 OK 765
	23.5	3/3	" "	0/3	730b, 2 OK 765
	12.8	2/3	2A; 1 OK 765	0/3	3 OK 765
7075-T73	33.0	0/3	3 OK 765	0/3	3 OK 765
CH70-T7 (cast)	32.0	0/3	1 OK <sup>a</sup> 730, 20K 765		
	22.0	0/3	3 OK 765		
	12.0	0/3	" "		

Specimens 4.08" O.D. x 3/16" thick by 1" wide. Parting plane in rings from die forgings located at section of maximum bending stress. Ring opened up to develop tensile stresses on inside surface.

(1) Times to failure:

- A indicates failure between 103 and 210 days
- B indicates failure between 211 and 289 days
- C indicates failure between 290 and 386 days

- a Removed from test at 730 days, metallographic examination confirmed that specimen was free of stress-corrosion cracking.
- b Removed from test at 730 days, metallographic examination detected incipient stress-corrosion cracking.

TABLE XIV. SUMMARY OF FLEXURAL FATIGUE TEST RESULTS OF C-RINGS UNDER HOOP TENSIONS EQUAL TO 80% OF DESIGN STRESSES

Alloy & C-Ring Stock Temper (Max. Test Stress, ksi)	Fatigue Lives for 3 or 4 Specimens, Cycles			
	Tests in Laboratory Environment (1)		Tests in Simulated Seacoast Environment (2)	
7075-T6 (37.9)	Die forged Rolled	18,000 20,800 43,600 119,000; 1.m.l. # = 37,300 No tests	32,900 41,300 47,800; 1.m.l. = 40,100 30,500 66,300 81,300; 1.m.l. = 54,900	
7079-T6 (37.4)	Die forged Rolled	29,800 37,400 40,400; 1.m.l. = 35,600 No tests	6,030 7,560 11,370; 1.m.l. = 8,030 9,800 16,000 19,940; 1.m.l. = 14,800	
X7080-T7 (34.6)	Die forged Rolled	2,682,000 3,263,000 8,838,000; 1.m.l. = 4,261,000 No tests	34,800 35,500 74,400; 1.m.l. = 45,100 100,800 116,300 171,200; 1.m.l. = 126,000	
2014-T6 (34.2)	Die forged Rolled	103,200 109,300 209,700; 1.m.l. = 133,200 No tests	14,090 41,200 149,600; 1.m.l. = 44,200 97,560 137,700 196,300; 1.m.l. = 130,500	
7075-T73 (33.0)	Die forged Rolled	49,400 741,700 1,483,000; 1.m.l. = 378,800 No tests	63,930 166,100 2,932,000; 1.m.l. = 224,000 206,900 239,450 430,200; 1.m.l. = 277,000	
CH70-T7 (32.0)	Premium cast	56,200 103,700 121,900; 1.m.l. = 89,200	62,200 267,500 418,700; 1.m.l. = 196,050	

(1) C-rings flexed at approximately 30 cps in laboratory air at 50% relative humidity.

(2) C-rings flexed at approximately 90 cphr, with 32-sec hold time at maximum stress for each cycle. Specimen enclosures subjected to 1-min injections of warm salt mist at 12-hr intervals. For balance of time specimens are exposed to circulating laboratory air at 50% relative humidity.

# 1.m.l. indicates log-mean-fatigue life.



TABLE XXVII. COMPARISON OF SPECIMEN LIVES IN CORROSION-FATIGUE AND VARIOUS TYPES OF STATIC-STRESS-CORROSION TEST

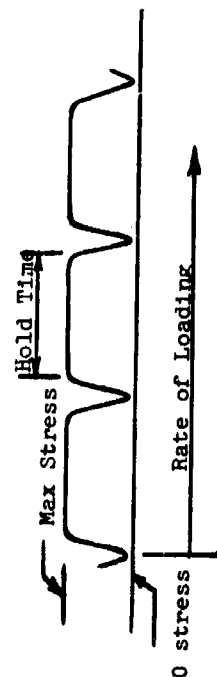
Alloy & Temper	Max. Test Stress, ksi	Material	Time to Failure <sup>a</sup> , days				
			Cylinders		C-Rings		
			Corrosion-Fatigue (Triplicate Tests)	Stress-Corrosion (Duplicate Tests)	Corrosion-Fatigue (Triplicate Tests)	Alternate-Immersion <sup>b</sup> (Duplicate Tests)	Stress-Corrosion Simulated Seacoast (Triplicate Tests)
7075-T6	37.9	Forged Rolled	3.5, 4.4, 5.5 10, 25, (55) <sup>c</sup>	7, 8 --	12 <sup>d</sup> , 15, 18 11, 24, 30	7, 7 44, 84	19, 20, 26 152, 160, 172
7079-T6	37.4	Forged Rolled	0.2, 1.7, 2.2 2.6, 3.6, 12.4	--	2.2, 2.8, 4.2 3.6, 6.7	1, 4 7, 14	6, 8, 11 40, 40, 54
X7080-T7	34.6	Forged Rolled	(32, 40, 47) (64, 85, 84)	--	(13, 13, 28) (38, 44, 64)	None in 84 None in 84	179, 179, 193 None in 1 year
2014-T6	34.2	Forged Rolled	2.4 to 3.6 5.9, 29, 71	--	5, 15, 55 36, 51, 77	3, 3 44, 84	8, 12, 32 249, 249

<sup>a</sup> Includes time at load only.

<sup>b</sup> Test in 3.5% NaCl solution. Cycle consisted of 10-min. immersion followed by 50 min. in air at 80°F and 45% relative humidity. All other tests (corrosion-fatigue or stress-corrosion) were conducted in simulated seacoast environment produced by saturating specimen enclosures with warm salt mist at 12-hr intervals. For balance of period specimens were exposed to circulating laboratory air at 50% relative humidity.

<sup>c</sup> Numbers in parenthesis indicate fatigue rather than stress corrosion failures.

<sup>d</sup> Underlined numbers indicate mixtures of stress-corrosion and fatigue cracking.



Load Cycles for Corrosion-Fatigue Tests

Cylinders		C-Rings	
Hold-time	5.4 min	32 sec	
Rate	9 cphr	90 cphr	



TABLE XXVIII  
RESULTS OF FATIGUE TESTS OF HYDRAULIC CYLINDERS  
IN NONCORROSIVE ENVIRONMENT

Alloy and Temper	Product	Cylinder Dimensions, in.		Spec. No.	Max. Test Stress ksi	Cycles to Failure	Description of Fatigue Crack (c)			
		O.D.	Wall				Point of Initia- tion (a)	Max. Depth, a, in.	Max. Length, 2c, in.	Shape
7075-T6	Die Forging	3.101	0.300	7	30.8	88,290	In	0.23	0.64	
				4	30.8	505,100	Out-P	0.28	0.96	
				6	37.9	22,840	In	0.23	0.66	
				8	37.9	31,760	In-P	0.17	0.44	
				9	37.9	40,760	In-P	0.20	0.58	
				5	37.9	68,260	In-P	0.15	0.44	
7079-T6	Die Forging	3.113	0.306	4	23.4	89,590	Out-P	0.31	0.85	
				5	23.4	149,900	In(b)	0.30	0.77	
				6	23.4	587,500	Out-P	0.21	0.61	
				7	37.4	3,960	Out-F	0.16	0.38	
				8	37.4	27,860	In-P	0.19	0.52	
				9	37.4	38,110	Out	0.20	0.50	
X7080-T7	Die Forging	3.161	0.330	6	21.6	1,361,500	In-P	0.30	0.98	
				4	28.1	80,630	In	0.27	0.88	
				5	28.1	147,560	Out	0.31	0.92	
				8	34.6	12,070	In-P	0.19	0.61	
				7	34.6	20,680	In	0.21	0.65	
				9	34.6	41,760	In-P	0.22	0.63	
2014-T6	Die Forging	3.177	0.338	5	21.4	2,176,800	Out	0.30	1.07	
				7	27.8	97,480	In	0.20	0.48	
				4	27.8	219,240	Out-P	0.24	0.72	
				8	34.2	46,050	In-P	0.17	0.44	
				10	34.2	65,590	In-P	0.20	0.50	
				9	34.2	87,160	In	0.18	0.64	
7075-T73	Die Forging	3.201	0.350	6	26.8	5,311,800	In-P	0.25	0.84	
				4	26.8	7,001,500	--	No Failure		
				7	33.0	39,280	In	0.26	0.87	
				8	33.0	48,790	In-P	0.23	0.70	
				9	33.0	49,560	In-P	0.28	0.80	
				5	33.0	57,310	In	0.23	0.82	
CH70-T7	Premium Casting	3.229	0.364	5	12.0	649,800	In(b)	0.36	0.83	
				6	12.0	714,100	In(b)	0.36	0.94	
				4	12.0	904,000	In(b)	0.36	0.89	
				7	32.0	10,170	In	0.36	1.39	
				8	32.0	10,370	In	0.28	1.65	
				9	32.0	10,970	In(b)	0.36	1.20	

(a) "In" or "Out" refers to interior or exterior surface of specimen;  
-P indicates failure in parting plane of die forgings.

(c) Fatigue cracks penetrated outer surface, stopping test, but there was no general failure. Specimens No. 7 and 8 of CH70-T7 developed cracks 5 and 6-1/2 in. long, respectively. In all other cases the fatigue cracks led to general instability failure, with splitting over entire length of test section.

(p) a = max. depth of fatigue crack through thickness of cylinder wall.  
2c = max. length of fatigue crack, normal to "a" direction

TABLE XXIX

FRACTURE MECHANIC. ANALYSIS OF FRACTURES IN VESSELS UNDER CYCLIC INTERNAL PRESSURE

Cyclic Test Environment	Ally and Temper	THE FORGINGS										ROLLED BOB									
		K <sub>IC</sub> , ksi√in.	Average Maximum Cyclic Stress, ksi	Depth, in.	Crack Descriptors, a, in.	a/2c, in.	q, in.	K <sub>IC</sub> , ksi√in.	K <sub>IC</sub> /K <sub>IC</sub>	K <sub>IC</sub> , ksi√in.	Average Maximum Cyclic Stress, ksi	Depth, in.	Crack Descriptors, a, in.	a/2c, in.	q, in.	K <sub>IC</sub> , ksi√in.	K <sub>IC</sub> /K <sub>IC</sub>				
X12-76	Ambient	15.9	18.9	0.30	1.92	0.156	1.23	0.244	18.2	1.14	16.8	0.31	0.86	0.361	1.88	0.165	15.0	0.89			
	Salt Fog	24.7	24.7	0.20	0.72	0.324	1.77	0.136	17.7	1.11	16.8	0.20	0.48	0.147	2.12	0.101	18.3	1.06			
		30.2	30.2	0.17	0.44	0.386	1.99	0.085	17.2	1.08	30.2	0.17	0.44	0.386	1.99	0.085	22.2	1.31			
		30.2	30.2	0.20	0.50	0.400	2.05	0.098	18.4	1.16	30.2	0.20	0.50	0.400	2.05	0.127	20.9	1.24			
7075-T6	Ambient	10.8	27.5	0.28	0.96	0.142	2.39	0.113	22.2	1.12	22.0	0.29	0.86	0.317	1.70	0.118	17.5	0.80			
	Salt Fog	27.5	27.5	0.23	0.64	0.360	1.88	0.125	19.0	0.96	21.1	0.23	0.64	0.360	1.88	0.125	16.6	0.76			
		33.8	33.8	0.15	0.44	0.386	1.99	0.085	23.3	1.15	33.8	0.15	0.44	0.386	1.99	0.085	21.8	0.99			
		33.8	33.8	0.20	0.53	0.395	1.82	0.110	20.2	0.97	33.8	0.20	0.53	0.395	1.82	0.110	23.5	1.07			
7075-T73	Ambient	20.6	23.6	0.25	0.84	0.298	1.63	0.153	18.0	0.87	24.3	0.25	0.84	0.298	1.63	0.153	24.7	1.02			
	Salt Fog	23.6	23.6	0.23	0.82	0.281	1.56	0.148	20.6	1.00	24.3	0.23	0.82	0.281	1.56	0.148	24.3	1.00			
		29.0	29.0	0.26	0.87	0.299	1.75	0.132	22.6	1.10	29.0	0.26	0.87	0.299	1.75	0.132	25.8	1.06			
		29.0	29.0	0.23	0.72	0.328	1.84	0.152	20.9	1.07	29.0	0.23	0.72	0.328	1.84	0.152	25.8	1.06			
7075-T6	Ambient	19.1	20.7	0.31	0.95	0.360	1.88	0.163	16.3	0.85	21.2	0.31	0.95	0.360	1.88	0.163	15.6	0.74			
	Salt Fog	20.7	20.7	0.21	0.61	0.344	1.82	0.115	13.7	0.72	20.7	0.21	0.61	0.344	1.82	0.115	16.7	0.79			
		33.1	33.1	0.16	0.38	0.421	2.04	0.078	18.0	0.94	33.1	0.16	0.38	0.421	2.04	0.078	19.6	0.93			
		31.1	31.1	0.20	0.50	0.400	2.05	0.098	20.2	1.06	31.1	0.20	0.50	0.400	2.05	0.106	21.0	0.99			
7075-T7	Ambient	19.4	19.1	0.30	0.98	0.306	1.66	0.181	15.6	0.80	22.0	0.30	0.98	0.306	1.66	0.181	24.4	1.11			
	Salt Fog	24.9	24.9	0.27	0.88	0.307	1.79	0.173	19.6	1.01	24.9	0.27	0.88	0.307	1.79	0.173	24.1	1.10			
		30.6	30.6	0.21	0.65	0.323	1.73	0.122	20.8	1.07	30.6	0.21	0.65	0.323	1.73	0.122	24.1	1.10			
		30.6	30.6	0.19	0.61	0.311	1.68	0.113	20.1	1.04	30.6	0.19	0.61	0.311	1.68	0.113	24.1	1.10			

Unclassified

Security Classification

DOCUMENT CONTROL DATA - R&D		
(Security classification of title, body of abstract and indexing annotation must be entered when the overall report is classified)		
1. ORIGINATING ACTIVITY (Corporate author) Alcoa Research Laboratories Aluminum Company of America		2a. REPORT SECURITY CLASSIFICATION Unclassified
		2b. GROUP
3. REPORT TITLE STRESS-CORROSION AND CORROSION-FATIGUE SUSCEPTIBILITY OF HIGH-STRENGTH ALUMINUM ALLOYS		
4. DESCRIPTIVE NOTES (Type of report and inclusive dates) June 1967 - November 1970 Final		
5. AUTHOR(S) (Last name, first name, initial) Nordmark, G. E., Lifka, B. W., Hunter, M. S., and Kaufman, J. G.		
6. REPORT DATE November 1970	7a. TOTAL NO. OF PAGES 124	7b. NO. OF REFS 9
8a. CONTRACT OR GRANT NO. F33615-67-C-1922	9a. ORIGINATOR'S REPORT NUMBER(S)	
b. PROJECT NO. 7381		
c.	9b. OTHER REPORT NO(S) (Any other numbers that may be assigned this report)	
d.	AFML-TR-70-259	
10. AVAILABILITY/LIMITATION NOTICES This document has been approved for publication and sale; its distribution is unlimited.		
11. SUPPLEMENTARY NOTES None	12. SPONSORING MILITARY ACTIVITY Air Force Materials Laboratory Air Force Systems Command Wright-Patterson Air Force Base, Ohio	
13. ABSTRACT <p>The "stress-corrosion-fatigue" performance of several high strength-aluminum alloys was investigated by tests of hydraulic cylinders and other types of specimens. Specimens were prepared from forgings and forging stock of alloys 2014-T6, 7075-T6, 7075-T73, 7079-T6, and X7080-T7 and from premium castings of alloy CH70-T7. The alternating internal pressure loading of the cylinders at frequencies between 0.15 and 20 cpm in corrosive environment included hold times at load of as much as 5.4 minutes. Corrosive environment was provided by a warm salt fog at 12 hour intervals.</p> <p>Alloy 7075-T73 rated best in the corrosion-fatigue tests; no stress-corrosion cracking occurred in this alloy, and the lives of forged cylinders subjected to repeated loadings to 80% of design stress in a corrosive environment were at least 10 times as long for this alloy as for forged cylinders of alloys 2014-T6, 7075-T6, or 7079-T6. Fractographic examination showed that stress-corrosion cracking as well as fatigue cracking occurred in alloys 2014-T6, 7075-T6, and 7079-T6 in the stress-corrosion-fatigue tests. The investigation demonstrated that stress corrosion and fatigue can interact under certain conditions to produce failures in shorter times and fewer cycles than for either phenomenon occurring by itself.</p>		

DD FORM 1473  
JAN 64

Unclassified

Security Classification

Unclassified

Security Classification

16	KEY WORDS	LINK 1	LINK 2	LINK 3	LINK 4	LINK 5
corrosion-fatigue	axial-aluminum					
stress-corrosion	metallography					
Internal	fracture-mechanics					
pressure	cracking					
hydraulic	fractography					
cylinders	frequency					
carriage	aluminum alloys					
corrosion	7075-T6					
rolled rod	7075-T7					
cracking	7079-T6					
mechanical properties						
fracture	X7080-T7					
toughness	2014-T6					
load	CH70-T7					
fatigue						
pressure						

INSTRUCTIONS

1. **ORIGINATING ACTIVITY:** Enter the name and address of the contractor, subcontractor, grantee, Department of Defense activity or other organization (corporate author) issuing the report.

2a. **REPORT SECURITY CLASSIFICATION:** Enter the overall security classification of the report. Indicate whether "Restricted Data" is included. Marking is to be in accordance with appropriate security regulations.

2b. **GROUP:** Automatic downgrading is specified in DoD Directive 5200.10 and Armed Forces Industrial Manual. Enter the group number. Also, when applicable, show that optional markings have been used for Group 3 and Group 4 as authorized.

3. **REPORT TITLE:** Enter the complete report title in all capital letters. Titles in all cases should be unclassified. If a meaningful title cannot be selected without classification, show title classification in all capitals in parentheses immediately following the title.

4. **DESCRIPTIVE NOTES:** If appropriate, enter the type of report, e.g., interim, progress, summary, annual, or final. Give the inclusive dates when a specific reporting period is covered.

5. **AUTHOR(S):** Enter the name(s) of author(s) as shown on or in the report. Enter last name, first name, middle initial. If military, show rank and branch of service. The name of the principal author is an absolute minimum requirement.

6. **REPORT DATE:** Enter the date of the report as day, month, year; or month, year. If more than one date appears on the report, use date of publication.

7a. **TOTAL NUMBER OF PAGES:** The total page count should follow normal pagination procedures, i.e., enter the number of pages containing information.

7b. **NUMBER OF REFERENCES:** Enter the total number of references cited in the report.

8a. **CONTRACT OR GRANT NUMBER:** If appropriate, enter the applicable number of the contract or grant under which the report was written.

8b, 8c, & 8d. **PROJECT NUMBER:** Enter the appropriate military department identification, such as project number, subproject number, system numbers, task number, etc.

9a. **ORIGINATOR'S REPORT NUMBER(S):** Enter the official report number by which the document will be identified and controlled by the originating activity. This number must be unique to this report.

9b. **OTHER REPORT NUMBER(S):** If the report has been assigned any other report numbers (either by the originator or by the sponsor), also enter this number(s).

10. **AVAILABILITY/LIMITATION NOTICES:** Enter any limitations on further dissemination of the report, other than those

imposed by security classification, using standard statements such as:

- (1) "Qualified requesters may obtain copies of this report from DDC."
- (2) "Foreign announcement and dissemination of this report by DDC is not authorized."
- (3) "U. S. Government agencies may obtain copies of this report directly from DDC. Other qualified DDC users shall request through \_\_\_\_\_."
- (4) "U. S. military agencies may obtain copies of this report directly from DDC. Other qualified users shall request through \_\_\_\_\_."
- (5) "All distribution of this report is controlled. Qualified DDC users shall request through \_\_\_\_\_."

If the report has been furnished to the Office of Technical Services, Department of Commerce, for sale to the public, indicate this fact and enter the price, if known.

11. **SUPPLEMENTARY NOTES:** Use for additional explanatory notes.

12. **SPONSORING MILITARY ACTIVITY:** Enter the name of the departmental project office or laboratory sponsoring (paying for) the research and development. Include address.

13. **ABSTRACT:** Enter an abstract giving a brief and factual summary of the document indicative of the report, even though it may also appear elsewhere in the body of the technical report. If additional space is required, a continuation sheet shall be attached.

It is highly desirable that the abstract of classified reports be unclassified. Each paragraph of the abstract shall end with an indication of the military security classification of the information in the paragraph, represented as (TS), (S), (C), or (U).

There is no limitation on the length of the abstract. However, the suggested length is from 150 to 225 words.

14. **KEY WORDS:** Key words are technically meaningful terms or short phrases that characterize a report and may be used as index entries for cataloging the report. Key words must be selected so that no security classification is required. Identifiers, such as equipment model designation, trade name, military project code name, geographic location, may be used as key words but will be followed by an indication of technical context. The assignment of links, rules, and weights is optional.

Unclassified

Security Classification